

STATE OF CALIFORNIA DEPARTMENT OF TRANSPORTATION  
**TECHNICAL REPORT DOCUMENTATION PAGE**  
 TR0003 (REV. 10/98)

1. REPORT NUMBER CA11-1226	2. GOVERNMENT ASSOCIATION NUMBER	3. RECIPIENT'S CATALOG NUMBER
4. TITLE AND SUBTITLE Online Freeway Corridor Deployment of Anonymous Vehicle Tracking for Real Time Traffic Performance		5. REPORT DATE September 28, 2010
7. AUTHOR(S) Stephen G. Ritchie, Yeow Chern Andre Tok, Shin-Ting (Cindy) Jeng, Hang Liu, Sarah Hernandez, Jinheoun Choi		6. PERFORMING ORGANIZATION CODE
9. PERFORMING ORGANIZATION NAME AND ADDRESS Institute of Transportation Studies University of California, Irvine Irvine, CA 92697-3600		8. PERFORMING ORGANIZATION REPORT NO. #UCI-0279
12. SPONSORING AGENCY AND ADDRESS California Department of Transportation Division of Research and Innovation, MS-83 1227 O Street; Sacramento CA 95814		10. WORK UNIT NUMBER 3763
15. SUPPLEMENTAL NOTES		11. CONTRACT OR GRANT NUMBER 65A0279
16. ABSTRACT <p>The need for advanced, accurate and comprehensive traffic performance measures in increasingly saturated traffic networks is stretching the effectiveness of existing conventional point-based loop detector traffic data. This study had two objectives. The first was the evaluation of two emerging technologies – Sensys Magnetometers and Blade Inductive Signature System – to assess their potential in providing advanced traffic performance measures using vehicle signature data. The second was the expansion and deployment of the Real-time Traffic Performance Measurement System (RTPMS) to provide section-based traffic performance measures under actual operating conditions. As a part of this deployment, a communications framework was implemented to provide real-time communications of signature feature data between field units and a central vehicle re-identification server. A new improved online interactive web-user interface was also developed to provide users with real-time as well as historical traffic performance measurements.</p>		13. TYPE OF REPORT AND PERIOD COVERED Final Report
17. KEY WORDS Traffic performance measurement, advanced technologies, inductive loop detector, real time measurement	18. DISTRIBUTION STATEMENT No restrictions. This document is available to the public through the National Technical Information Service, Springfield, VA 22161	
19. SECURITY CLASSIFICATION (of this report) Unclassified	20. NUMBER OF PAGES 136	21. PRICE

## **DISCLAIMER STATEMENT**

This document is disseminated in the interest of information exchange. The contents of this report reflect the views of the authors who are responsible for the facts and accuracy of the data presented herein. The contents do not necessarily reflect the official views or policies of the State of California or the Federal Highway Administration. This publication does not constitute a standard, specification or regulation. This report does not constitute an endorsement by the Department of any product described herein.

For individuals with sensory disabilities, this document is available in Braille, large print, audiocassette, or compact disk. To obtain a copy of this document in one of these alternate formats, please contact: the Division of Research and Innovation, MS-83, California Department of Transportation, P.O. Box 942873, Sacramento, CA 94273-0001.

# **Deployment of a Vehicle Tracking System for an Online Real-Time Freeway Traffic Performance Measurement**

**Final Report  
Federal Report #UCI-0279**

*Prepared for:*

**State of California Department of Transportation  
Division of Research & Innovation  
Office of Technology Applications**

**September 2010**

**State of California Department of Transportation  
Division of Research & Innovation  
Office of Technology Applications**

**Deployment of a Vehicle Tracking System for an  
Online Real-Time Freeway Traffic Performance  
Measurement**

**Final Report  
#UCI-0279**

**Authors:  
Stephen G. Ritchie  
Yeow Chern Andre Tok  
Shin-Ting (Cindy) Jeng  
Hang Liu  
Sarah Hernandez  
Jinheoun Choi**

**Institute of Transportation Studies  
University of California  
Irvine, CA 92697-3600**

## **ACKNOWLEDGMENT**

The research presented in this report was sponsored by the California Department of Transportation (Caltrans), Division of Research and Innovation (DRI) with Fred Yazdan as the project manager.

The contents of this report reflect the views of the authors who are responsible for the facts and the accuracy of the data presented herein. The contents do not necessarily reflect the official views or policies of the State of California. This report does not constitute a standard, specification, or regulation.

The authors gratefully acknowledge the assistance of Ron Flemming and Chris Van Wagenen, Department of Parking and Transportation, Brian Fuller and Karric Kwong, Sensys Networks Inc., University of California, Irvine, Fred Yazdan, John Slonaker and Nadine Martins, California Department of Transportation and the California Highway Patrol Officers and staff at the San Onofre Inspection Facility in conducting this research.

**EXECUTIVE SUMMARY**

Effective real-time traffic detection systems which are able to obtain accurate, detailed and timely freeway performance measures are a prerequisite for efficient transportation system operations. Advanced real-time traffic performance measurement provides timely and detailed assessment of traffic conditions and is the cornerstone for achieving optimal operations of the freeway network. It is therefore imperative that Caltrans obtain experience with different detection technologies and performance measurement systems in actual operating environments, in order to obtain the greatest benefit at least cost for California travelers on the state highway system.

There has been sustained research in the development of advanced traffic surveillance systems through the investigation of various technologies. However, while many have shown potential to be less pavement-intrusive, few have achieved performance levels that rival the conventional loop detection system. In fact, loop detection systems remain the most robust surveillance technology with an expected lifespan that equals or exceeds pavement service life. However, the need for advanced, accurate and comprehensive traffic performance measures in increasingly saturated traffic networks is stretching the effectiveness of conventional point-based loop detector traffic data. This is because point-based aggregate volume and occupancy data do not provide the required fidelity or the sophistication to accurately describe the complex characteristics of congested traffic across sections, where conditions vary dynamically both in time and space.

This study had two objectives. The first was the evaluation of two emerging technologies – Sensys™ Magnetometers and Blade™ inductive system – to assess their potential in providing advanced traffic performance measures using vehicle signature data. The second was the expansion and deployment of the Real-time Traffic Performance Measurement System (RTPMS), which uses inductive signature data obtained from upgraded hardware at field cabinets connected to existing

inductive loop infrastructure to provide advanced section-based traffic performance measures under actual operating conditions.

The study on Blade™ inductive system yielded proposed sensor configurations that may be suitable for obtaining speed profiles from vehicles to enable recovery of vehicle inductive signatures that have been distorted by acceleration effects.

The investigation on Sensys™ wireless magnetometer revealed the potential of Sensys™ in providing reliable conventional traffic data such as volume and occupancy information as well as to augment the Inductive Loop Detector (ILD) signature system through heterogeneous transformation of signatures between ILD and Sensys™ sensors. The results from the analysis of conventional data indicated that volume counts from Sensys™ deviated from ILDs by about six percent. However, occupancy measures at the test site were significantly higher than ILDs. Spikes in occupancy measurements were also a concern, as they appeared abruptly and seemed to be random in nature. The investigation of transformation between ILD and Sensys™ revealed significant data errors in Sensys™ signatures which have been attributed to dropped data packets during wireless communication between the sensors and access point. The errors were recovered where possible, and subsequent analyses indicated that Sensys™ signatures were not compatible with ILD signatures. However, because their features were independent from ILD signatures, data fusion of these two technologies could help to improve the performance of advanced traffic surveillance applications if the reliability of Sensys™ signatures can be addressed.

The components of the prototype RTPMS first developed under PATH Task Order 5304 were refined and improved for full deployment on the Northbound I-405 freeway corridor in the City of Irvine, California. Modifications were made to the RTPMS to improve the reliability of connections from multiple field units to a central vehicle re-identification server, located in the California Traffic Management Laboratories (CTMLabs) on the University of California, Irvine campus.

A new improved integrated web-user interface using advanced interactive web technologies was developed to provide advanced queries for retrieving detailed graphical as well as text-based real-time and archived traffic performance measure reports such as section and corridor travel times, section speeds and densities and station volumes by vehicle class. A repository for access to archived signature data was also developed. This resource will allow the research community to further investigate the potential of ILD signatures in providing improved traffic surveillance applications.

**TABLE OF CONTENTS**

ACKNOWLEDGMENT .....iv

EXECUTIVE SUMMARY .....v

TABLE OF CONTENTS ..... viii

LIST OF FIGURES .....xi

LIST OF TABLES .....xv

CHAPTER 1 INTRODUCTION..... 1

    1.1 Background ..... 1

    1.2 Report Outline .....2

CHAPTER 2 A REVIEW AND EVALUATION OF REAL-TIME POINT  
AND SECTION-BASED FREEWAY PERFORMANCE MEASURES.....3

    2.1 Overview .....3

    2.2 Literature Review .....5

        2.2.1 Speed and Travel Time .....6

        2.2.2 Flow.....8

        2.2.3 Density .....9

    2.3 Data Collection..... 11

    2.4 Model Selection and Development ..... 12

        2.4.1 Selected Point-Based Models Implemented..... 12

        2.4.2 Development of Section-Based Models ..... 13

        2.4.3 Development of Data and Performance Measures Ground  
                Truth ..... 15

    2.5 Comparisons of Point-based and Section-based Freeway  
        Performance Measures ..... 17

    2.6 Conclusions ..... 20

CHAPTER 3 ANALYSIS OF EMERGING TECHNOLOGIES .....21

    3.1 Background ..... 21

    3.2 Overview of Technologies ..... 22

        3.2.1 Blade Inductive Signatures..... 22

        3.2.2 Sensys Wireless Magnetometers ..... 24

- 3.3 Blade™ Inductive Signatures.....26
  - 3.3.1 Study Sites.....26
  - 3.3.2 Configuration Analysis .....28
- 3.4 Analysis of Sensys™ in Conventional Mode.....36
  - 3.4.1 Data Description.....37
  - 3.4.2 Analysis of Results.....38
- 3.5 Analysis of Quality and Repeatability of Sensys™ Data in Signature Mode.....41
  - 3.5.1 Study Sites and Data .....42
  - 3.5.2 Signature Mode Issues .....45
  - 3.5.3 Sensys™ Signature Quality Analysis.....46
  - 3.5.4 Sensys™ Signature Repeatability Analysis .....59
- 3.6 Investigation of Heterogeneous Transformation between Sensys™ and Inductive Loop Signatures.....67
  - 3.6.1 Study Site .....68
  - 3.6.2 Signal Preprocessing: Matching ILD and Sensys™ Signatures .....68
  - 3.6.3 Correlation Analysis.....70
  - 3.6.4 Exploratory Heterogeneous Transformation Analysis.....72
- 3.7 Summary of Findings .....76
  - 3.7.1 Blade™ Inductive Sensors .....76
  - 3.7.2 Analysis of Sensys™ Data in Conventional Mode.....76
  - 3.7.3 Analysis of Quality and Repeatability of Sensys™ Data in Signature Mode .....77
  - 3.7.4 Investigation of Heterogeneous Transformation between Inductive Loop and Sensys™ Signatures.....77
- CHAPTER 4 REAL-TIME TRAFFIC PERFORMANCE MEASUREMENT SYSTEM: FIELD AND COMMUNICATIONS DEPLOYMENT.....78
  - 4.1 Overview of Field, Communications and Data Processing Framework .....78

- 4.2 Field Hardware Configuration .....81
  - 4.2.1 Recommended Traffic Cabinet Hardware Components .....81
  - 4.2.2 Field Data Processing System (Field Unit).....82
  - 4.2.3 Advanced Loop Detector Cards .....84
- 4.3 Performance Measurement System.....85
- 4.4 Database Server Architecture.....85
  - 4.4.1 Lookup Tables.....86
  - 4.4.2 Signature Table .....89
  - 4.4.3 REID Table .....90
- 4.5 Field Deployment.....91
- CHAPTER 5 REAL-TIME TRAFFIC PERFORMANCE
  - MEASUREMENT SYSTEM: WEB SERVER DEPLOYMENT .....94
    - 5.1 Overview of Web and Database Framework .....94
    - 5.2 Web Server Design.....94
    - 5.3 RTPMS Web Interface Modules .....95
      - 5.3.1 Real-time Google Maps interactive navigation interface.....95
      - 5.3.2 Real-Time Performance Measures .....97
      - 5.3.3 Historical Query Interface .....102
      - 5.3.4 Signature Data Repository .....108
- CHAPTER 6 CONCLUSION .....110
  - 6.1 Alternative Advanced Traffic Surveillance Technologies .....110
  - 6.2 Real-time Traffic Performance Measurement System .....111
  - 6.3 Implementation Strategies and Future Research .....112
- REFERENCES.....115

**LIST OF FIGURES**

Figure 2-1 PeMS, REID, Base and ground truth travel time and speed measures ..... 18

Figure 2-2 PeMS, REID, Base and ground truth flow and density measures ..... 19

Figure 2-3 Correlation between REID and GT Travel Time Measures ..... 20

Figure 3-1 Comparison of Round and Blade™ Inductive Loop Sensor Signatures of a Tractor Pulling a Semi-Trailer ..... 23

Figure 3-2 Characteristics of a Blade™ Inductive Signature ..... 24

Figure 3-3 Wireless magnetometers ..... 25

Figure 3-4 Installation of Sensys™ sensors ..... 26

Figure 3-5 UCI Commercial Vehicle Study Testbed ..... 27

Figure 3-6 Location of UCI Detector Testbed ..... 28

Figure 3-7 Example of inductive loop signatures from narrow double Blade inductive sensors showing wheel locations and body signature profile ..... 29

Figure 3-8 Southbound San Onofre Data Collection Study Site ..... 31

Figure 3-9 Installation of Permanent Blade Sensors ..... 31

Figure 3-10 Sample of signatures from permanent double 8-inch Blade™ inductive sensors ..... 32

Figure 3-11 Study Site in University of California, Irvine at Bison Ave ..... 33

Figure 3-12 Installation of 8-inch Surface Mounted Blade™ Inductive Sensors at Bison Ave Study Site at the University of California, Irvine ..... 34

Figure 3-13 Sample Blade Inductive Signatures of Passenger Vehicle from Blade™ Inductive Sensors with 8 inch Longitudinal Spacing ..... 35

Figure 3-14 Sample Blade Inductive Signatures of Single Unit Truck from Blade™ Inductive Sensors with 8 inch Longitudinal Spacing ..... 35

Figure 3-15 Sample Blade Inductive Signatures of Tractor with Single Low-boy Trailer from Blade™ Inductive Sensors with 8 inch Longitudinal Spacing ..... 36

Figure 3-16 Layout of inductive loop and Sensys™ sensors used to obtain aggregate measures along NB I-405 freeway .....37

Figure 3-17 Scatter plot comparison of five-minute Volume measures between ILD and Sensys™ sensors .....38

Figure 3-18 Scatter plot comparison of five-minute Occupancy measures between ILD and Sensys™ sensors .....39

Figure 3-19 Time-of-day comparison of 5-minute occupancy measures between ILD and Sensys .....40

Figure 3-20 Example of Sensys™ magnetometer signatures .....42

Figure 3-21 Wireless magnetometer setup at upstream station .....44

Figure 3-22 Detector stations with sensor layout in Detector Testbed along northbound I-405 freeway in Irvine, California. ....45

Figure 3-23 Example of a signature with dropped sections.....46

Figure 3-24 Total number of vehicles by lane across datasets .....48

Figure 3-25 Percentage of no-drop signatures by lane across datasets.....49

Figure 3-26 Data quality analysis for HOV Lane 1 .....51

Figure 3-27 Data quality analysis for HOV Lane 2 .....52

Figure 3-28 Data quality analysis for Mainline Lane 1 .....53

Figure 3-29 Data quality analysis for Mainline Lane 2 .....54

Figure 3-30 Data quality analysis for Mainline Lane 3 .....55

Figure 3-31 Data quality analysis for Mainline Lane 4 .....56

Figure 3-32 Dataset 1 Jan 9 2009.....57

Figure 3-33 Dataset 2 April 28 2009 .....58

Figure 3-34 Dataset 3 May 12 2009.....58

Figure 3-35 Comparison for repeatable signatures across lanes by dataset.....60

Figure 3-36 Cumulative distribution plot showing percentage of non-repeatable signatures below corresponding correlation coefficient for HOV Lane 1 and HOV lane 2 across datasets.....61

Figure 3-37 Cumulative distribution plot showing percentage of non-repeatable signatures below corresponding correlation coefficient for Mainline Lane 1 and Mainline lane 2 across datasets .....62

Figure 3-38 Cumulative distribution plot showing percentage of non-repeatable signatures below corresponding correlation coefficient for Mainline Lane 3 and Mainline Lane 4 across datasets ..... 63

Figure 3-39 Cumulative distribution plot showing percentage of non-repeatable signatures below corresponding correlation coefficient for the Jan 9 2009 dataset across lanes..... 65

Figure 3-40 Cumulative distribution plot showing percentage of non-repeatable signatures below corresponding correlation coefficient for the April 28 2009 dataset across lanes..... 66

Figure 3-41 Cumulative distribution plot showing percentage of non-repeatable signatures below corresponding correlation coefficient for the May 12 2009 dataset across lanes..... 67

Figure 3-42 Extracting features from an ILD signature for heterogeneous transformation analysis ..... 73

Figure 3-43 Extracting features from a Sensys™ signature for heterogeneous transformation analysis ..... 74

Figure 3-44 Percentage of vehicles with minimum number of Sensys™ target features predicted correctly ..... 75

Figure 4-1 RTPMS Module Framework..... 79

Figure 4-2 RTPMS Architecture..... 80

Figure 4-3 Traffic cabinet showing advanced loop detector cards and rack-mounted field computer ..... 81

Figure 4-4 Field Unit processes ..... 83

Figure 4-5 Additional hardware components of field unit..... 84

Figure 4-6 Communications Framework for RTPMS ..... 93

Figure 5-1 RTPMS Web and Database Framework ..... 94

Figure 5-2 Sample Traffic Performance Interface from Google Maps..... 95

Figure 5-3 Google Maps-based RTPMS Interface ..... 96

Figure 5-4 Detector Station Information Display from Google Maps-based RTPMS Interface..... 97

Figure 5-5 Real-time Performance Measures interactive user input query interface ..... 98

Figure 5-6 Origin-Destination Travel Time Matrix for the S. CA-133 - Red Hill Corridor ..... 99

Figure 5-7 Sample Lane-Lane Travel Time Matrix Format ..... 100

Figure 5-8 Sample Lane-Lane Section Speed Display ..... 101

Figure 5-9 Sample Section Speeds and Densities Display ..... 102

Figure 5-10 Historical Performance Measures Query Inputs ..... 103

Figure 5-11 Sample Corridor Travel Time by Facility Display..... 104

Figure 5-12 Sample Corridor Speed by Facility Display..... 105

Figure 5-13 Sample Corridor Average Delay Timeline Chart Display (minutes per vehicle)..... 106

Figure 5-14 Sample Corridor Total Delay Timeline Chart Display (Vehicle-Hours)..... 107

Figure 5-15 Sample Section-based Density Contour Map..... 108

Figure 5-16 Signature Data Repository ..... 109

**LIST OF TABLES**

Table 2-1 Summary of Point-Based, Section-Based, and Ground truth Performance Measure Models..... 16

Table 2-2 Evaluations of Performance Measures by Selected Models .....20

Table 3-1 Summary of Data Collection Exercises for Sensys™ Investigation .....43

Table 3-2 Summary of Sensys Data Collections at the Sand Canyon Detector Testbed along the Northbound I-405 freeway to evaluate Access Point location ..... 47

Table 3-3 Number of signature pairs by correlation values between ILD and Sensys™ Z-Axis..... 70

Table 3-4 Number of signature pairs by correlation values between ILD and Sensys™ X-Axis ..... 71

Table 3-5 Number and Percentage of signature pairs by correlation values between ILD and Sensys™ Z-Axis..... 71

Table 4-1 Corridor Lookup Table (LOOKUP\_CORRIDORS)..... 86

Table 4-2 Detector Card Lookup Table (LOOKUP\_DET\_CARD\_LN)..... 87

Table 4-3 Section Lookup Table (LOOKUP\_SECTIONS) ..... 88

Table 4-4 Corridor Lookup Table (LOOKUP\_SECT\_CORR)..... 88

Table 4-5 Station Information Lookup Table (LOOKUP\_STATIONS)..... 89

Table 4-6 Signature Table (RTPMS\_VEH\_SIG) ..... 90

Table 4-7 REID Results Table (RTPMS\_REID\_OUTPUT)..... 90

Table 4-8 List of RTPMS detector stations with deployment status ..... 92

Table 5-1 Detector Stations corresponding to I-405 Northbound corridor from South of the CA-133 Freeway to Red Hill ..... 99

## **DISCLAIMER STATEMENT**

This document is disseminated in the interest of information exchange. The contents of this report reflect the views of the authors who are responsible for the facts and accuracy of the data presented herein. The contents do not necessarily reflect the official views or policies of the State of California or the Federal Highway Administration. This publication does not constitute a standard, specification or regulation. This report does not constitute an endorsement by the Department of any product described herein.

For individuals with sensory disabilities, this document is available in Braille, large print, audiocassette, or compact disk. To obtain a copy of this document in one of these alternate formats, please contact: the Division of Research and Innovation, MS-83, California Department of Transportation, P.O. Box 942873, Sacramento, CA 94273-0001.

## **CHAPTER 1 INTRODUCTION**

### **1.1 Background**

Effective real-time traffic detection systems which are able to obtain accurate, detailed and timely freeway performance measures are a prerequisite for efficient transportation system operations. Advanced real-time traffic performance measurement provides timely and detailed assessment of traffic conditions and is the cornerstone for achieving optimal operations of the freeway network. It is therefore imperative that Caltrans obtain experience with different detection technologies and performance measurement systems in actual operating environments, in order to obtain the greatest benefit at least cost for California travelers on the state highway system.

There has been sustained research in the development of advanced traffic surveillance systems through the investigation of various technologies. However, while many have shown potential to be less pavement-intrusive, few have achieved performance levels that rival the conventional loop detection system. In fact, loop detection systems remain the most robust surveillance technology with an expected lifespan that equals or exceeds pavement service life. However, the need for advanced, accurate and comprehensive traffic performance measures in increasingly saturated traffic networks is stretching the effectiveness of conventional point-based loop detector traffic data. This is because point-based aggregate volume and occupancy data do not provide the required fidelity or the sophistication to accurately describe the complex characteristics of congested traffic across sections, where conditions vary dynamically both in time and space. PATH Task Order (TO) 5304 accomplished the development of a simulated freeway real-time traffic performance measurement system using actual peak-period data obtained from the Northbound Interstate-405 (I-405) freeway in Irvine and the development of an advanced commercial vehicle classification system using Blade™ inductive sensors. The simulated system, called the Real-time Traffic Performance Measurement System (RTPMS), demonstrated an ability to produce accurate and

reliable section-based performance measures using actual travel time measures obtained from re-identified vehicles across freeway sections. Hence, the next logical step in developing this system for potential implementation is an online freeway corridor deployment under actual operating conditions.

It was also found in TO 5304 that while conventional inductive loop sensors perform sufficiently well to obtain good measurements of travel time information under varying traffic conditions, signatures from inductive loop sensors do suffer from distortion under stop-and-go situations when vehicles are subject to significant acceleration and deceleration relative to their speed. While such traffic conditions are unlikely to affect aggregate travel time measures significantly, they may affect the ability to obtain accurate origin-destination and route information. In addition, while inductive loop technology is relatively robust, it still requires significant labor and coordination for new sensors to be installed or replaced on freeways. Hence, there is a need to identify potential alternative technologies that may provide the advanced traffic surveillance potential of inductive loop signature systems as well as the ability to integrate seamlessly with them. Review of two potential sensor technologies—Blade™ inductive sensors and Sensys™ wireless magnetometers—have revealed potential to address these problems, and are investigated in this study.

## **1.2 Report Outline**

This report consists of six chapters, including this chapter. Chapter 2 provides a review and evaluative comparison between point and section-based traffic measures, and discusses the advantages of section-based measures. Chapter 3 presents the analysis of emerging signature-capable traffic detector technologies which have potential to yield section-based traffic measures. The Blade™ inductive system and Sensys™ Magnetometer are investigated here. Chapter 4 describes the field and communications deployment of the Real-time Traffic Performance Measurement System (RTPMS). Chapter 5 presents the web server deployment of RTPMS. Descriptions of the web and database framework as well as web interface modules are presented in this chapter. Chapter 6 presents the conclusions of this study.

## **CHAPTER 2 A REVIEW AND EVALUATION OF REAL-TIME POINT AND SECTION-BASED FREEWAY PERFORMANCE MEASURES**

### **2.1 Overview**

A safe and efficient freeway system is reliant upon the ability to monitor and detect traffic conditions in real-time. Real-time measurements of speed, density, flow, and travel time are examples of some of the key traffic performance measures used in determining the state of a network. The performance measures are also useful for advanced traffic management such as automatic incident detection, adaptive freeway ramp metering, traveler information systems, vehicle routing, model calibration, and emergency management (1, 2). In order to facilitate implementation of any advanced traffic management system, the accuracy of these key measures plays an important role.

The most common methods used to gather freeway traffic performance measures are point-based and are mostly derived from inductive loop detectors. Data from point locations are then used to estimate conditions along entire links, i.e., the road segment between two consecutive detector locations. Point-based freeway performance measures have been widely used for traffic surveillance and management. For instance, the Freeway Performance Measurement System (PeMS) used by the California Department of Transportation collects point data from 22,000 loop sensors in California to provide real-time performance measures (3). However, this approach has many inherent inaccuracies (4-8) as estimating section measures from point data may require providing approximations of vehicle length (9 - 12) when using single loops.

Acquiring accurate freeway traffic performance measures would involve directly measuring traffic parameters over the length of a link, rather than at single points. Intelligent Transportation Systems (ITS) technologies such as video imaging, license plate matching, cellular phone tracking, automatic vehicle identification (AVI), and vehicle re-identification (REID) are capable of producing direct section-

based measures. Among the aforementioned technologies, REID has made it possible to obtain direct section-based performance measures from loop detectors. This approach aims to match either individual vehicles by using inductive loop signature features (5, 13, 14, 15), or platoons of vehicles by matching vehicle lengths (16, 17, 18). Researchers have found that section-based measures are arguably better than point-based measures. For instance, Sun et al. (1999) indicated that during congested and moderate flow conditions, section-based measures of travel time and density had errors of less than 4% (60). Accordingly, Oh et al. (2005) stated that point measures are not an accurate depiction of freeway performance, and developed a Level of Service model based on section-measures for use in real-time freeway analysis (7). More specifically, Jeng et al. (2007) have shown the increased accuracy of section-based measures via a vehicle re-identification approach.

Although the improvement in accuracy of section-based freeway measurement over point-based freeway measurement seems clear, the comparison has rarely been made explicitly, and most studies have focused on travel time estimation (19-27). Therefore, this study provides an initial comparative evaluation of the accuracy and reliability of point-based and section-based models in terms of real-time freeway performance measurements. The most common real-time performance measures of speed, travel time, count, and density will be discussed.

This chapter is organized into five sections. The first section presents a review of current practices for point-based and section-based freeway traffic performance measures including speed, travel time, count, and density. The second section describes the performance measurement models developed around section-based vehicle re-identification techniques and an outline of the key point-based measurements to which the section-based models will be compared. The third section presents the comparison results. The conclusions are offered in the fourth section.

## 2.2 Literature Review

Real-time freeway traffic performance measurements commonly rely on point-based variables obtained from inductive loop detectors since they are the most popular form of detection system and have been widely deployed on freeways. The general measurements obtained from single Inductive Loop Detectors (ILDs) are count and occupancy. The speed, flow, and density are then estimated for a link using the occupancy and count data obtained from the loops. Significant efforts have been made to improve the accuracy of such estimates from inductive loop detectors for travel time and speed (17, 19 - 28), for flow and count (10, 18, 23, 25, 29, 30), and for density (6, 31, 32, 33).

Other existing detection technologies are also suitable for providing traffic speed and counts including magnetic, passive infrared, microwave radar true presence, passive acoustic, and video image processing (VIP) (34, 35, 36). In terms of increasing the accuracy of section related measures, VIP technologies appear to have the most potential and are the least costly of those listed (34), but often have poor performance under changing weather conditions (37). Inductive loop detectors show the least error (2 to 3%) for counts and for speeds (1.2 to 10%) whereas VIP technologies show errors of 1.6 to 15% and 0.8 to 12%, respectively (37). Several additional technologies also aim at producing better travel time and density estimates including electronic distance-measuring instruments (DMIs), license plate matching, cellular phone tracking, automatic vehicle identification (AVI), Blue Tooth Readers, and automatic vehicle location (AVL), but most are costly, have privacy issues, and their accuracies are uncertain (38). For this report, existing round and square loops as well as additional new technologies- Blade Inductive Loops and Sensys Magnetometers were investigated. However, this chapter focuses on only the section measures derived from round and square loops, as later chapters are dedicated to discussion of the performance of the additional two technologies. Therefore, in the remainder of this section, research relating to each of the performance measures is discussed.

### 2.2.1 Speed and Travel Time

Speed and travel time are very closely related measures, as travel time can be computed from speed estimates and vice versa. The estimation of speeds and travel times can be grouped into three categories: single point detector based estimation, adjacent point detector based estimation, and section-based data estimation. Travel time found by first calculating the speed at a single point detector and then extrapolating to get the link travel time is referred to as a single point speed-based travel time estimation model. The extrapolation of the speed is equivalent to developing a trajectory of the vehicle as it traverses the link, and relies on the presence of dual loop detectors, or an estimation of the g-factor (9) which is defined as the inverse of the effective vehicle length, or knowledge of the vehicle's inductive signature. Adaptations and improvements in speed estimation have been made by altering the g-factor or vehicle length estimate (9, 11, 12, 39), as well as by evaluating vehicle signature data (28, 40, 41, 60). The *Travel Time Data Collection Handbook* (59) states that the extrapolation technique is the simplest and most widely accepted method for estimating travel time from inductive loop detectors. In estimating speed from a single loop detector, researchers are able to obtain time-mean-speed. However, most researchers conclude that the use of space-mean-speed rather than time-mean-speed in any model results in higher accuracy of travel time estimates (19, 20, 21, 42, 43). Data from adjacent detectors can be used to provide better estimates of travel time over a link, which is referred to as the adjacent point detector based estimation. The estimation errors for this method are in the range of 2 to 30 percent (19, 20, 21, 22, 42).

In a comparison of four well developed travel times estimation models, including instantaneous, time slice, dynamic time slice, and linear models, Li et al. (2006) showed that there was very little difference between each of the models, with the errors around 7 to 15 percent, while only the instantaneous model could be implemented in real-time. The researchers concluded that the use of the space-mean-speed rather than the time-mean-speed would reduce errors further by 2 percent (19). Cortes et al. (2002) examined the use of harmonic speed (a proxy for space-mean-

speed) calculated at adjacent point detectors, and combined via an averaging parameter resulted in 1.78 to 5.90 percent error for fairly congested conditions, and 4.11 to 14.31 percent error for severely congested conditions when compared to the simulated data mimicking 100 percent probe vehicle rates (20). Van Lint and van der Zijpp (2003) used a piecewise linear speed based trajectory method which modeled the speed over the link as a convex combination of vehicle speed from upstream and downstream adjacent loops. Their results showed mean relative errors of 0.76 percent for the linear method, and 5.94 percent for constant speed based trajectory methods (21). Holt et al. (2003) used microscopic traffic simulation to show that extrapolation based travel time models based on time-mean-speed underestimated travel times by 30 percent during congested periods where traffic reached 85 percent of capacity (42). Using the speeds from three adjacent detectors to estimate the speed path and trajectory between detectors, Sun et al. (2008) developed a real-time travel time estimation model resulting in less than 10 percent error over actual travel times (22).

The aforementioned studies relied on speed data from adjacent detectors to estimate the travel time. The second procedure for calculating travel time from adjacent point detectors depends on the count information and includes methods such as checking the conservation of vehicles, stochastic queuing theory, and cross-correlational based approaches (23, 25, 26). In short, flow-based approaches involve estimating the number of vehicles entering and exiting a link from point detectors at either end of the link, calculating the space-mean-speed, and then estimating the travel time. An early study based on this approach reported that the estimated travel times were in “qualitative agreement” with measuring 30-second data (23). Following up on this study, by replacing the calculation of space-mean-speed and density with the loop occupancy data rather than the flow/count data, researchers reported reduced errors (12 to 19 percent) compared to AVI data (24). Additionally, cross-correlation methods based on flow models confirm that using information gathered from both ends of a link can accurately estimate travel times (25, 26).

Various vehicle re-identification techniques have been developed for travel time estimation which use information from detectors at both ends of the link to produce better estimates of travel times (2, 5, 6, 8, 17, 27, 61). For this class of approaches, inductive loop count or signature data, for example, are gathered at the upstream and downstream detectors, and then matched either on an individual or vehicle platoon basis so that actual travel times are known. Reported errors for inductive signature based approaches range from 1 to 2 percent for moderate flow conditions and 3 to 4 percent for congested conditions (5, 6, 8, 61).

### **2.2.2 Flow**

Count, the number of vehicles that pass over a sensor, is a measure directly obtained from inductive loop sensors (3). Flow can be derived from count as the number of vehicles per second, minute, or hour that pass over a sensor. The terms count and flow, although they technically refer to different measurement units, are often considered interchangeable references. Flow has been shown to be an important factor in predicting freeway safety especially when the flow measurements and variations can be derived separately for each freeway lane (44). In fact, based on flow information, researchers can identify the types of crashes that are most likely to occur (44). More importantly, flow measures are related to freeway Level of Service (LOS) because they are applied to determine if the freeway is operating in congested or uncongested density conditions (45).

Errors in count measurements are usually caused by data transmission problems or cross-talk between sensors (36). It is estimated that for the California freeway network, 20 percent of loops may not be reporting accurate count information (46). Zhang et al (2007) reported that basic volume count modes of loop detectors have a positive mean error of around 0.91 percent, meaning they tend to over count (47).

In addition to count, cumulative count at a point sensor is also a popular measure. For instance, many density and travel time measurements are derived from

cumulative counts at the ends of a freeway section (18, 23, 25, 29). Cumulative counts can be used to enhance the accuracy of flow measures at a loop. Vanajakaski and Rilett (2004) corrected discrepancies in counts at detector stations by identifying instances when the conservation of vehicle principle was violated (30). By this approach, they were able to recapture missing and erroneous detector data.

Vehicle re-identification techniques involving loop detector signature analysis (5, 8,13,14) are able to provide more accurate flow measures, mainly because vehicles are matched on a one to one basis and thus if counts at two stations do not align, the vehicle path is known and the count can be corrected. Other re-identification techniques, such as those presented by Coifman (18) adopt the count and length measures provided by the point sensor and are thus prone to the same errors as previously discussed.

### **2.2.3 Density**

Density or concentration, defined as the number of vehicles per unit distance (36), and can be derived from loop occupancy (36, 48). Density is perhaps the most difficult traffic parameter to measure using inductive loop detectors since density is a spatial-temporal measure. Loop occupancy, i.e., the ‘on-time’ of the detector (36), is divided by the effective vehicle length, i.e., the length of a roadway traversed by the vehicle during the ‘on-time’ of the detector, to estimate the density of the section between detector locations (49). Most density measures based on loop detector data do not capture the spatial dimension of density since there is no way to track a vehicle’s trajectory without adopting advanced ITS approaches, thus there are many inaccuracies inherent in this density estimation method (5, 7, 43, 58). One such inaccuracy shown by Cassidy and Coifman (43) is that 30-second aggregated measures from loop detectors do not report the sufficient data (i.e., space-mean-speed) needed to apply the well known Greenshield’s model.

Another density estimation method involves the variations of the fundamental relationship between flow, speed, and density (51). Density ( $k$ ) can be derived from

speed ( $u$ ) and flow ( $q$ ), via the fundamental equation,  $q = uk$  (50). Hu and Yang (2008) developed a very simple method for calculating density from stationary loops by applying a parabolic relation between flow and density, and the results showed the parabolic curve fit the data with an R-squared of 0.985 (52).

The conservation of vehicles principle has also been applied for density estimation in conjunction with the fundamental equation. Using vehicle counts and speed profiles at the boundaries of a highway section, Gazis and Knapp (1971) applied the Kalman filtering technique to estimate the section density based on conservation of vehicles within the section and obtained 10 to 15 percent errors (29). Later researchers have adapted and expanded this model with similar approaches (53, 54, 55).

The Cell Transmission Model (CTM), a traffic flow model developed by Daganzo (56), has also been applied to loop data to estimate the density (31, 32, 57). Because of real-time implementation issues, simplified versions of the CTM have been developed (e.g. the Switching Mode Model (32, 57)), and both models provided better estimates of density compared to standard occupancy conversion methods. These models showed between 13 to 14 percent error and between 4 to 5 percent error for flow estimation (32, 57).

All of these studies use point data to estimate section density. However, incorporating vehicle trajectory over space and time into density estimation would greatly improve the accuracy (5, 8, 17). Herrera and Bayen (33) showed that the combination of data from mobile sensors (GPS tracking in individual vehicles) and stationary loop data significantly improved the accuracy of density estimates from 57.8 percent error for point sensor data only to 12.7 percent error with trajectory data provided. Vehicle reidentification techniques are capable of providing vehicle trajectory information and are thus very suitable for real-time density estimation. By matching only as few as 5 percent of vehicles Coifman (18) estimated section density with 7 percent error over groundtruthed data, predicting that with a higher match rate

and knowledge of lane change behavior, the accuracy of density estimates could be improved further (18). With a 66 percent match rate, Sun et al (6) estimated density with only 1 percent error, compared to around 50 percent error for standard point measures.

### **2.3 Data Collection**

There are two types of data used in this study: point and section. The point data were obtained from the PeMS database (3) and the section data were collected from the field, both for the Detector Testbed located on Northbound I-405 freeway, in Irvine, California. 30-second and 5-minute data for flow, occupancy, and speed from loops at Laguna Canyon (LC, PeMS ID #1209176 ML and 1209177 HOV, Post mile 2.35) and Sand Canyon (PeMS ID# 1201159 ML and 1201157 HOV, Post mile 2.89) were downloaded from PeMS for Tuesday, May 12th, 2009 to coincide with the section data gathered that day. The loops at these two locations are not the same as the loops in the Detector Testbed, but they are located less than 0.12 miles from the Testbed loops for comparison. In addition, the data from LC station were not applied because it is too close to a merging section, and therefore, experiences increased lane changing behavior.

Vehicle signature data from three detector locations at Laguna Canyon 1 (LC1), Sand Canyon (SC), and the Sand Canyon Off-Ramp (SC-Off) were collected on Tuesday, May 12th, 2009 from 6:00AM to 10:00AM, comprising the AM peak period. The signature data were collected at detector locations that contained double square inductive loop detectors via advanced loop detector cards located in the traffic cabinets adjacent to the freeway. Although double loop signature data was obtained, only one loop's data of the double loops was applied (14).

Camcorders were set up at each of the three locations and the entire data collection was recorded. The camcorder clocks were synchronized with a GPS clock, and then the signature timestamps were synchronized to the video timestamps. Ground truth data was obtained from nine discrete time periods (6:35AM, 7:00AM,

7:35AM, 8:00AM, 8:10AM, 8:20AM, 8:35AM, 9:00AM and 9:35AM) in which three to five minutes of the video data were analyzed. Congested and uncongested conditions were represented in this data set. A total number of 4,287 vehicles were re-identified between stations.

## 2.4 Model Selection and Development

### 2.4.1 Selected Point-Based Models Implemented

For comparison of point-based freeway performance measures with section-based freeway performance measures, two point-based estimation methods that are implementable in real-time, were adopted in this study: the PeMS approach (3) and a Base model. For each of the measures, the data were aggregated over all lanes at each station for the detectors. Flow data were obtained from PeMS and aggregated into one-minute intervals. The other measures are described below.

#### 2.4.1.1 Speed

For speed estimation, PeMS applies a modified g-factor approach to report five minute aggregated speeds for all single loop detector locations (3) as shown in Equation (1). Speed is directly available from the PeMS database for five minute aggregation for the upstream and downstream detectors within the study site. The Base model speed is calculated as the average of the upstream and downstream point speeds as shown in Equation (2):

$$speed_{SC}(t) = \frac{flow_{SC}(t)}{occupancy_{SC}(t) \times g\ factor_{SC}(t)} \quad (1)$$

$$speed(t) = \frac{speed_{SC}(t) + speed_{LC}(t)}{2} \quad (2)$$

### 2.4.1.2 Travel Time

PeMS travel time was estimated by extrapolating the speed at the downstream detector over the length of the link, as in Equation (3). For the Base model, the travel time was calculated from the PeMS five-minute speed data at the Laguna Canyon (LC) and Sand Canyon (SC) stations by applying the instantaneous travel time model shown in Equation (4) (19).

$$travel\ time(t) = \frac{link\ length}{speed(t)} \quad (3)$$

$$travel\ time(t) = \frac{2 \times link\ length}{speed_{SC}(t) + speed_{LC}(t)} \quad (4)$$

### 2.4.1.3 Density

Density is not reported by PeMS, nor is there a method provided in the HCM for directly measuring density in the field. PeMS reports occupancy and suggests occupancy as a surrogate for density over a link by applying Equation (5). The Base model for density is calculated by Equation (6) (50) where  $L_v$  is the average vehicle length, 15.46 ft (3), and  $L_D$  is the length of the detector, 6 ft. The average vehicle length is the daily average from PeMS vehicle length estimates for Tuesday at the SC station.

$$density = (occupancy) \times (g\ factor) \quad (5)$$

$$density = \frac{52.8}{L_v + L_D} \times (\%occupancy) \quad (6)$$

## 2.4.2 Development of Section-Based Models

As mentioned in section 2.2, a vehicle reidentification approach based on inductive loops (REID) is used in this study (8). All of the measures are aggregated results at

one-minute intervals. The flow is obtained from calculation of the number of vehicle signature profiles at each time interval, and the calculations of the other measures from the REID data are described below.

#### 2.4.2.1 Travel Time

The travel times of each matched vehicle are obtained directly from the REID data. Travel time is calculated as in Equation (7).

$$\begin{aligned} \text{travel time}_{SC-LC}(t) &= (\text{arrival time}_{SC}) - (\text{arrival time}_{LC}) \\ \text{where } LC &\text{ is the upstream station of Laguna Canyon and} \\ SC &\text{ is the downstream station of Sand Canyon} \end{aligned} \quad (7)$$

#### 2.4.2.2 Speed

The section speed is calculated from the section travel time generated from the REID algorithm as seen below in Equation (8). This speed calculation does not rely on an estimation of the g-factor, but only the travel times of the matched vehicles in the REID algorithm. Hence, the estimated section speed is a space-mean-speed measure.

$$\text{speed}_{SC-LC}(t) = \frac{\text{link length}_{SC-LC}}{\text{travel time}_{SC-LC}(t)} \quad (8)$$

#### 2.4.2.3 Density

For this study, density is calculated by counting the number of vehicles present on the link during a specified time interval. For the specified time interval, if the travel time of a vehicle is greater than the length of the time interval, the vehicle is considered to be present on the link and thus contributes to the link density. For the REID data, a scaling factor is applied to account for the vehicles that are present but not matched. This factor is the percentage of the matched vehicles for each time interval, i.e. the number of total vehicles in the time period divided by the number of matched vehicles for the same time period. It should be noted that the density

estimation presented here is not explicitly real-time, but this measure could be improved with future research.

### **2.4.3 Development of Data and Performance Measures Ground Truth**

The data ground truth in this study was established from manual counts and visual observation of the video data. From the ground truth of matched vehicles, travel time and flow can be obtained. Performance measures from data ground truth are calculated in the same way as with REID data.

The summary of abovementioned measures based on different approaches is listed in Table 2-1:

Table 2-1 Summary of Point-Based, Section-Based, and Ground truth Performance Measure Models

Performance Measure	Point-Based Models		Section-Based Model	Ground truth Data
	PeMS	Base		
<b>Travel Time</b>	$travel\ time = \frac{link\ length}{speed}$	$travel\ time(t) = \frac{2 \times link\ length}{speed_{sc}(t) + speed_{lc}(t)}$	$travel\ time_{sc-lc}(t) = (arrival\ time_{sc}) - (arrival\ time_{lc})$ where <i>LC</i> is the upstream station of Laguna Canyon and <i>SC</i> is the downstream station of Sand Canyon	$travel\ time_{sc-lc}(t) = (arrival\ time_{sc}) - (arrival\ time_{lc})$ where <i>LC</i> is the upstream station of Laguna Canyon and <i>SC</i> is the downstream station of Sand Canyon
<b>Speed</b>	$speed^2 = \frac{flow}{occupancy \times g\ factor^1}$  1. Modified g-factor 2. Smoothed speed estimate	$speed(t) = \frac{speed_{sc}(t) + speed_{lc}(t)}{2}$  1. Average of upstream and downstream speeds	$speed_{sc-lc}(t) = \frac{link\ length_{sc-lc}}{travel\ time_{sc-lc}(t)}$  1. Provided by REID data	$speed_{sc-lc}(t) = \frac{link\ length_{sc-lc}}{travel\ time_{sc-lc}(t)}$  1. Provided by video data
<b>Flow</b>	1 minute aggregated flow rate	1 minute aggregated flow rate	1 minute aggregated flow rate	1 minute aggregated flow rate
<b>Density</b>	$density = (occupancy) \times (g\ factor)$	$density = \frac{52.8}{L_v + L_d} \times (\%occupancy)$	Estimated from travel time	Estimated from travel time

## 2.5 Comparisons of Point-based and Section-based Freeway Performance Measures

In this section, comparisons between each of the four performance measures (speed, travel time, flow, and density listed in Table 2-1) are presented and discussed. Figure 2-1 and Figure 2-2 show the PeMS, REID, Base, and ground truth (GT) data for each performance measure. The performances of the PeMS, REID, and Base models against GT datasets are summarized in Table 2-2 by the Mean Absolute Percentage Error (MAPE) shown in Equation (9). Figure 2-3 shows the correlation between the REID and ground truth data for travel time.

$$MAPE = \frac{1}{n} \sum_n \left| \frac{x_{MODEL} - x_{GT}}{x_{GT}} \right| \times 100\%$$

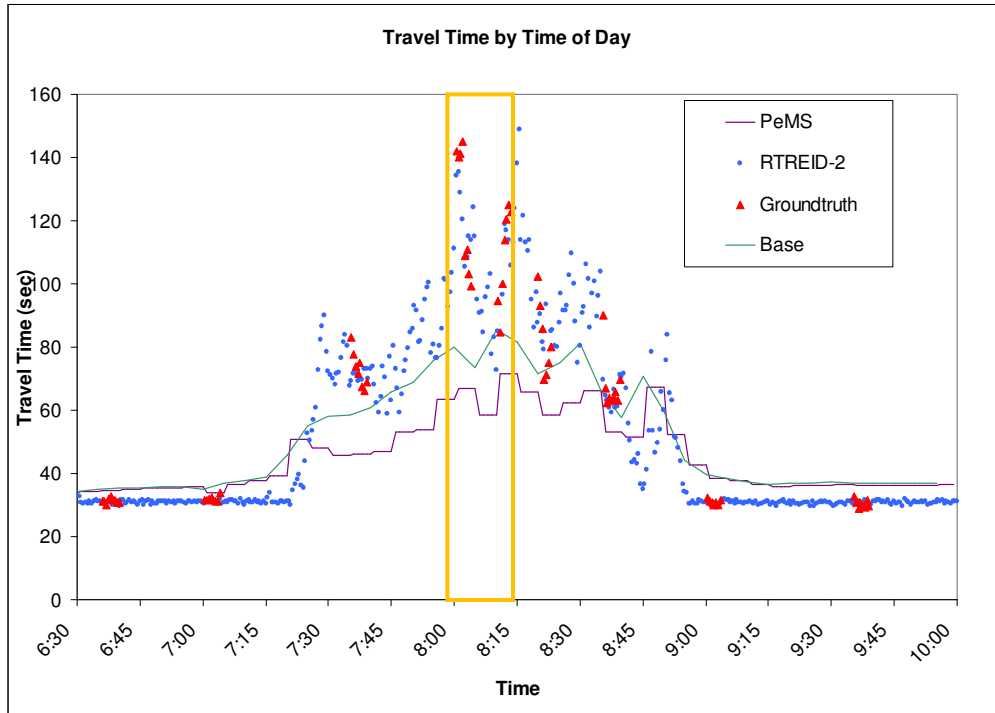
where

$x_{MODEL}$  is the performance measure of the model being compared (9)

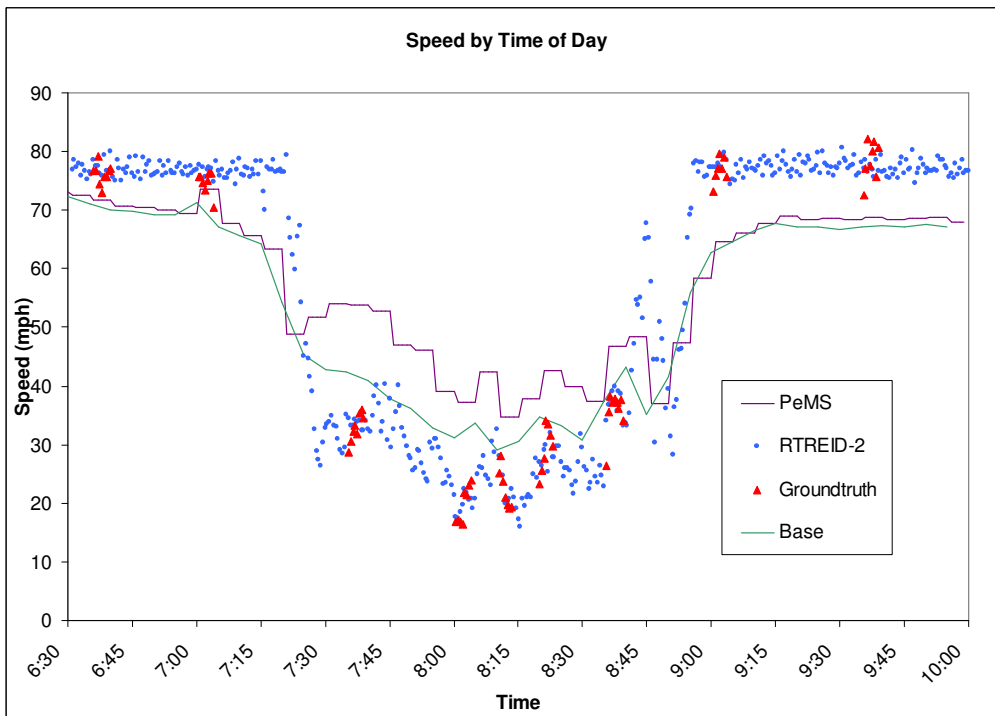
$x_{GT}$  is the performance measure of the groundtruthed data

$n$  is the number of samples in the data set

It can be seen in Figure 2-1(a) that there is a sharp peak in ground truth travel time at about 8:00AM. After this peak the ground truth travel time decreases significantly before increasing again at about 8:10AM. This observation is accurately captured by REID but not well captured by the PeMS and Base models. For the overall dataset, the REID data showed the lowest MAPE compared to the MAPEs and correlations of the PeMS and Base data. These results indicate the superiority of section-based REID performance measures in providing better estimates of real traffic conditions, especially during congested conditions.

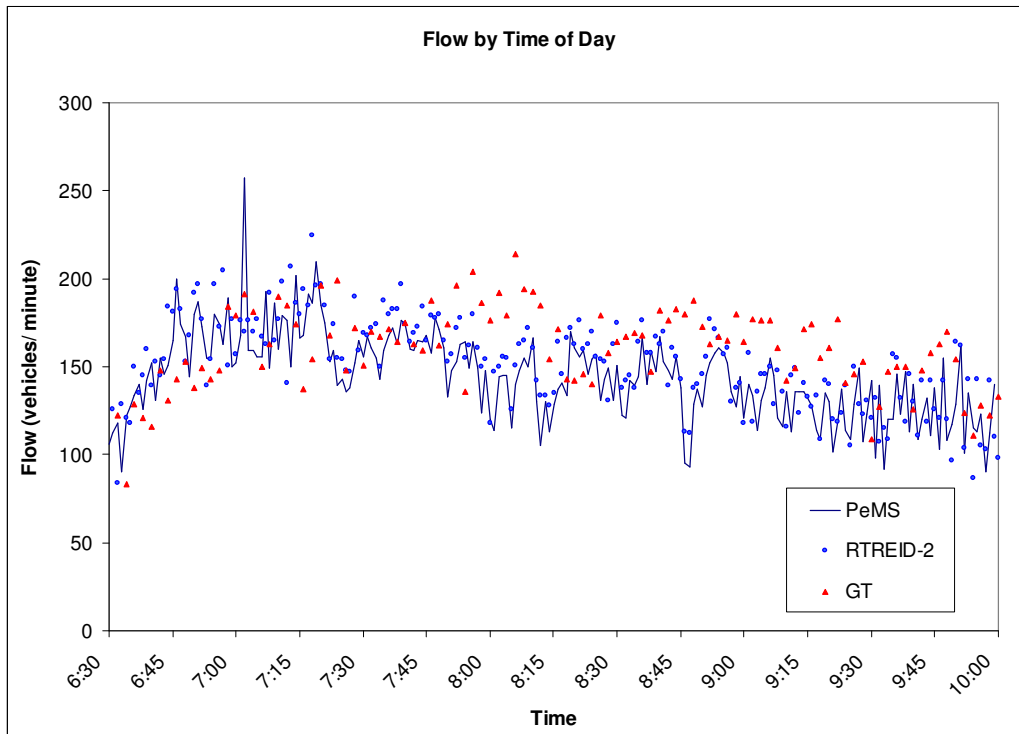


(a)

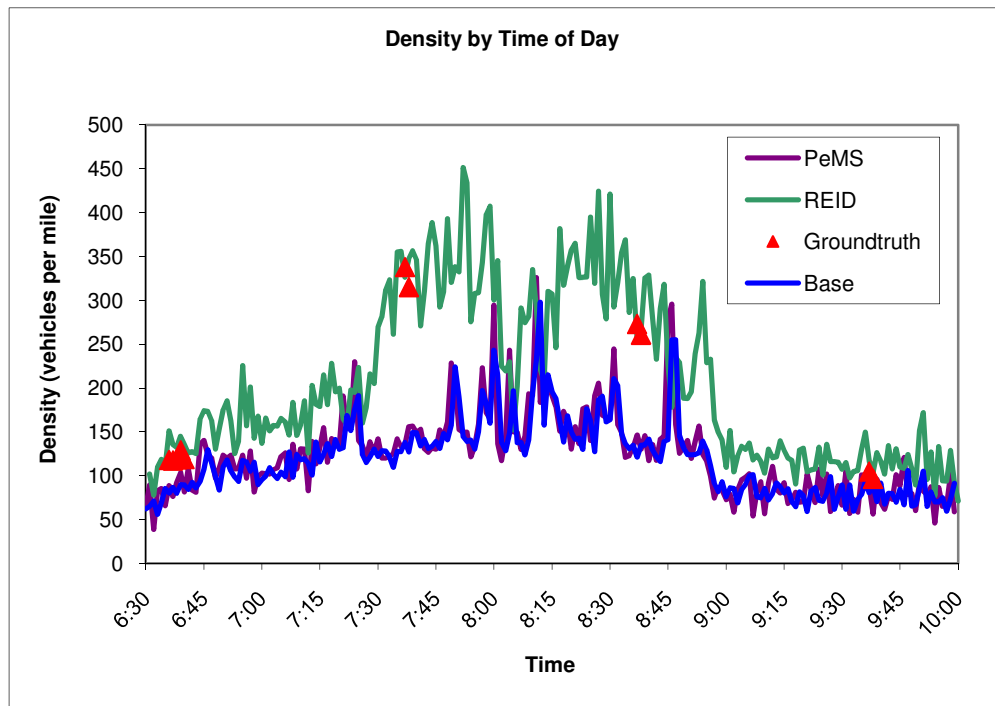


(b)

Figure 2-1 PeMS, REID, Base and ground truth travel time and speed measures



(a)



(b)

Figure 2-2 PeMS, REID, Base and ground truth flow and density measures

Table 2-2 Evaluations of Performance Measures by Selected Models

REID TT vs GT TT	ALL	6:36:00 AM	7:00:30 AM	7:35:30 AM	8:00:30 AM	8:10:30 AM	8:20:00 AM	8:35:30 AM	9:00:30 AM	9:35:30 AM
MAPE TT	5.26%	2.43%	2.46%	7.18%	8.36%	6.89%	10.16%	6.07%	2.87%	4.33%

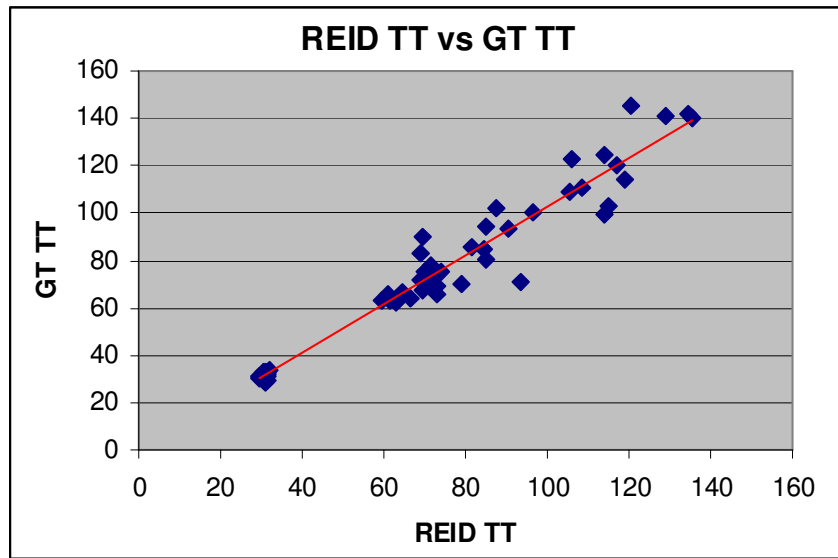


Figure 2-3 Correlation between REID and GT Travel Time Measures

## 2.6 Conclusions

The analysis performed in this chapter has demonstrated that section-based performance measures are more accurate than point-based measures. In general, the section-based REID performance measures can better estimate ground truth traffic conditions than the two point based models used in this study (the PeMS approach and the Base model), especially in congested conditions.

## **CHAPTER 3 ANALYSIS OF EMERGING TECHNOLOGIES**

### **3.1 Background**

While conventional inductive loop sensors perform sufficiently well to obtain good measurements of travel time information under varying traffic conditions, they may not be well suited for obtaining accurate origin-destination and route information due to occurrences of distorted vehicle signatures under stop-and-go situations. This serves as impetus for further investigation of alternative surveillance technologies which have the potential to address these challenges. The Blade™ inductive sensor and the Sensys™ wireless magnetometer technologies have been identified as two candidate traffic surveillance technologies for this study.

The preliminary study of the Blade™ inductive sensor technology performed in PATH Task Order 5304 found that Blade™ inductive sensors have the potential to address this problem, and may show greater suitability for implementation on arterial streets in the future as well. This is because Blade™ sensors span the entire width of each lane, thereby minimizing signature irregularities caused by off-centered vehicles. In addition, they have a much shorter sensor length in the direction of vehicle travel, and hence are able to obtain more detailed inductive vehicle signatures for additional potential to improve the performance of advanced traffic surveillance.

Sensys™ wireless magnetic sensors have recently emerged as potential candidates for advanced traffic surveillance systems. Implementation tests indicate that these sensors require less installation effort and time compared with conventional inductive loop sensors, as each sensor requires only a four-inch diameter core cut in the center of each lane. In addition, Sensys™ wireless magnetometers transmit data wirelessly to a roadside access point. This relieves the need for additional pavement cuts and roadside trenching for lead cable installation, which aids in reducing traffic performance and safety impact by minimizing road

closure times. Hence, they offer an attractive low-cost alternative to inductive loops for freeway traffic surveillance applications.

## **3.2 Overview of Technologies**

### **3.2.1 Blade Inductive Signatures**

The Blade™ is a new configuration of the loop sensor which can provide more detailed signature information than traditional round or square inductive loops. It combines the advantages of axle-based systems as well as inductive signature-based conventional loop sensors. In addition, its short traverse length addresses the integration issues found in conventional loop sensors and its full lane coverage ensures uniform sensitivity over the entire lane width of traffic. Figure 3-1 shows a comparison of signatures obtained via a conventional preformed round inductive loop sensor and a Blade™ inductive sensor obtained from a single tractor trailer. This modified configuration combines the ability of obtaining high fidelity inductance signatures of the vehicle undercarriage as well as axle configuration information, as shown in Figure 3-2. This fusion of information within a single sensor technology provides the potential for further improvement in vehicle classification and other advanced Intelligent Transportation Systems (ITS) applications.

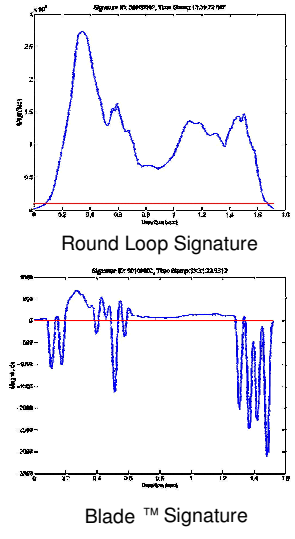


Figure 3-1 Comparison of Round and Blade™ Inductive Loop Sensor Signatures of a Tractor Pulling a Semi-Trailer

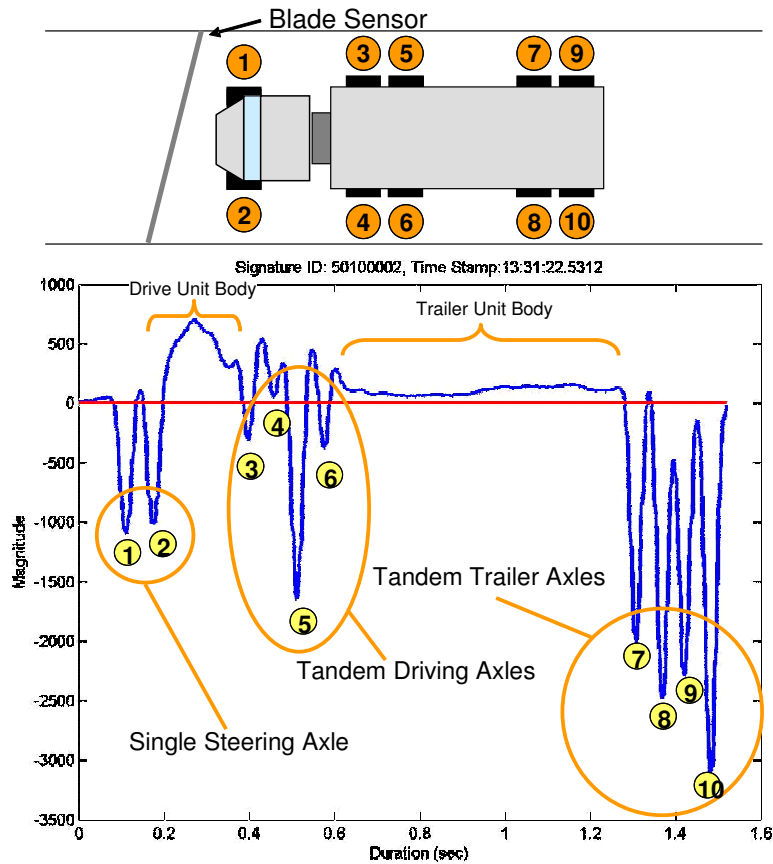
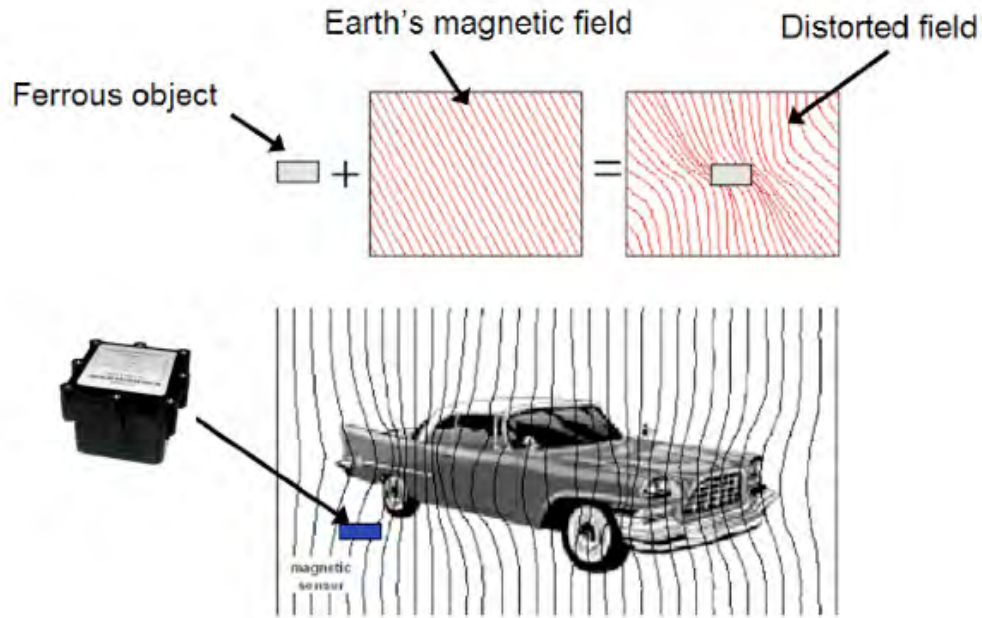


Figure 3-2 Characteristics of a Blade™ Inductive Signature

### 3.2.2 Sensys Wireless Magnetometers

The Sensys™ wireless magnetic sensor, or magnetometer, works by detecting the change in the Earth's magnetic field caused by the ferrous parts of a vehicle that passes over it (Figure 3-3). The wireless sensor generates data in three dimensions: x, y, and z. The x-axis, y-axis, and z-axis measure the change in magnetic flux in the direction of travel, perpendicular to the direction of travel, and perpendicular to the ground, respectively.



(Source: Cheung and Varaiya, 2007, Traffic Surveillance by Wireless Sensor Networks: Final Report, California PATH Research Report, UCB-ITS-PRR-2007-4)

Figure 3-3 Wireless magnetometers

Sensys™ sensors offer several advantages over conventional inductive loop sensors: With wireless technology, Sensys™ sensors do not require lead-in cables that would necessitate pavement cuts or roadside trenching. In addition, the sensors have a significantly smaller footprint compared with conventional inductive loop sensors. Because of these reasons, Sensys™ sensors are comparatively easier and quicker to install (see Figure 3-4) and maintain and have the potential to reduce traffic impacts due to shorter lane closure periods.

Sensys™ magnetometers are investigated in both conventional and signature modes in the following sections of this chapter.

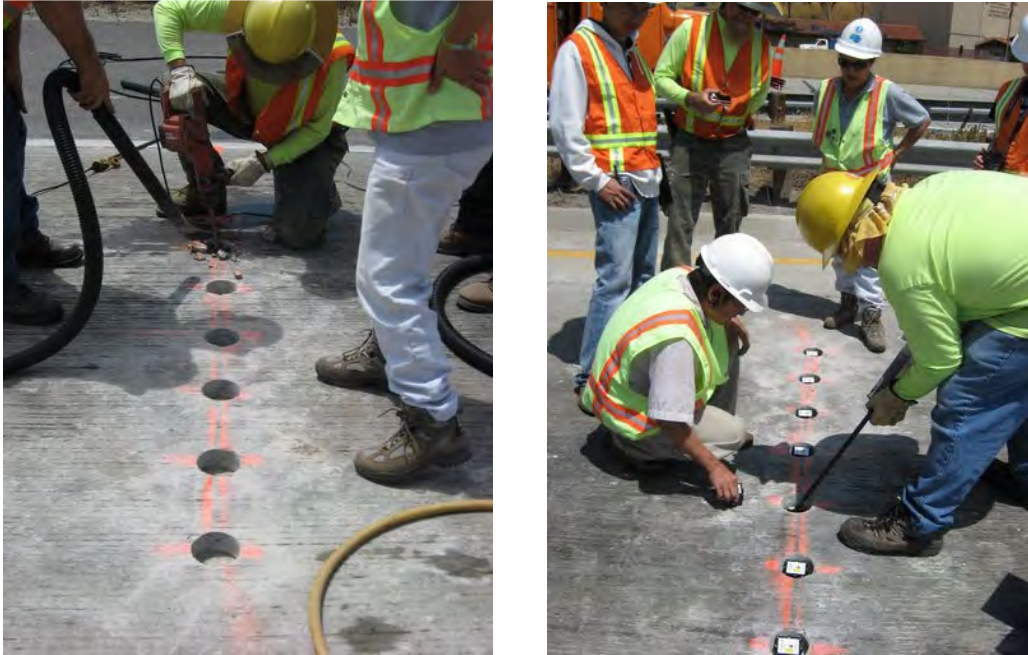


Figure 3-4 Installation of Sensys™ sensors

### 3.3 Blade™ Inductive Signatures

#### 3.3.1 Study Sites

Two study sites were instrumented to investigate the Blade™ inductive signature technology: the University of California, Irvine (UCI) Commercial Vehicle Study (CVS) Testbed and the UCI Detector Testbed. Both study sites are described in the following sections.

##### 3.3.1.1 UCI Commercial Vehicle Study Testbed

The UCI CVS Testbed is located at the California Highway Patrol (CHP) Southbound I-5 Truck Weigh and Inspection Station in San Onofre, between Los Angeles and San Diego as shown in Figure 3-5. I-5 is a major truck route in Southern California, and truck volumes at the site are high. The UCI CVS Testbed is an ideal site for investigating commercial vehicles due to the high volume and variety of commercial vehicles that enter the site daily. It has a single lane entrance ramp from the Southbound I-5, which expands into three lanes approaching the weighing scales followed by a single lane exit ramp back to the mainline freeway. Two locations at

the UCI CVS Testbed are available for detector deployments: the entrance ramp into the weigh and inspection station and the exit ramp. The distance between these stations is approximately 0.35 miles.

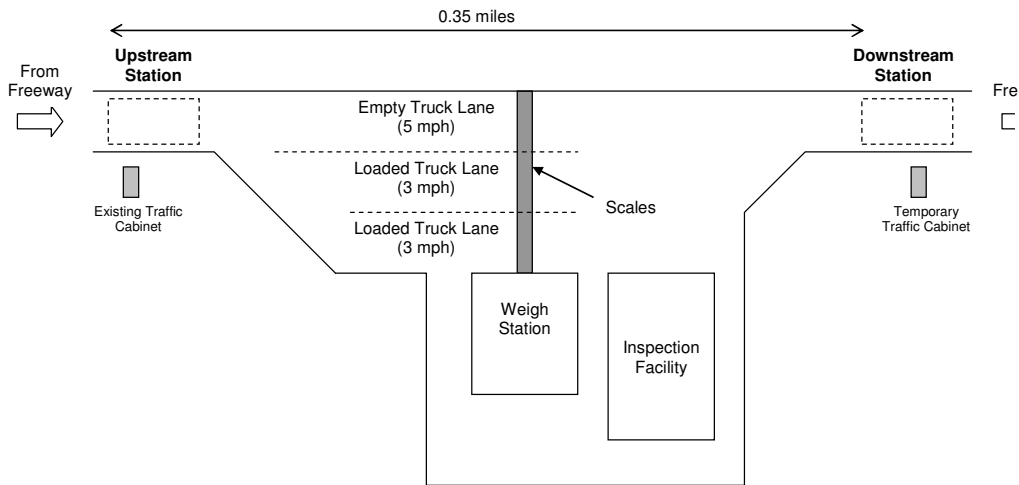


Figure 3-5 UCI Commercial Vehicle Study Testbed

### 3.3.1.2 UCI Detector Testbed

The UCI Detector Testbed is located within the UCI campus on westbound Bison Ave towards the SR-73 freeway as shown in Figure 3-6, upstream of the intersection with California Ave. Bison Ave serves as one of the main arterials for traffic entry and egress to the University and provides access to the nearest freeway – the SR-73. Hence, it is an ideal location for obtaining a large dataset with heterogeneous vehicle types.

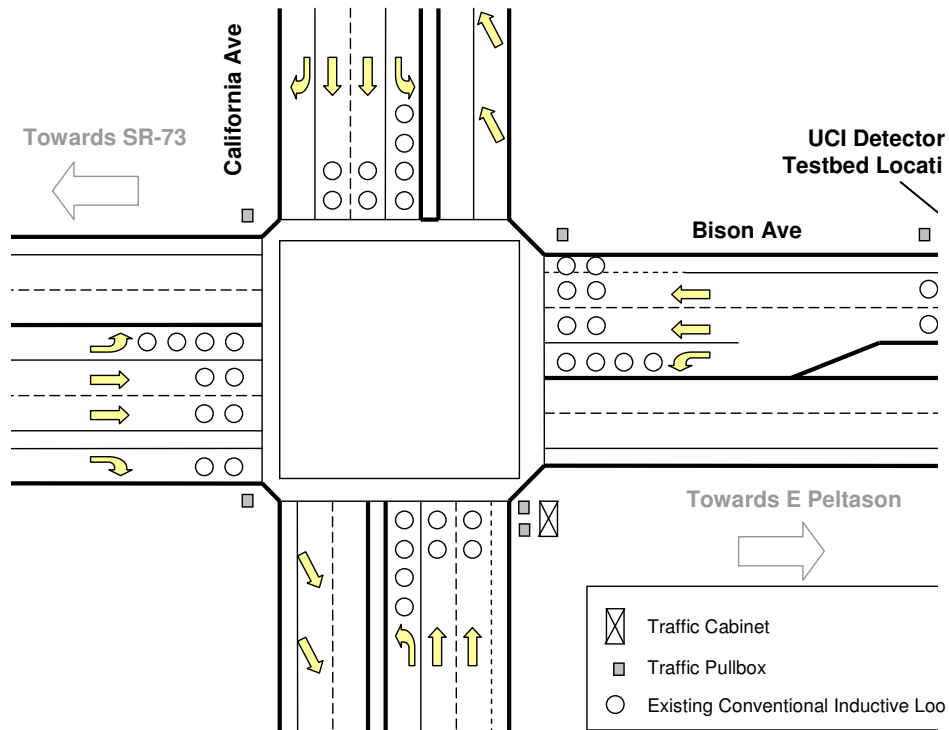


Figure 3-6 Location of UCI Detector Testbed

### 3.3.2 Configuration Analysis

This study involves investigating various Blade™ inductive sensor configurations for advanced surveillance applications as well as to develop the required technical specifications for this study. The purpose of this study is to determine ideal configurations and installation guidelines for the Blade™ inductive sensor applications.

#### 3.3.2.1 Previously investigated configurations

##### 3.5-inch Diagonal Surface Mounted Blades™ with 6 feet longitudinal spacing

The 3.5-inch diagonal surface mounted sensors with 6 feet longitudinal spacing configuration was investigated in May 2006 at the UCI CVS Testbed. This configuration was designed and fabricated by Inductive Signature Technologies Inc (IST), the manufacturer of the IST-222 advanced detector cards and possesses several advantages: The entire sensor loop can easily fit into a single strip of 4-inch Bithuthane tape. Also, due to its narrow profile, the sensor generates very distinct

wheel spikes in relation to the body signature as shown in Figure 3-7. In this figure the blue line represents the vehicle passing over the leading, or upstream, sensor, whereas the pink line represents the vehicle passing over the trailing, or downstream sensor. The two signatures should be relatively similar, with the downstream sensor displaced in time from the upstream signature.

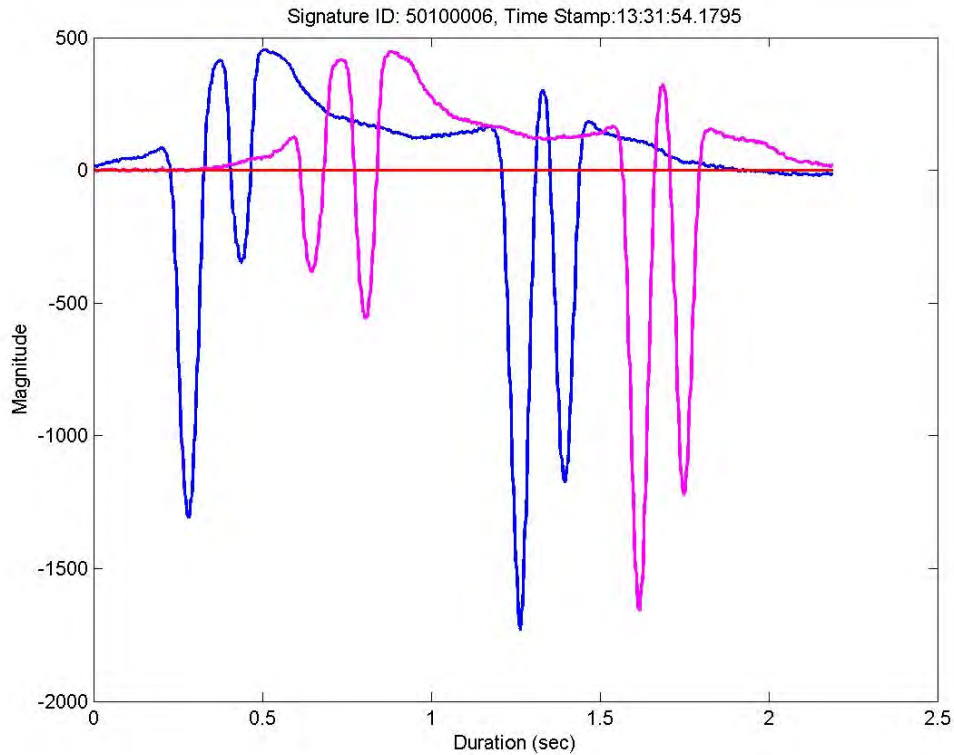


Figure 3-7 Example of inductive loop signatures from narrow double Blade inductive sensors showing wheel locations and body signature profile

The signatures obtained from this configuration have demonstrated excellent potential for commercial vehicle classification applications. The 6-foot longitudinal separation between the sensor pair seems adequate to address inductance interference issues. However, the separation is too large to detect the speed profile—changes in speed as a vehicle traverses the sensor—which is required for correcting acceleration-distorted signatures.

### 3.5-inch Diagonal Surface Mounted Blades™ with 1 foot longitudinal spacing

A subsequent investigation was performed in March and April, 2008, to investigate the potential to estimate speed profiles from Blade™ inductive sensors using a shorter longitudinal separation. In this study, 3.5-inch diagonal surface-mounted sensors with 1-foot longitudinal spacing configuration were installed at the UCI Detector Testbed. This close proximity between sensor pairs enabled the development of the Speed PRofile INterpolation Temporal-Spatial (SPRINTS) transformation model, which is used to correct signatures that have been distorted by acceleration and deceleration effects, such as those caused by stop-and-go traffic conditions. However, due to the closer spacing, occasional interference was detected in the inductance signal. Also, due to its narrow profile, high-profile vehicles tend to yield lower magnitude signatures from these sensors. There can be a potential concern for vehicle detection accuracy when the background noise is significant.

#### **3.3.2.2 Currently investigated configurations**

Two configurations have been investigated in this study: permanent in-pavement and temporary surface-mounted Blade™ sensors.

##### Permanent In-Pavement Blades™

The permanent in-pavement Blade™ sensor configurations were designed under the recommendations of IST. Three sets of permanent in-pavement Blade inductive sensors were installed at the UCI CVS Testbed on the entrance ramp into the weigh and inspection station as well as the exit ramp to the freeway as shown in Figure 3-8. The configurations vary by traversal length: 8 inches, 16 inches and 24 inches. Each configuration consists of Blade inductive sensor pairs abutting each other, with five turns of inductive loop wire in each sensor. The installation at the exit ramp to the freeway is shown in Figure 3-9.

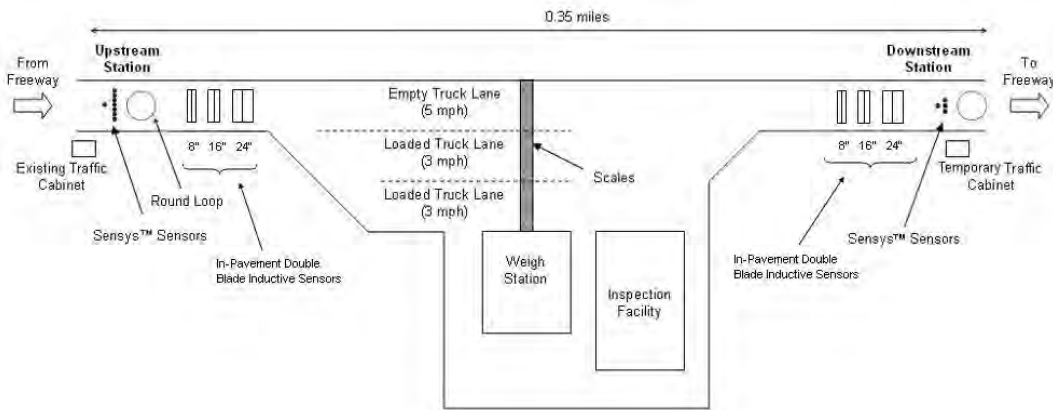


Figure 3-8 Southbound San Onofre Data Collection Study Site



Figure 3-9 Installation of Permanent Blade Sensors

Preliminary analysis results indicate the presence of significant cross-talk interference between inductive loop sensor pairs. This conclusion was determined from observations of Blade™ signatures obtained, which regularly exhibited either

significant differences in signature magnitudes between sensor pairs and inconsistent wheel spike features in the signatures as shown in Figure 3-10. The resolutions of these observed issues are pending further investigation by IST.

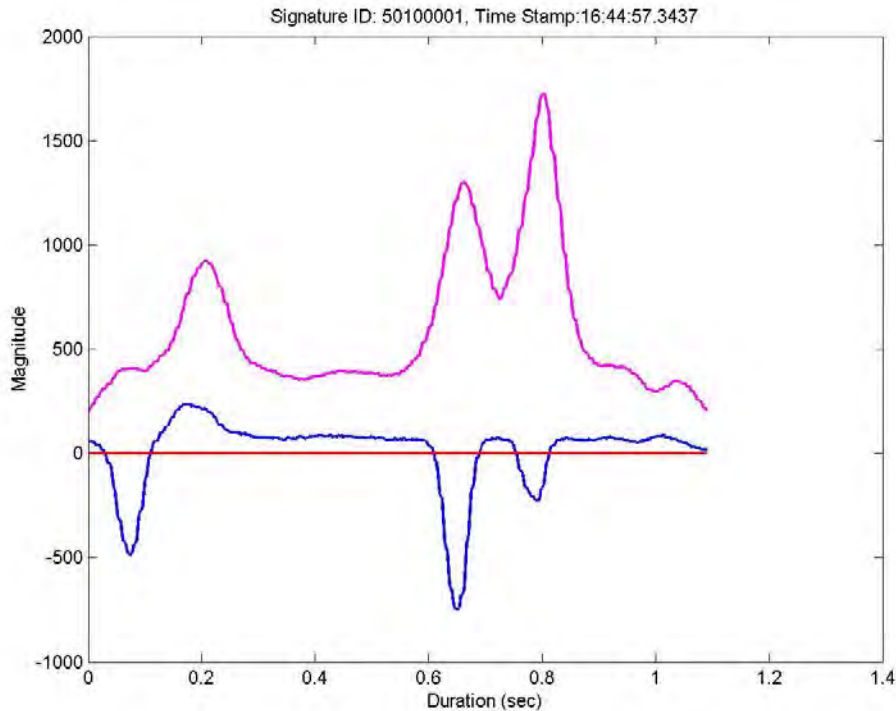


Figure 3-10 Sample of signatures from permanent double 8-inch Blade™ inductive sensors

#### 8-inch Surface-Mounted Blades with 2 feet spacing

A subsequent investigation was performed at the UCI Detector Testbed to determine the effect of increasing the longitudinal distance between the Blade™ inductive sensor pairs.

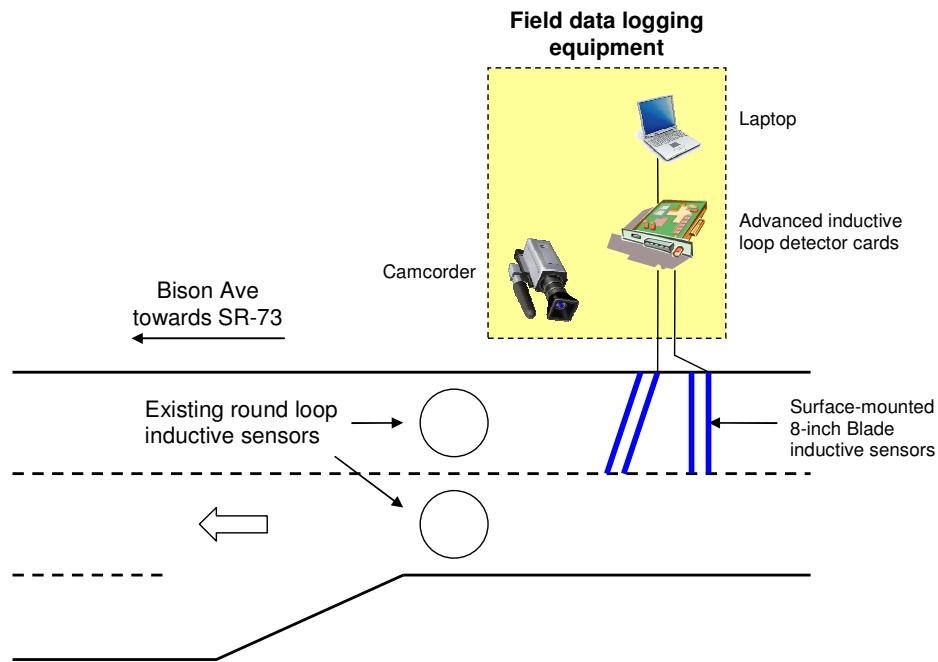


Figure 3-11 Study Site in University of California, Irvine at Bison Ave

Two sets of double Blade inductive sensors were installed on the rightmost lane: a pair of diagonal and a pair of perpendicular Blade™ inductive sensors. The diagonal pair of sensors was installed at 20 degrees from perpendicular to the direction of travel, similar to the orientation used in previous studies. All sets of Blade™ inductive sensors were fabricated with three turns of wire, which conforms to the Caltrans specifications for conventional inductive loop sensors. In addition, the sensors had a traversal length of 8 inches and spanned 12 feet, covering the entire lane width. Sensor pairs were spaced longitudinally at a distance of two feet between the leading edges. Figure 3-12 shows the installation of these sensors at the Bison Ave study site.

Advanced inductive loop detector cards were connected to a laptop for inductive signature data logging via the universal serial bus (USB) interface. Inductive signature data was collected in a continuous stream via proprietary software provided by Inductive Signature Technologies (IST) – the manufacturers of the advanced inductive loop detector cards. Video data was collected simultaneously

using a side-fire camcorder to provide ground truth of the vehicles traversing the Blade™ inductive sensors (as shown in Figure 3-11). The clocks of the laptop and camcorder were matched with a handheld GPS unit to ensure synchronization between the signature and video data.



Figure 3-12 Installation of 8-inch Surface Mounted Blade™ Inductive Sensors at Bison Ave Study Site at the University of California, Irvine

Figure 3-13 to Figure 3-15 show examples of vehicles with their corresponding Blade™ inductive signatures obtained from these installed sensors. Analysis of the signature data revealed that background noise is still occasionally present in these configurations. When background noise is observed, re-initializing the detector cards would occasionally resolve the noise issue.

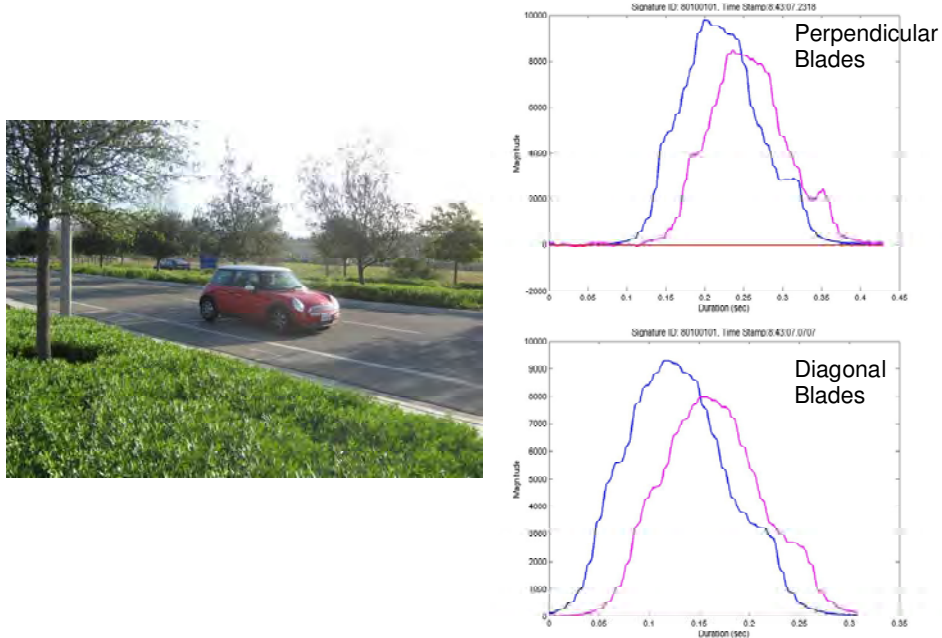


Figure 3-13 Sample Blade Inductive Signatures of Passenger Vehicle from Blade™ Inductive Sensors with 8 inch Longitudinal Spacing



Figure 3-14 Sample Blade Inductive Signatures of Single Unit Truck from Blade™ Inductive Sensors with 8 inch Longitudinal Spacing

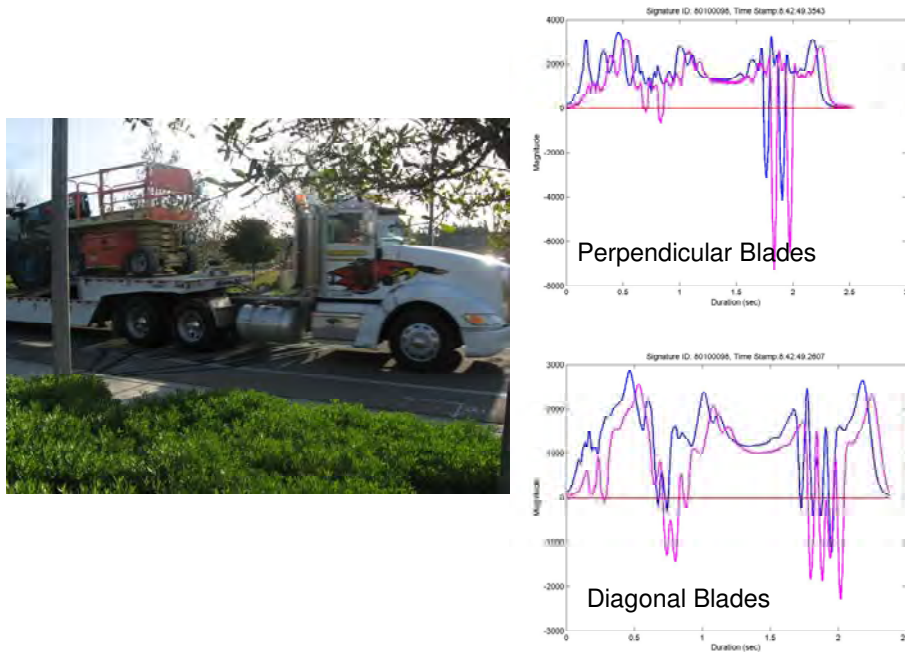


Figure 3-15 Sample Blade Inductive Signatures of Tractor with Single Low-boy Trailer from Blade™ Inductive Sensors with 8 inch Longitudinal Spacing

It was also observed that wheel spikes are absent from many passenger vehicle signatures. In addition, wheel spikes are sometimes inverted or missing from one or both signatures of large commercial vehicles, resulting in signature repeatability issues. These observed errors necessitate further investigation into more geometric configurations of Blade inductive sensors before a recommendation can be made for the specification of the permanent Blade™ inductive sensor configuration. The current recommended configurations are 8-inch Blades spaced longitudinally at 3 feet or 6-inch Blades spaced longitudinally at 2 feet.

### 3.4 Analysis of Sensys™ in Conventional Mode

This section describes the evaluation of the compatibility between traffic measures obtained from Inductive Loop Detectors (ILDs) and Sensys™ wireless magnetometers, and the potential of Sensys™ as a substitute for existing ILD's. Point-based estimation methods from the California freeway Performance

Measurement System (PeMS) and Sensys™ technology were examined for this study. Data was collected from the Detector Testbed on Northbound I-405 freeway at Sand Canyon Rd. Comparisons were made over five-minute aggregated volume and occupancy measures from the mainline sensors (as shown within orange box in Figure 3-16) to determine disparities between the two sensor technologies under various traffic conditions and time of day.

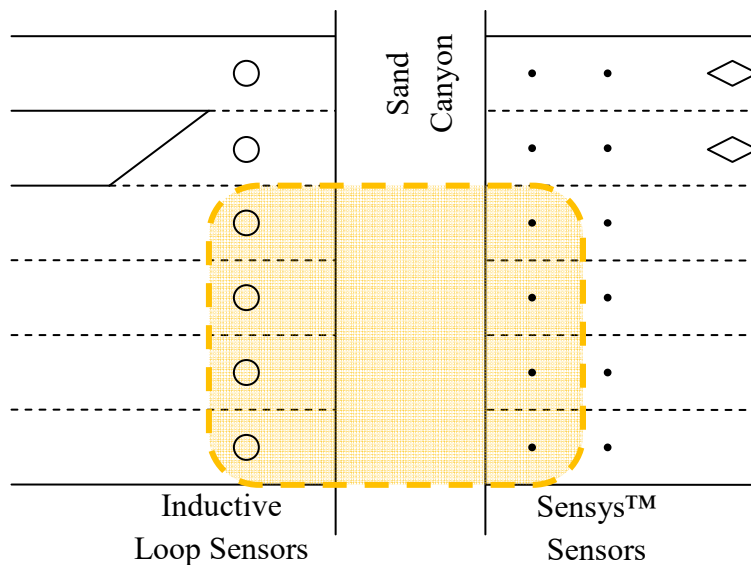


Figure 3-16 Layout of inductive loop and Sensys™ sensors used to obtain aggregate measures along NB I-405 freeway

### 3.4.1 Data Description

ILD data was obtained from PeMS, while Sensys™ data was manually collected via a field unit connected to the Sensys™ Access Point via Ethernet. Five-minute aggregated data was collected and analyzed for three consecutive days—from March 2nd through 4th, 2010. Both sensor technologies were evaluated in the single-sensor configuration mode, reflecting the configuration mostly used in the State of California.

### 3.4.2 Analysis of Results

This section describes the analysis of volume and occupancy results obtained from ILD and Sensys™. Scatter plot comparisons of paired ILD and Sensys™ volumes and occupancies for each observed five-minute time interval across the 72-hour duration of the data collection effort are shown in Figure 3-17 and Figure 3-18, respectively.

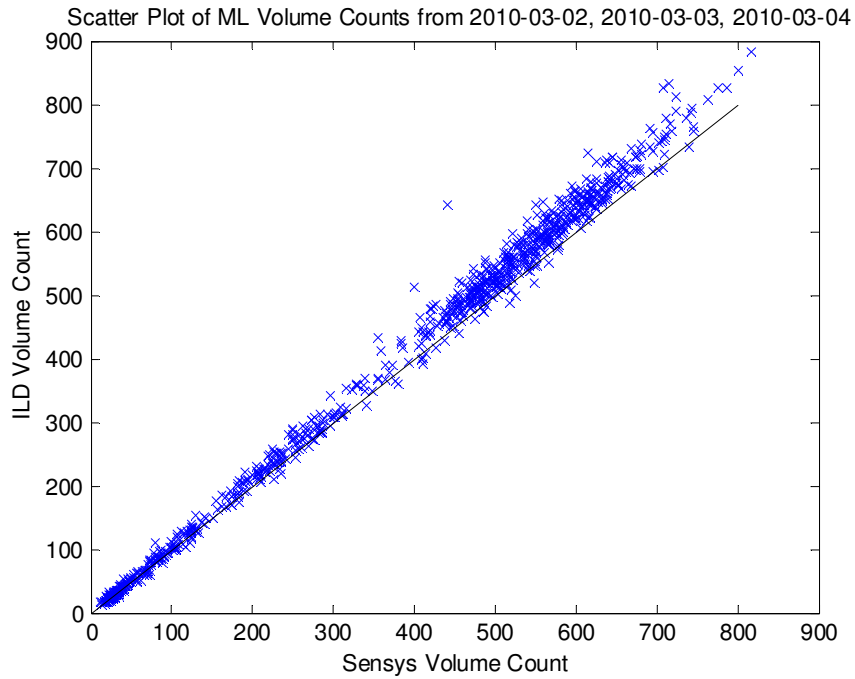


Figure 3-17 Scatter plot comparison of five-minute Volume measures between ILD and Sensys™ sensors

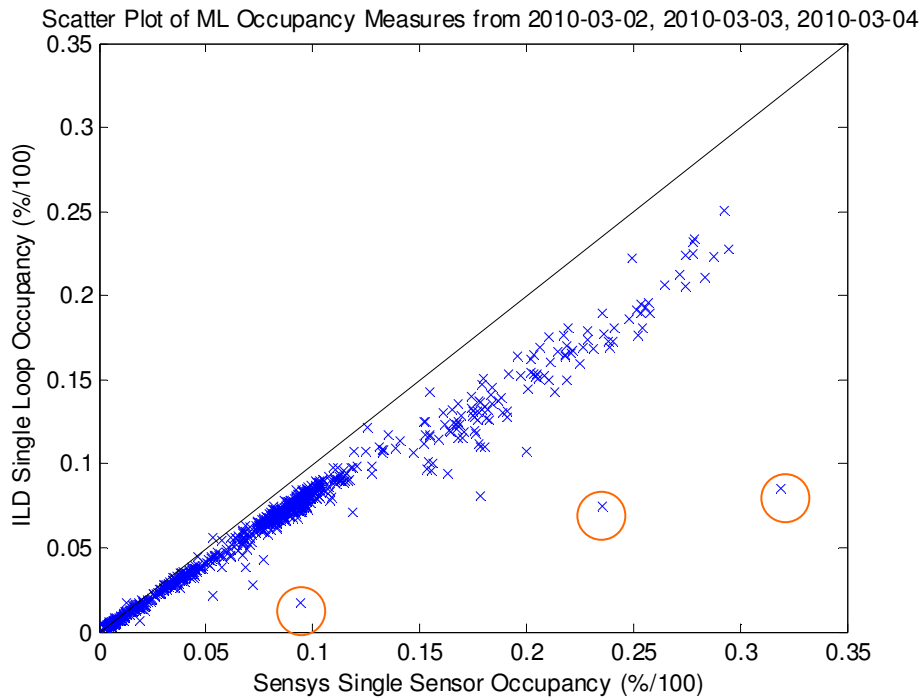


Figure 3-18 Scatter plot comparison of five-minute Occupancy measures between ILD and Sensys™ sensors

Figure 3-17 shows that there is generally good correlation between the ILD and Sensys™ volume measures. However, Sensys™ volume counts tend to be lower than ILD, and the errors are generally proportional with volume. The average error of five-minute aggregated volume counts from Sensys™ was 6.05 percent. The five-minute occupancy measurement errors from Sensys™ were found to be more significant compared with volume. The average error in occupancy measurements from Sensys™ was 25.87 percent.

Figure 3-18 shows that Sensys™ occupancy measures are systematically larger than corresponding ILD measures. In addition, some observations of occupancy spike measurements from Sensys™ where Sensys™ measures were much larger than ILDs (circled in Figure 3-18). Figure 3-19 shows the time-of-day plot of 5-minute occupancy measures from ILD and Sensys™. The black, blue and red lines show ILD occupancy measures, Sensys™ occupancy measures and measure differences, respectively. The observed Sensys™ occupancy spikes (indicated in

orange boxes in Figure 3-19) appear and disappear very abruptly in contrast to the corresponding ILD measurements, which do not exhibit any abrupt change. The causes of these spikes cannot be explained due to the aggregate nature of the analysis. However, a separate analysis<sup>1</sup> has highlighted the possibility of influence of large trucks from adjacent lanes, which is a possible explanation for these observations.

The systematic occupancies errors in Sensys™ could be addressed by applying a correction factor of 0.769 estimated via linear regression, which yields a corresponding coefficient of determination of 0.961. This implies that Sensys™ occupancy measures are highly correlated with measures from ILDs. However, the correction factor can only be reliably determined if there are ILDs in close proximity to installed Sensys™ sensors on the same facility. The correction factors obtained in this study may not be transferrable due to the sensitivity of Sensys™ measures to the earth's magnetic field, which may vary with location.

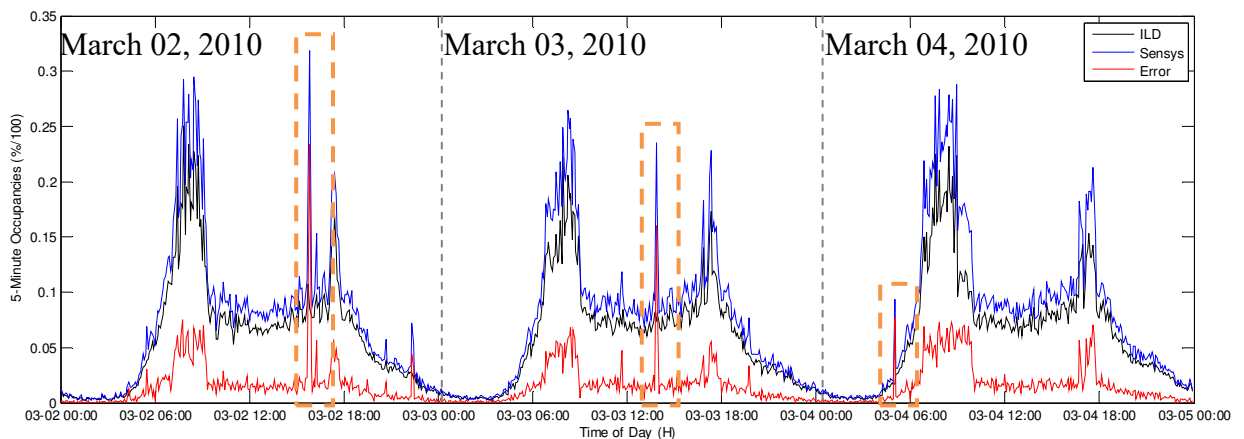


Figure 3-19 Time-of-day comparison of 5-minute occupancy measures between ILD and Sensys

<sup>1</sup> Palen, J. 2008. Sensys and Loop Detector Evaluation Report (not released to public), Caltrans DRI.

### **3.5 Analysis of Quality and Repeatability of Sensys™ Data in Signature Mode**

The investigations described in this section relate to the operations of Sensys™ magnetometers in signature mode. As a vehicle traverses each sensor, resulting magnetic flux changes are recorded at 128 samples per second to yield individual vehicle magnetic signatures.

Unlike in conventional modes of operation where only aggregated traffic measures are transmitted at predefined intervals, Sensys™ magnetometers send signatures of vehicles after each vehicle detection event, resulting in a significant increase in data transfer between the sensors and access point. However, signature data provides the possibility for advanced traffic surveillance applications such as vehicle re-identification, which will be investigated in this study.

Vehicle signatures generated from Sensys™ magnetometers are generally different from those acquired from traditional inductive loop detectors. Figure 3-20 shows two sample Sensys™ magnetometer signatures.

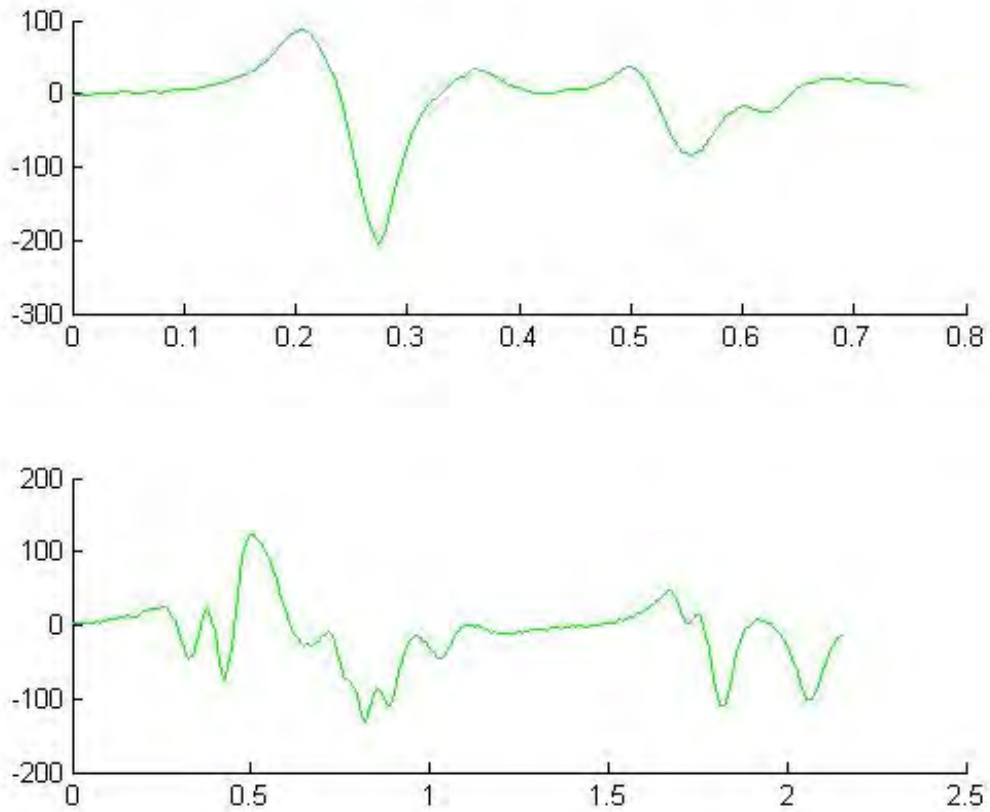


Figure 3-20 Example of Sensys™ magnetometer signatures

### 3.5.1 Study Sites and Data

Two locations were used in this study: the UCI CVS Testbed at the San Onofre Truck Weigh and Inspection Facility in San Onofre, California, and Detector Testbed on Northbound I-405 freeway in Irvine, California. The evaluation of Sensys™ magnetometer signatures involved seven independent data-collection efforts. A summary of these data collection exercises is shown in Table 3-1.

Table 3-1 Summary of Data Collection Exercises for Sensys™ Investigation

	Location, Date & Time Period	Purpose	Detector Stations	Post Mile	Sensor Config	Video
I	SB San Onofre Weigh Facility May 27 2008 – June 03 2008	Sensys Evaluation	Freeway Exit Ramp	-	Single Round ILD, Sensys Array	Yes
			Freeway Entrance Ramp	-	Single Round ILD, Sensys Array	Yes
II	NB I-405 in Irvine Dec 15 2008	Sensys Evaluation	Sand Canyon	2.99	Double Sensys Sensys AP @ 30'	No
III	NB I-405 in Irvine Jan 7 2009 – Jan 9 2009	Sensys Evaluation	Sand Canyon	2.99	Double Sensys Sensys AP @ 30'	No
IV	SB San Onofre Weigh Facility Feb 24 2009	Repositioning of Access Point Evaluation	Freeway Exit Ramp	-	Sensys Array Sensys AP @ 8'	No
V	SB San Onofre Weigh Facility Feb 26 2009	Repositioning of Access Point Evaluation	Freeway Exit Ramp	-	Sensys Array Sensys AP @ 6'	No
VI	NB I-405 in Irvine Apr 6 2009	Repositioning of Access Point Evaluation	Sand Canyon	2.99	Double Sensys Sensys AP @ 15'	No
VII	NB I-405 in Irvine May 12 2009	Sensys Evaluation Heterogeneous REID	Laguna Canyon	2.23	Double Square ILD	Yes
			Laguna Canyon 2	2.35	Single Round ILD	Yes
			Sand Canyon Off Ramp	2.99	Double Square ILD	Yes
			Sand Canyon	2.99	Double Square ILD Double Sensys Sensys AP @ 15'	Yes

### UCI CVS Testbed at the San Onofre Truck Weigh and Inspection Facility

A description of the UCI CVS Testbed is described in Section 3.3.1.1. For this study, each detector station is instrumented with single 6-foot conventional inductive round loop sensors together with an array of wireless magnetometers. The array of magnetometers at the upstream detector station consists of a leading sensor followed by a set of seven sensors spaced equally at 1 foot laterally across the lane and 6 feet downstream from the leading sensor. At the downstream detector station, a single leading sensor was installed with three sensors spaced equally at 1 foot laterally across the lane and 6 feet downstream from the leading sensor. Figure 3-21 shows the actual setup of the cabinet with a pole-mounted wireless access point and the array of seven sensors at the upstream station.

Communications with the wireless magnetometers is achieved via a wireless access point physically connected to the PC via a Cat-5 Ethernet cable. The wireless

magnetometers were configured to transmit signature data at 128 samples per second in 16 sample packets for each detected vehicle. All data was logged into the PC hard drive, to be later retrieved for analysis after data collection.



Figure 3-21 Wireless magnetometer setup at upstream station

#### Detector Testbed (Northbound I-405 Freeway in Irvine)

The Detector Testbed on Northbound I-405 freeway study site in Irvine consists of four detector stations spanning a distance of 0.63 miles in the northbound direction, as shown in Figure 3-22. The freeway corridor consists of between five and seven lanes, and one high occupancy lane (HOV). A buffer lane that separates the HOV lane from the other mainline lanes exists from the south end of the study site and extends to the Jeffery interchange, except for a stretch at the vicinity of the Sand Canyon interchange that allows entry into and exit from the HOV lane.

Each detector station consists of single square or double round conventional inductive loop sensors embedded in each lane of the freeway that are connected to advanced inductive loop detector cards located in the traffic cabinets adjacent to the freeway. The advanced inductive loop detector cards are connected to the field computer, an industrial PC running Windows 2000 operating system, via a USB

interface. These advanced inductive loop detector cards process inductance signals, induced by the vehicles passing over the loops, at 1200 samples per second, while a client program logs these in binary format to the PC hard drive. Each of the three PCs' clocks were set with a GPS clock prior to each data collection exercise so that they could be synchronized with the camcorder clocks, which were also set to the GPS clock.

In addition, the Sand Canyon detector station is equipped with double Sensys™ magnetometers in each lane, located in the center of each conventional square inductive loop sensor. Sensys™ sensor pairs corresponding to each lane are spaced 20 feet apart.

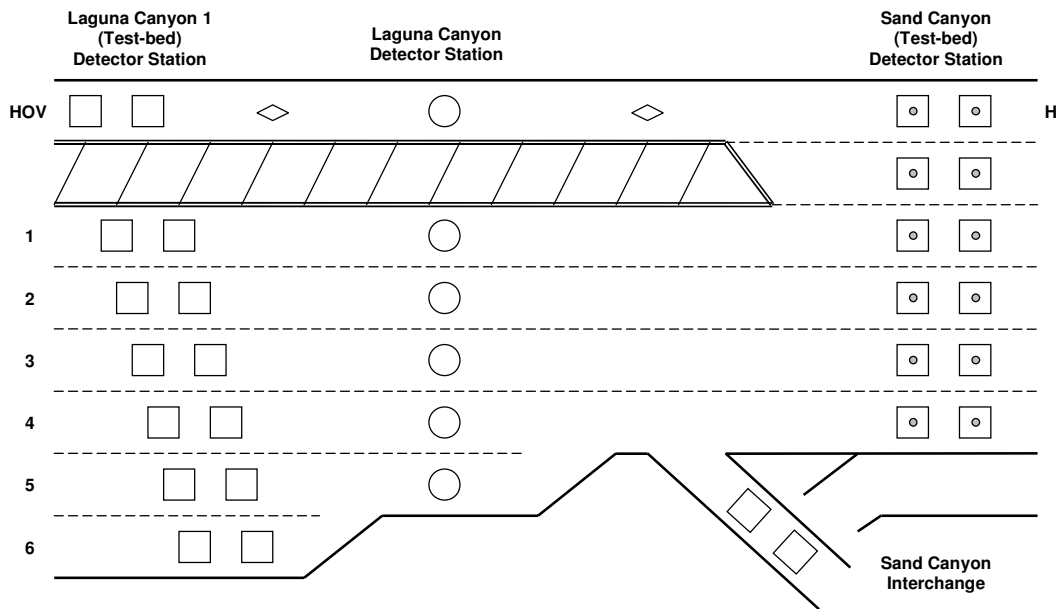


Figure 3-22 Detector stations with sensor layout in Detector Testbed along northbound I-405 freeway in Irvine, California.

### 3.5.2 Signature Mode Issues

Due to the larger data storage requirements for signature data compared with conventional data, the buffer memory equipped with each sensor is unable to provide

persistent storage of signature data in the event of dropped communications between the Sensys™ sensors and the Sensys™ Access Point. Hence, data packets from the Sensys™ sensors to Sensys™ Access Point are not re-transmitted in the occurrence of dropped data packet events when operating in signature mode. Consequently, these dropped communication events result in dropped data packets within affected vehicle signatures, which may cause significant loss of data associated with vehicle features. These data packet drops are observed as sustained stationary magnitude signals across all three axes of the Sensys™ signature. Figure 3-23 shows an example of a vehicle signature with dropped data packets. Hence, an initial investigation was performed to further evaluate the causes and potential solutions to minimize the observed dropped Sensys™ signature data packets.

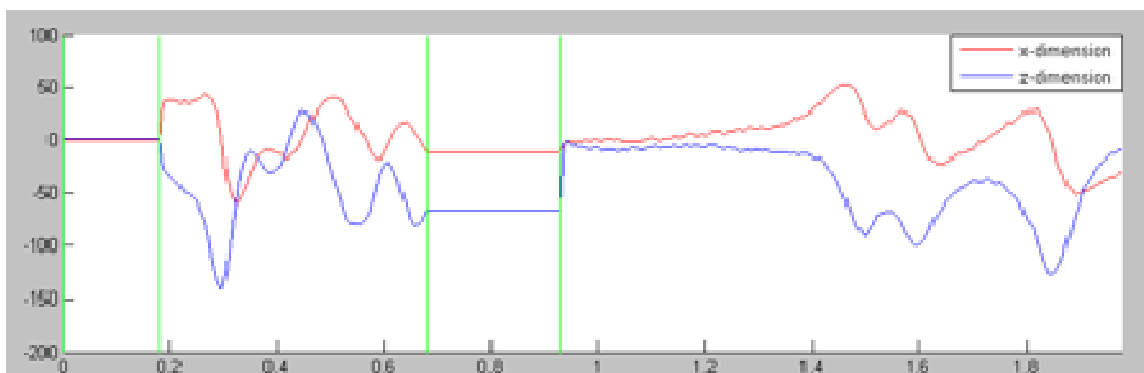


Figure 3-23 Example of a signature with dropped sections

### 3.5.3 Sensys™ Signature Quality Analysis

#### 3.5.3.1 Overview

A preliminary analysis of signature quality was first performed at the San Onofre Truck Weigh and Inspection facility. During this analysis phase, Sensys™ signatures were evaluated corresponding to Sensys™ Access Point elevations of approximately 15 feet down to 8 feet and 6 feet to determine if physical proximity of the Sensys™ Access Point to the sensors was a factor of concern.

Results indicated that data drops were not significantly improved by the relocating the Sensys™ Access Point. However, this investigation was performed on

a single lane adjacent to the Sensys™ Access Point. Hence, a more in-depth analysis was performed to further investigate the effect of the elevation of the Sensys™ Access Point on signature quality to assess the sensitivity of dropped packets with the Sensys™ Access Point elevation. This analysis was performed on data obtained from three separate data collection efforts on the I-405 study site, with the Sensys™ Access Point placed at approximate elevations of 30 feet and 15 feet.

A brief description of each data collection is shown in Table 3-2. The investigation would determine if the data drops are possibly caused by vehicles in adjacent lanes and by vehicles traversing over the traveled lane of the sensors, blocking the line of sight between the Sensys Access Point and the Sensys Magnetometer. Figure 3-24 compares the total volume of vehicles analyzed by lane for each data collection period

Table 3-2 Summary of Sensys Data Collections at the Sand Canyon Detector Testbed along the Northbound I-405 freeway to evaluate Access Point location

Dataset no.	Date	Time	AP Status
1	Jan 09, 2009	07:15 – 08:15 (1 hour)	Original height ~ 30'
2	Apr 28, 2009	15:30 - 19:30 (4 hours)	Lowered to ~15'
3	May 12, 2009	06:30 - 11:00 (4.5 hours)	Lowered to ~15'

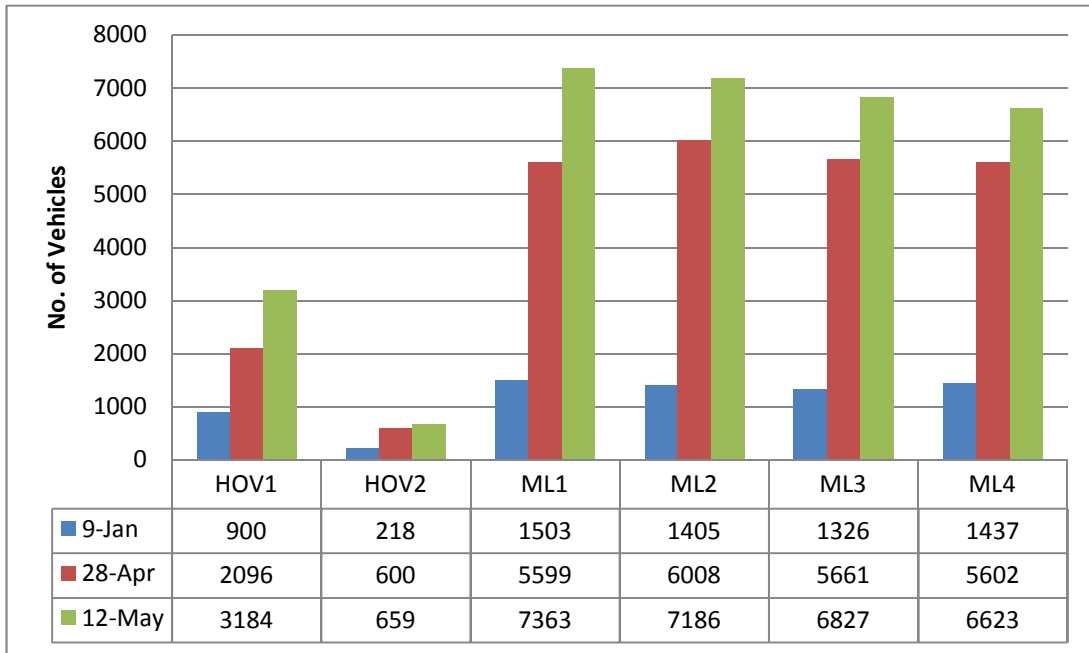


Figure 3-24 Total number of vehicles by lane across datasets

Figure 3-25 shows the percentage of Sensys vehicle signatures with no detected data drop by lane and compared across datasets. It can be observed that the results for HOV lanes across all datasets were similar. However, data quality across datasets for the main line lanes had some observable differences: Dataset 2 consistently performed best while dataset 1 performed worst. Due to the variability in traffic conditions across datasets this preliminary result was not considered conclusive. Hence, subsequent evaluations were performed analysing the signature quality by duration characteristics and across lanes to further investigate the cause of the signature data drops. These results are presented in the following sections.

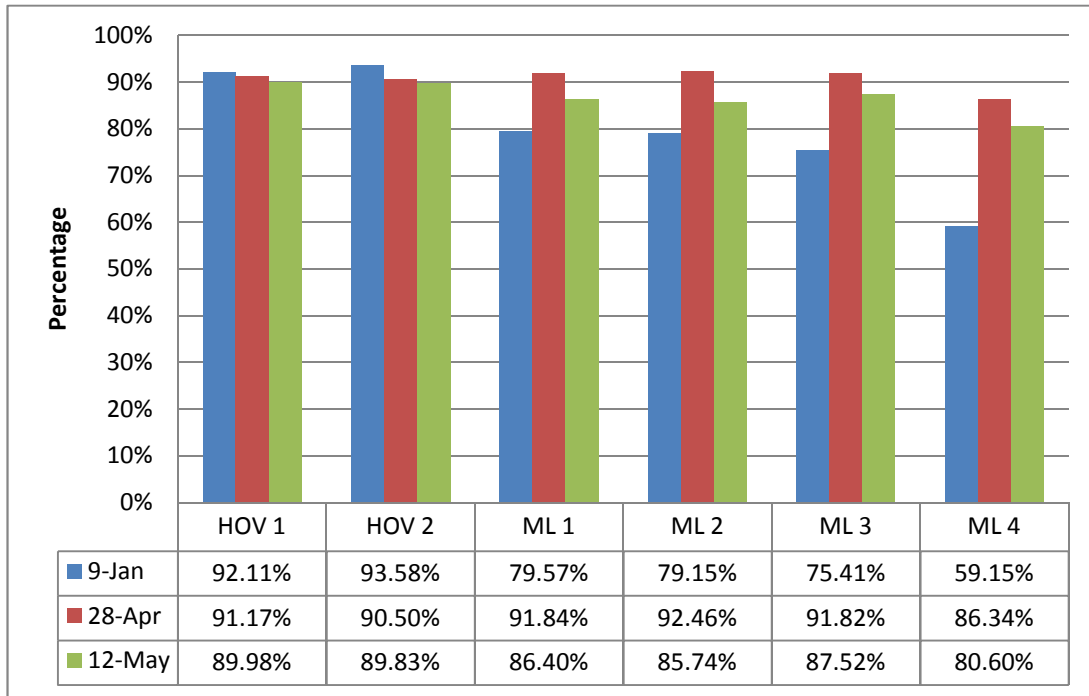


Figure 3-25 Percentage of no-drop signatures by lane across datasets

### 3.5.3.2 Sensys™ Data Quality Analysis across Datasets by Lane

Following the preliminary analysis identifying overall rates of signature data packet drops by lane and across datasets, a more rigorous analysis was performed by investigating the relationship of data packet loss by the duration of individual signatures recorded. Figure 3-26 to Figure 3-31 presents this data quality analysis results for each lane.

#### Duration distribution

The statistical mode, i.e. the most frequently occurring value, of durations is 0.3 sec across all lanes for all datasets. It can be inferred that dataset 2 experienced the lowest congestion indicated by a lower proportion of high duration signatures.

#### Signature data packet drops

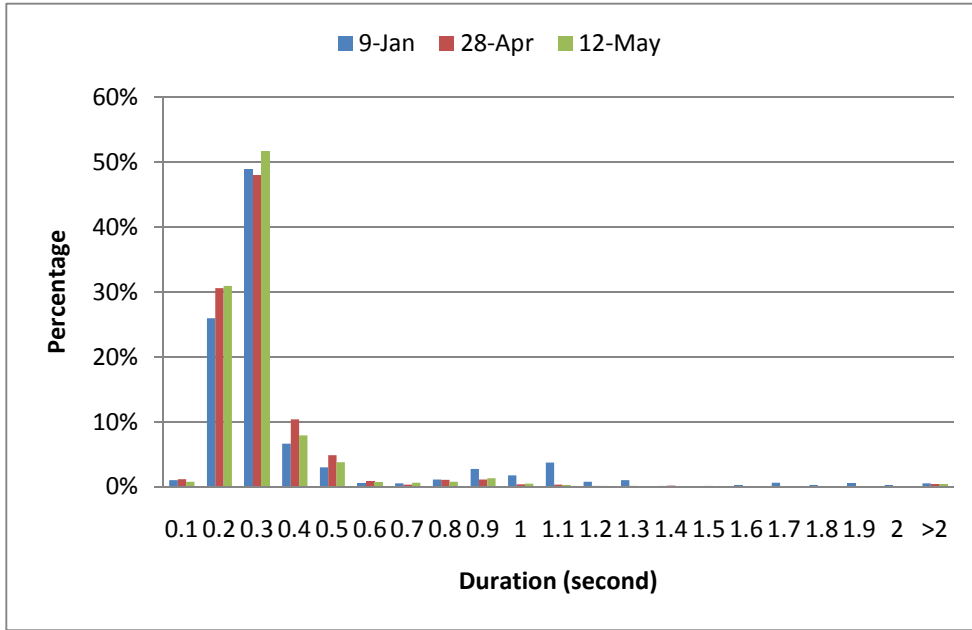
There is an observable inverse relationship trend between signature quality (percentage of signatures) and signature duration. The local instability at higher duration intervals (greater than 1.0 sec) is attributed to low observed sample sizes at

these duration intervals. Also, the results indicate that signatures with less than 0.3 seconds duration experience a low rate of packet drops.

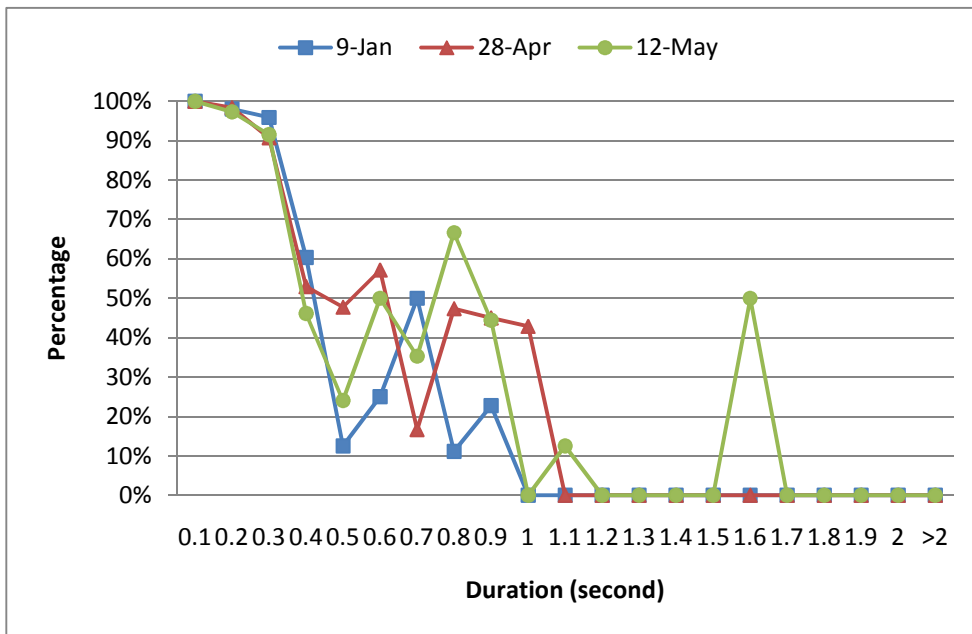
Dataset 2 experienced the lowest rate of signature data packet loss overall, and features the Sensys™ Access Point at the lower position. Dropped signature packets were most significant for dataset 1 as a whole, but this observation is at least partly attributed to dataset 1 being the most congested.

The figures also indicate that lowering the Sensys™ Access Point may provide marginal improvement for the two right-most lanes for duration ranges between 0.6 and 1.0 seconds as shown in Figure 3-30 and Figure 3-31. No significant difference is observable in the other lanes.

This duration analysis by lane indicates that signature quality may be more significantly affected by the time a vehicle spends over the sensor (duration), which correlates with poorer performance in congested periods than the Sensys™ Access Point location. This implies that the signature data packet loss is more likely influenced by the communications operations limitations between the Sensys™ Magnetics Sensors and Access Point than due to external physical influences.

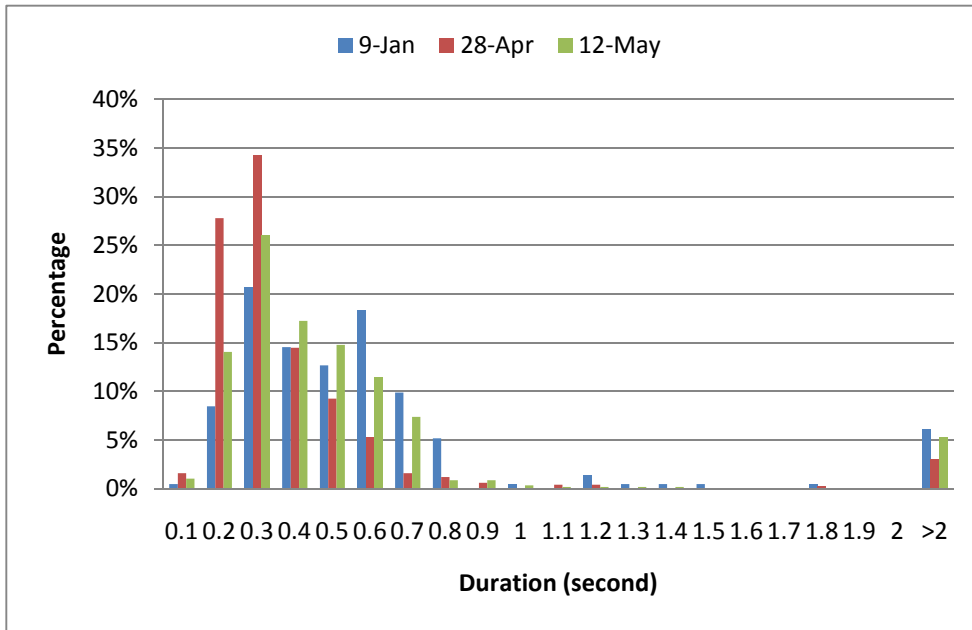


(a) Signature distribution by duration

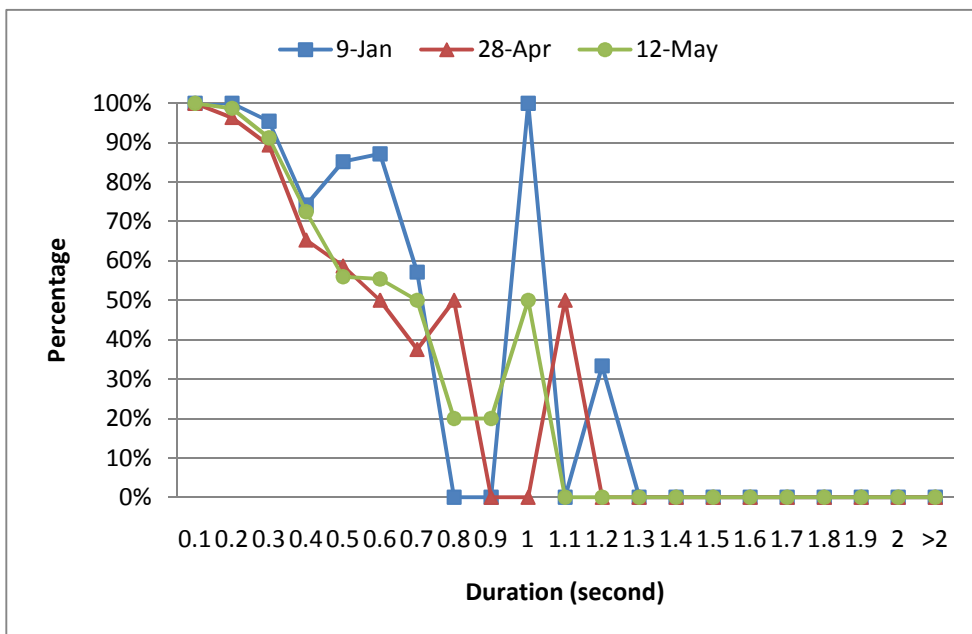


(b) Percentage of signatures with no data packet loss by duration

Figure 3-26 Data quality analysis for HOV Lane 1

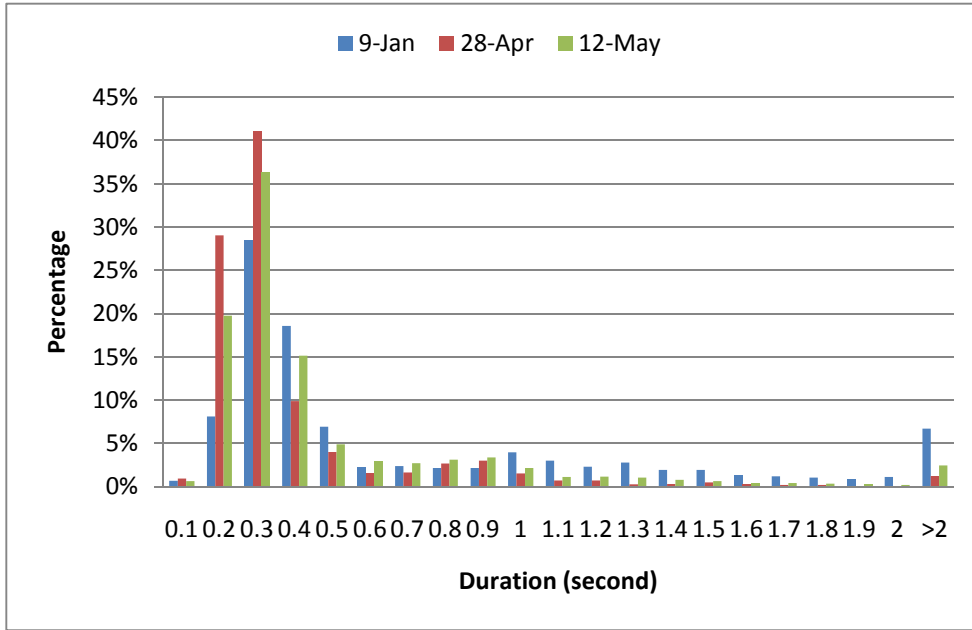


(a) Signature distribution by duration

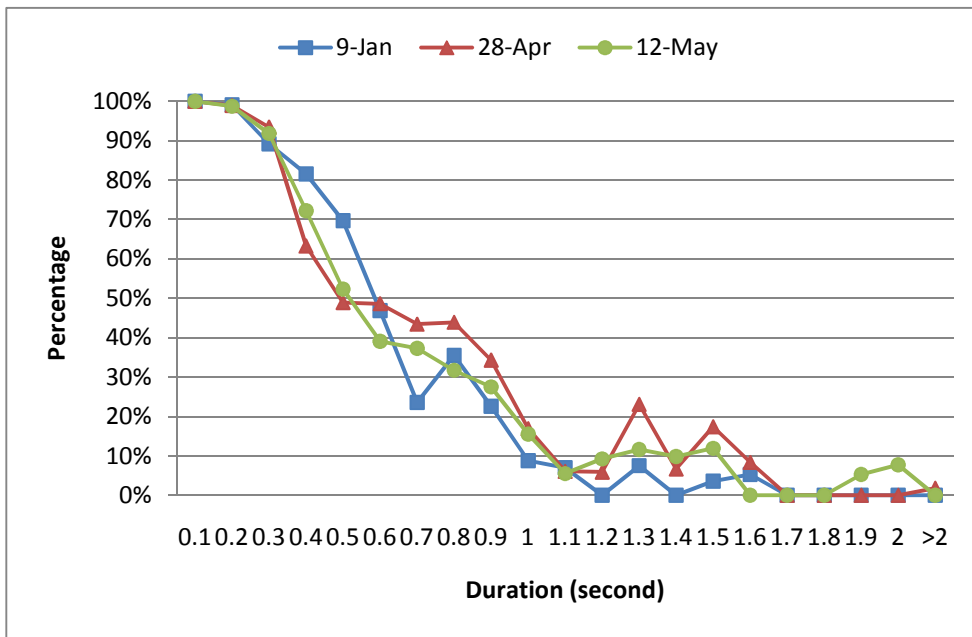


(b) Percentage of signatures with no data packet loss by duration

Figure 3-27 Data quality analysis for HOV Lane 2

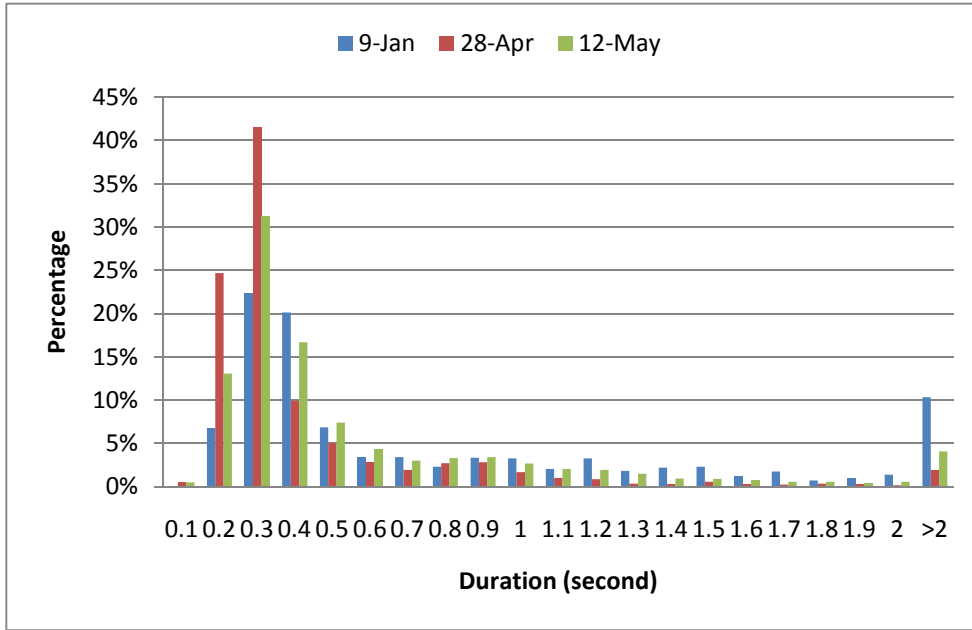


(a) Signature distribution by duration

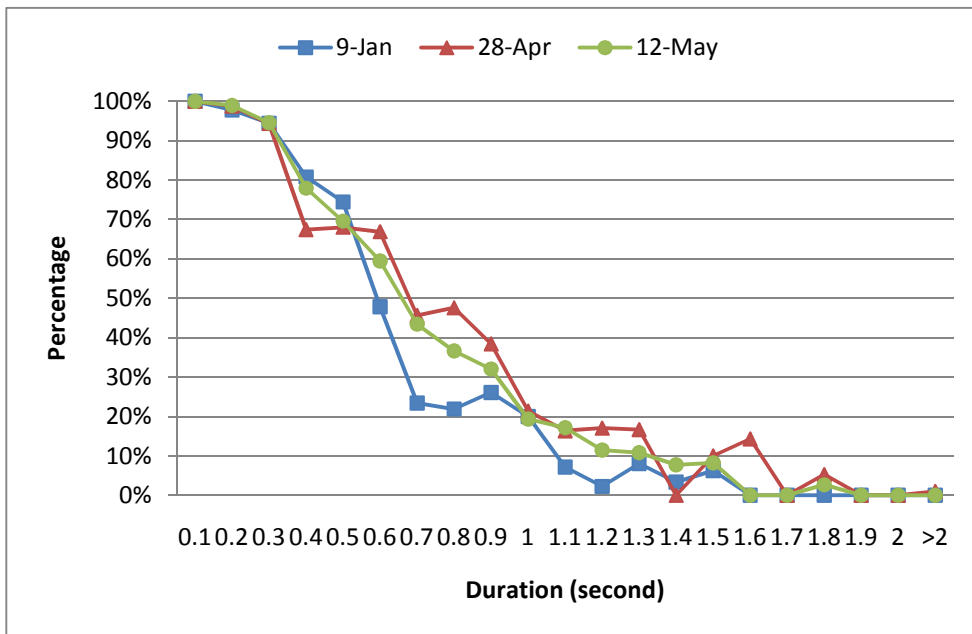


(b) Percentage of signatures with no data packet loss by duration

Figure 3-28 Data quality analysis for Mainline Lane 1

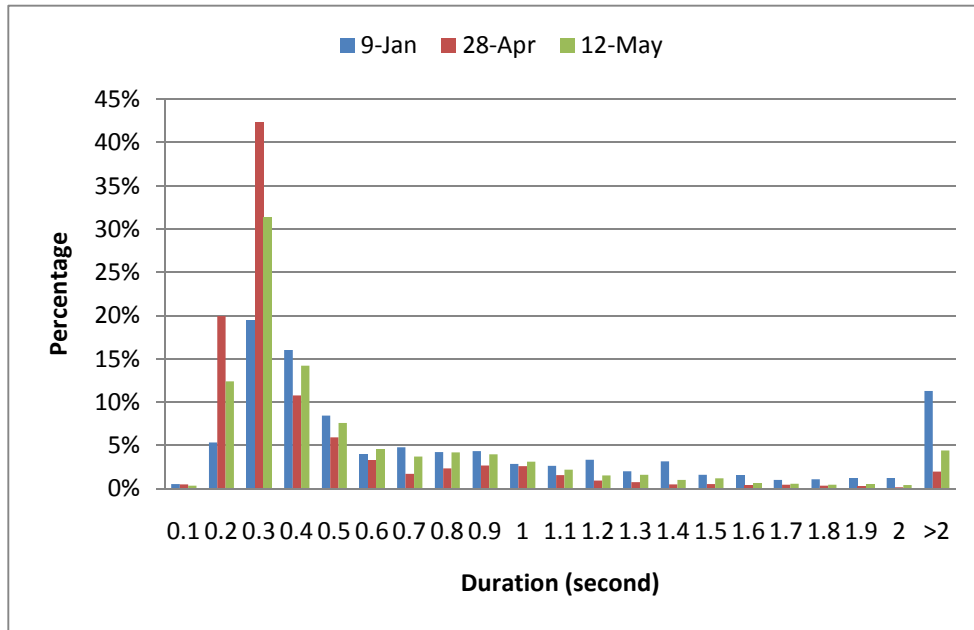


(a) Signature distribution by duration

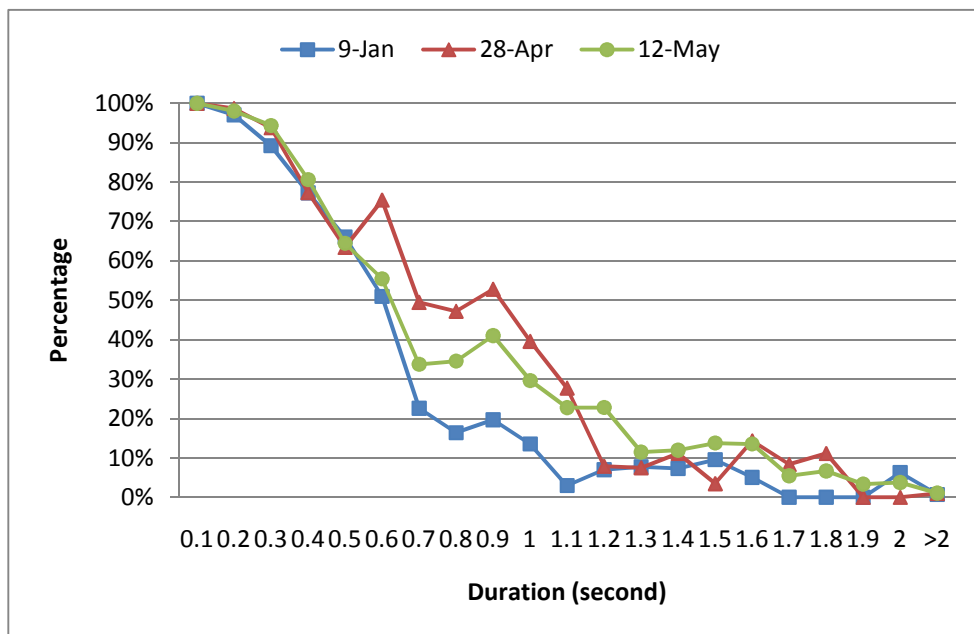


(b) Percentage of signatures with no data packet loss by duration

Figure 3-29 Data quality analysis for Mainline Lane 2

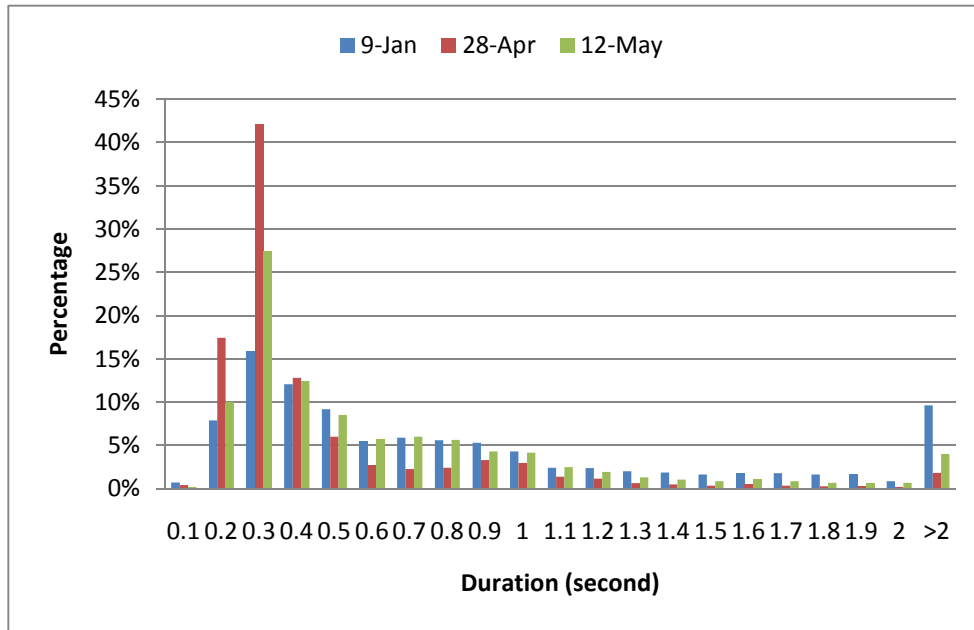


(a) Signature distribution by duration

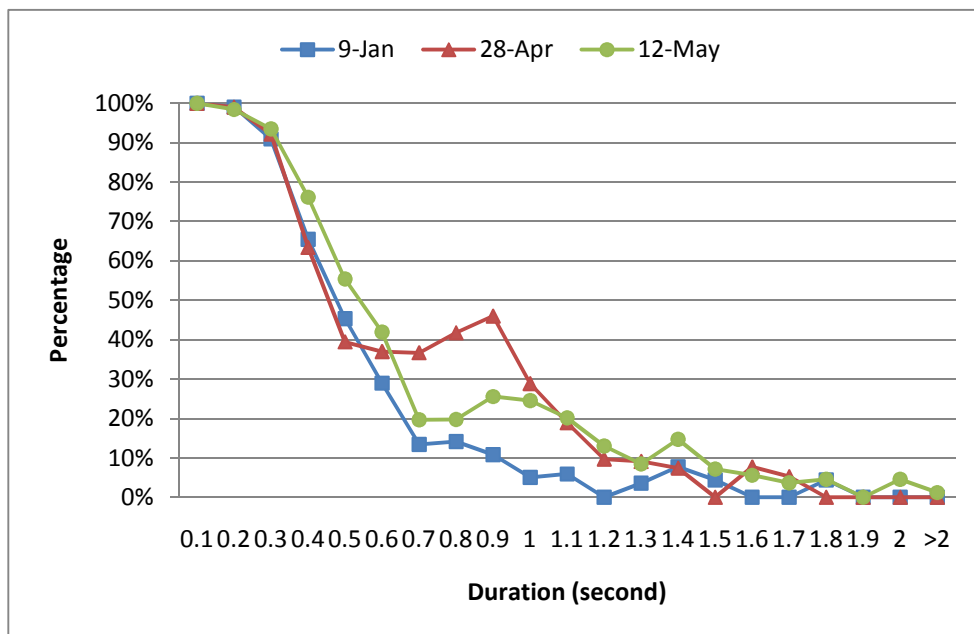


(b) Percentage of signatures with no data packet loss by duration

Figure 3-30 Data quality analysis for Mainline Lane 3



(a) Signature distribution by duration



(b) Percentage of signatures with no data packet loss by duration

Figure 3-31 Data quality analysis for Mainline Lane 4

### 3.5.3.3 Sensys™ Data Quality Analysis across Lanes by Dataset

Following the duration analysis of signature packet loss of Sensys signatures by dataset, a further analysis was performed to investigate the variability of data packet loss across lanes within each dataset. Figure 3-32 to Figure 3-34 show plots representing the percentage of signature data packet loss occurrences with signature duration across lanes for each dataset, respectively. The results show that the trends of signature data packet loss with signature duration are similar across all lanes. This indicates that the signature data packet loss due to the location of the Sensys™ Access Point from the Sensys™ sensors are likely to be negligible.

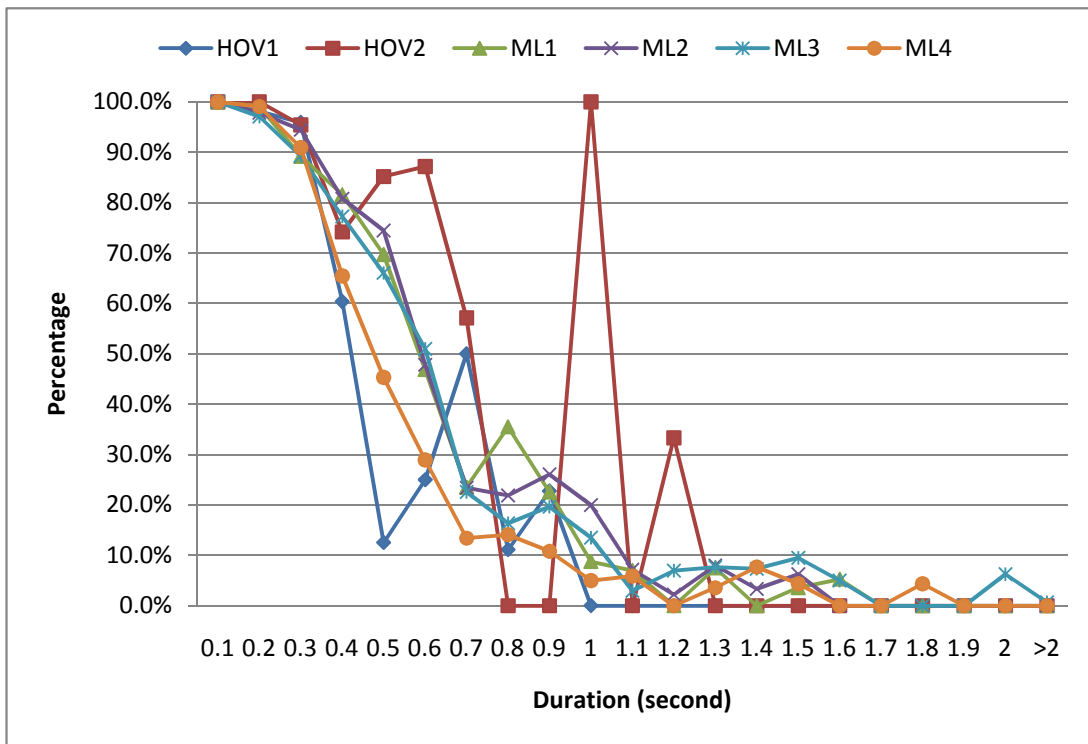


Figure 3-32 Dataset 1 Jan 9 2009

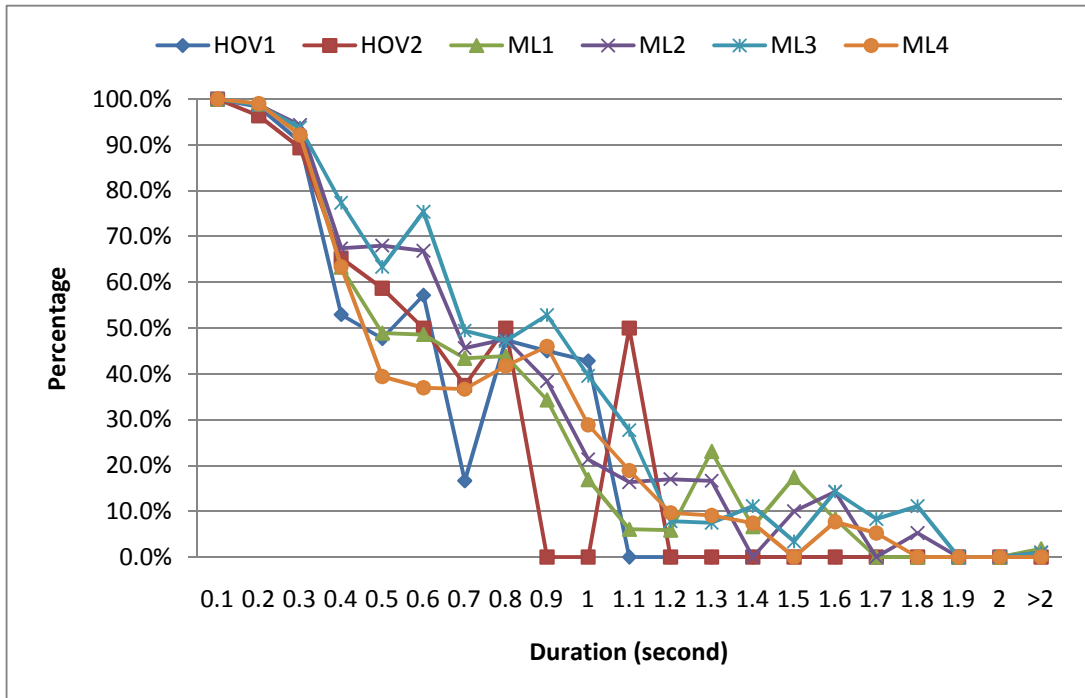


Figure 3-33 Dataset 2 April 28 2009

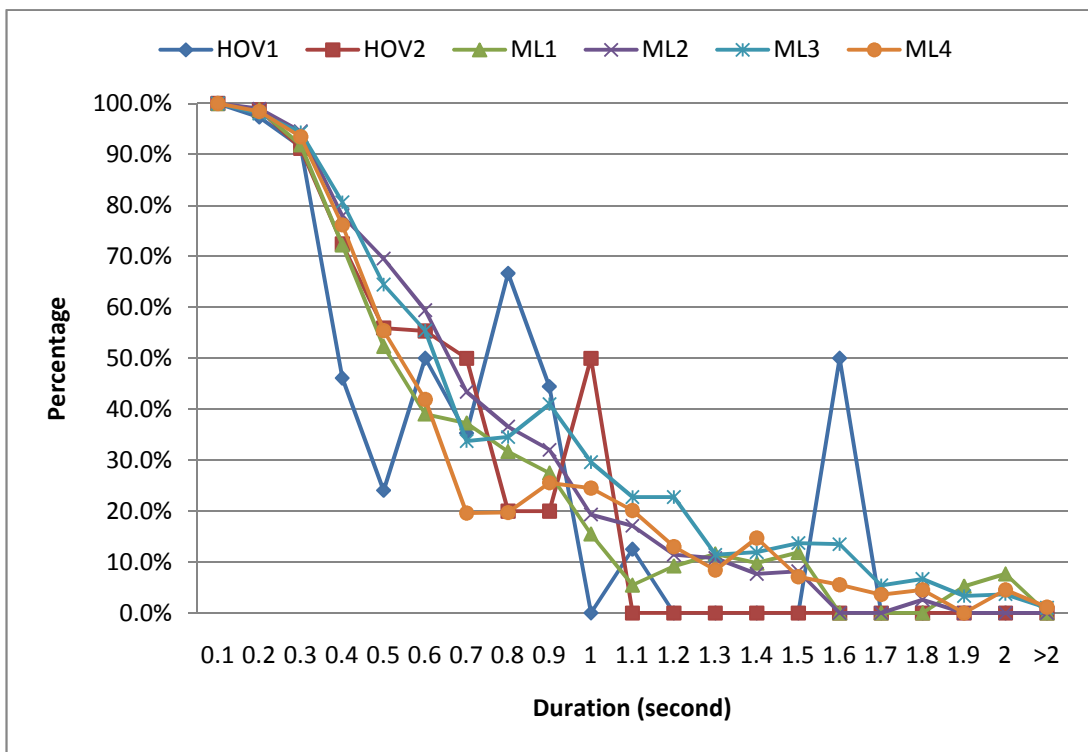


Figure 3-34 Dataset 3 May 12 2009

### 3.5.4 Sensys™ Signature Repeatability Analysis

The Sensys™ signature repeatability analysis provides a preliminary evaluation of the suitability of Sensys™ signatures for section-based vehicle re-identification. Correlation analysis was used in this investigation to compare the similarity between the front and rear signature pairs corresponding to the Sensys™ sensors installed on each lane. The correlation coefficient obtained indicates the strength and direction of a relationship between two random variables, which in this case refers to the signatures from the leading and trailing sensors, and is a measure of how well the two signatures match each other.

The correlation coefficient used in this analysis is the Pearson product-moment correlation coefficient, which is obtained by dividing the covariance of the two variables by the product of their standard deviations. The correlation coefficient  $\rho_{X,Y}$  between two random variables  $X$  and  $Y$  with expected values  $\mu_X$  and  $\mu_Y$  and standard deviations  $\sigma_X$  and  $\sigma_Y$  is defined as:

$$\rho_{X,Y} = \frac{\text{cov}(X, Y)}{\sigma_X \sigma_Y} = \frac{E((X - \mu_X)(Y - \mu_Y))}{\sigma_X \sigma_Y}$$

Prior to correlation analysis, signatures identified with dropped data packets are first removed from each dataset. Then, a comparison of repeatability across lanes and datasets is performed by identifying the proportion of repeatable signatures. The correlation coefficient threshold used for this analysis is 0.9 (i.e. any pair of signatures with correlation coefficient bigger than 0.9 is regarded as a good match). The comparison of repeatability across lanes and datasets is presented in Figure 3-35.

It can be observed that lanes HOV2 and ML4 have the worst repeatability performance. Lanes HOV1, ML1, ML2 and ML3 show similar repeatability performance. The likely cause of this observation in HOV2 is that it acts as an entry and egress lane between the mainline lanes and HOV1. This likely results in a larger

proportion of vehicles performing lane changing manouvers over HOV2, which would cause the observed signature repeatability issues.

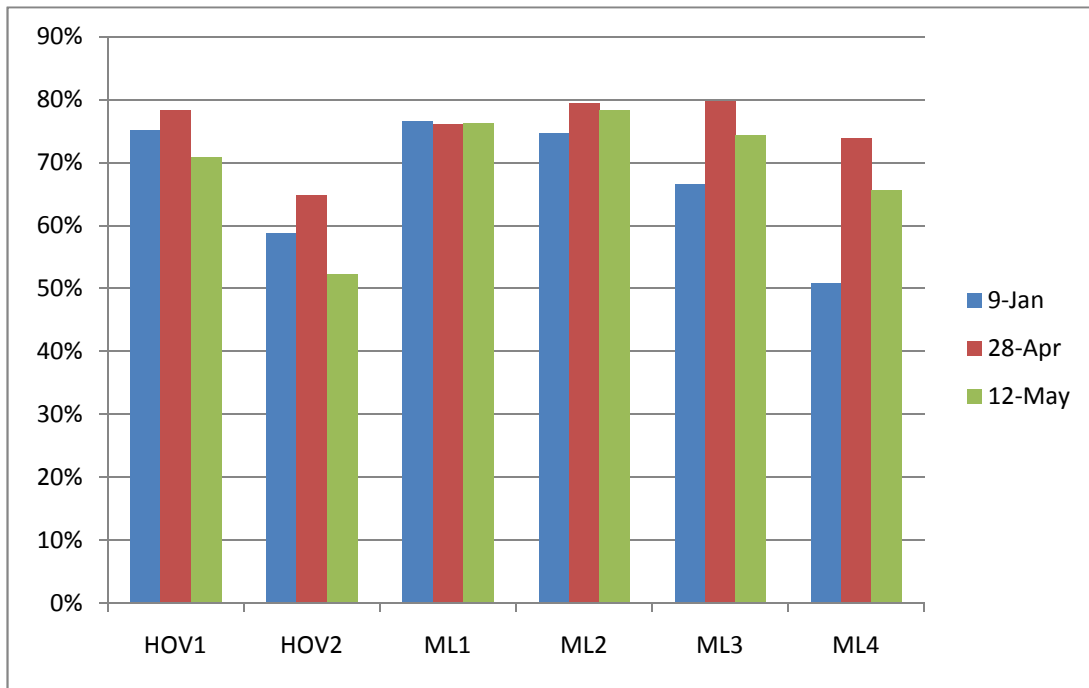


Figure 3-35 Comparison for repeatable signatures across lanes by dataset

A comparison between Figure 3-25 and Figure 3-35 shows that signature repeatability follows the same pattern as proportion of signatures without dropped data packets in general, especially for the mainlines. This implies that, both signature quality and signature repeatability improve under better traffic conditions.

**3.5.4.1 Sensys™ Signature Repeatability Analysis By Lanes Across Datasets**

Figure 3-36 to Figure 3-38 show the cumulative correlation coefficient for the cumulative distribution plots grouped by lanes across datasets. These plots present the percentage of non-repeatable signatures corresponding with associated correlation coefficient threshold values used. Hence, a higher curve would indicate poorer repeatability corresponding to the associated lane and dataset. A range of coefficient threshold values from 0.55 to 0.95 have been presented. The overall

results obtained from these plots are in agreement with the conclusions drawn from Figure 3-35.

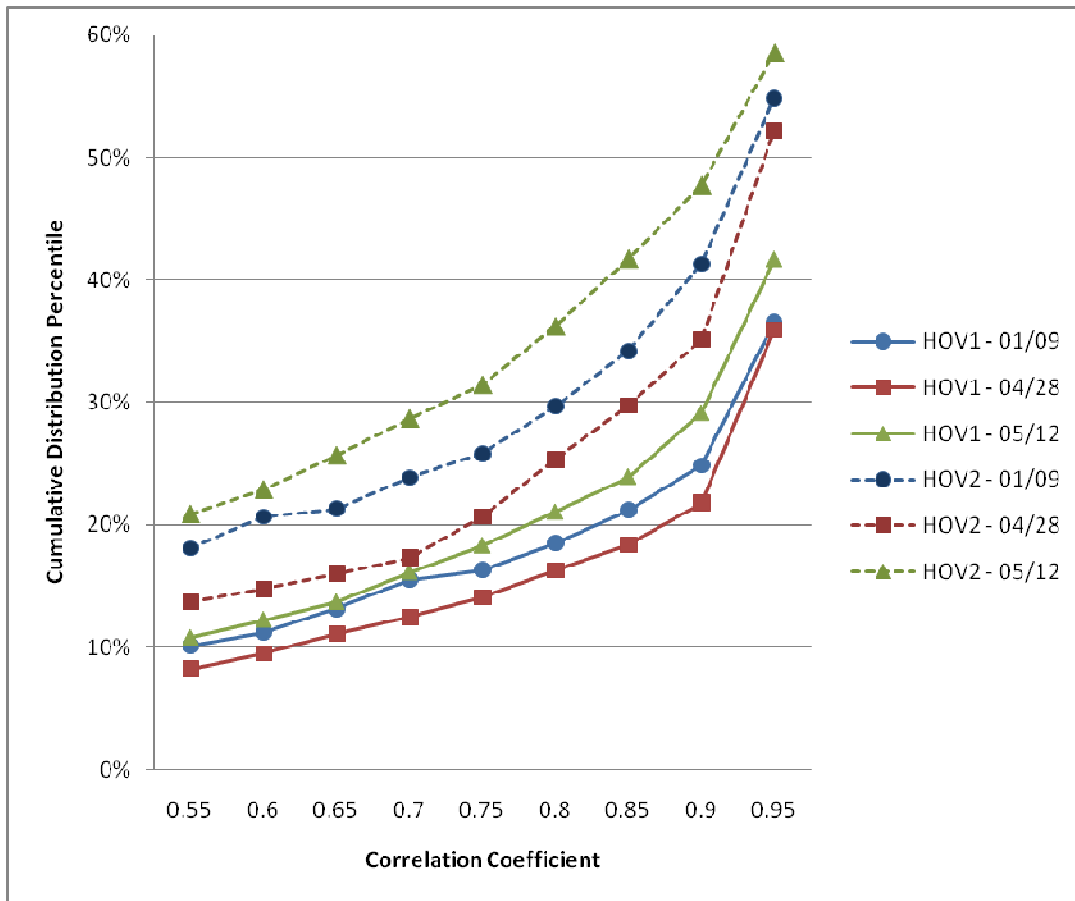


Figure 3-36 Cumulative distribution plot showing percentage of non-repeatable signatures below corresponding correlation coefficient for HOV Lane 1 and HOV lane 2 across datasets

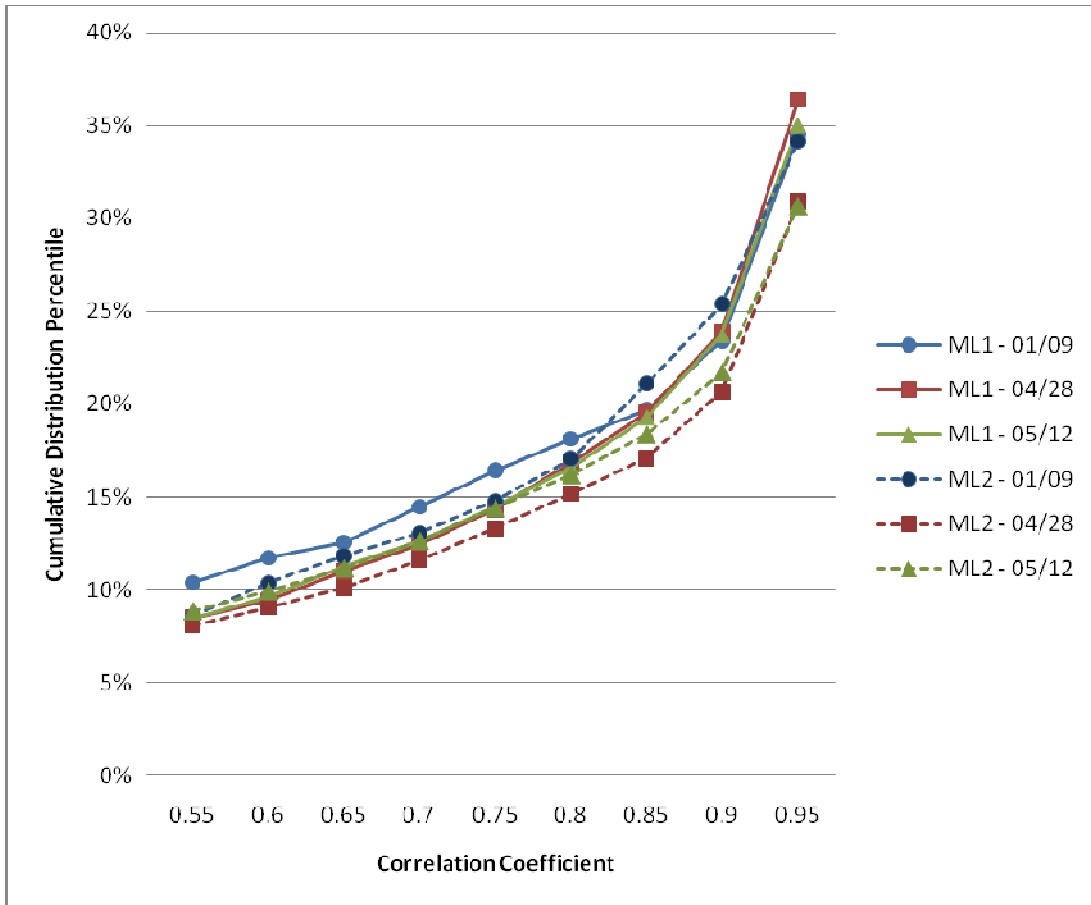


Figure 3-37 Cumulative distribution plot showing percentage of non-repeatable signatures below corresponding correlation coefficient for Mainline Lane 1 and Mainline lane 2 across datasets

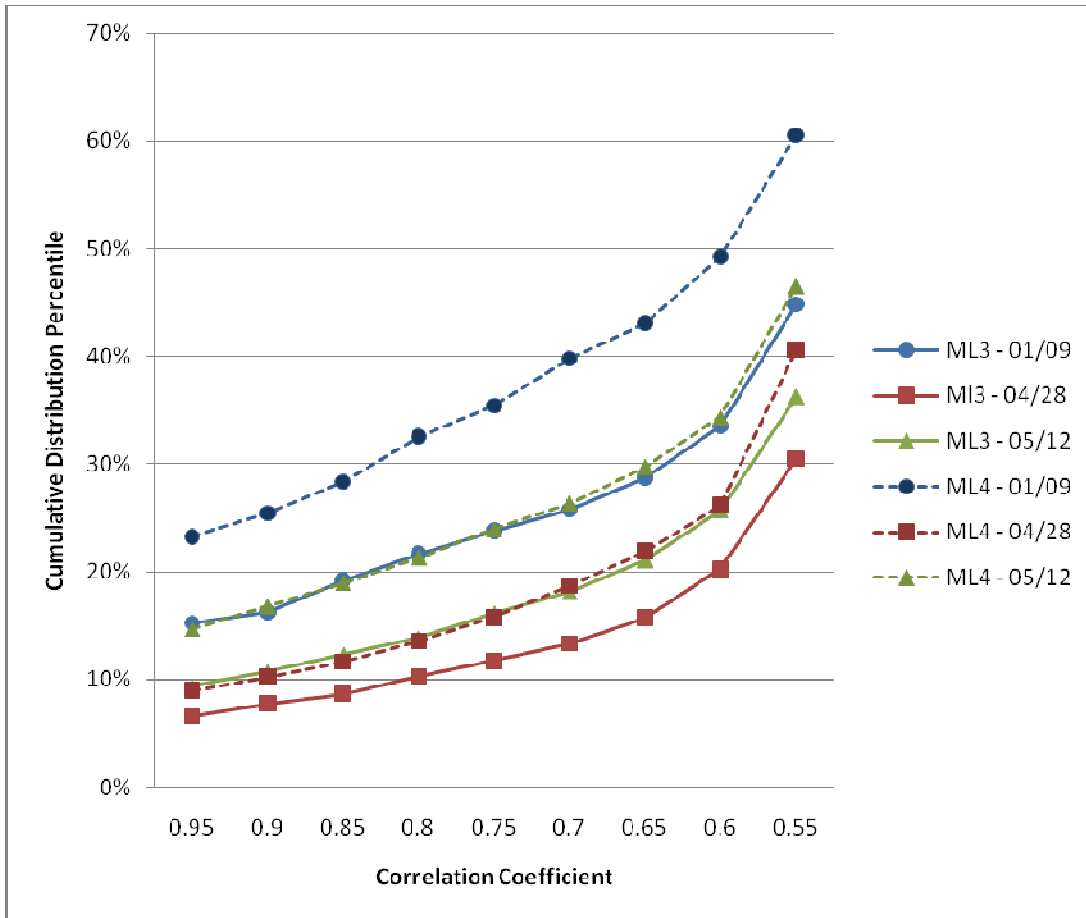


Figure 3-38 Cumulative distribution plot showing percentage of non-repeatable signatures below corresponding correlation coefficient for Mainline Lane 3 and Mainline Lane 4 across datasets

**3.5.4.2 Sensys™ Signature Repeatability Analysis By Dataset Across Lanes**

Figure 3-39 to Figure 3-41 show the cumulative distribution plots for the cumulative correlation coefficient of lanes grouped by datasets. These figures present the disparity in signature repeatability across lanes. The plots present the percentage of non-repeatable signatures corresponding with associated correlation coefficient threshold values used. Hence, a higher curve would indicate poorer repeatability corresponding to the associated lane and dataset. A range of coefficient threshold values from 0.55 to 0.95 have been presented. These figures show that lanes HOV1, ML1, ML2 and ML3 consistently perform best across datasets, while lanes HOV2 and ML4 perform worst. Hence, there appears to be no association of signature repeatability with the distance of the Sensys™ sensors from the Sensys™ Access Point. This analysis further indicates that the distance and relative location between the Sensys™ Access Points and Sensys™ sensors probably have little effect on the repeatability of the signature pairs obtained from each lane.

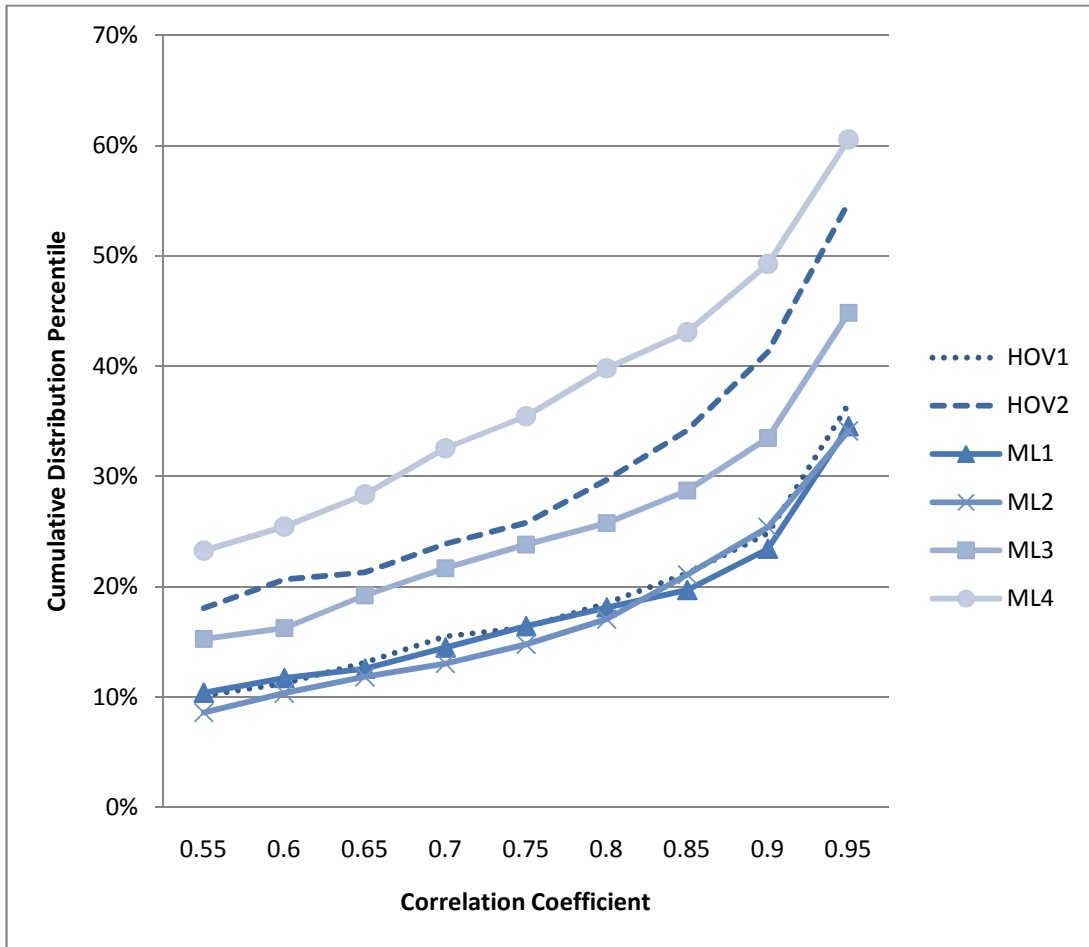


Figure 3-39 Cumulative distribution plot showing percentage of non-repeatable signatures below corresponding correlation coefficient for the Jan 9 2009 dataset across lanes

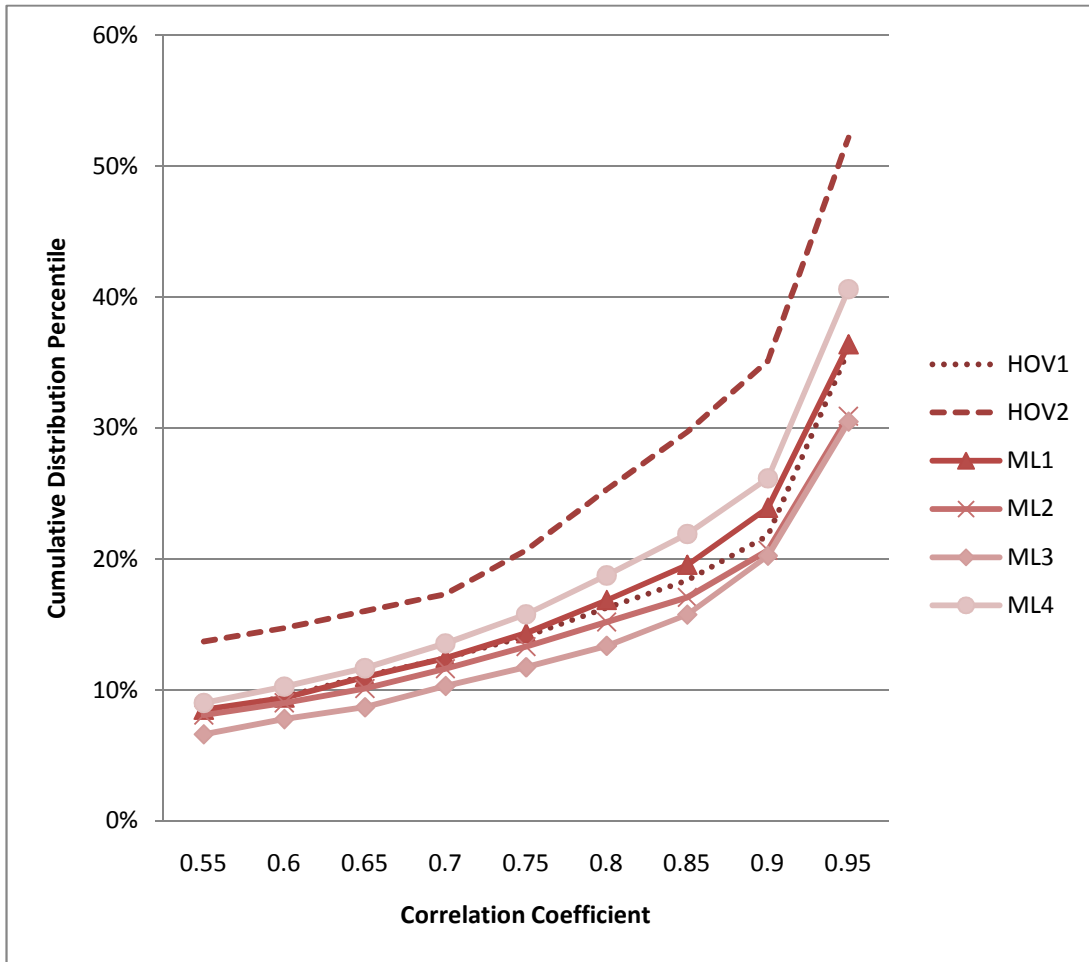


Figure 3-40 Cumulative distribution plot showing percentage of non-repeatable signatures below corresponding correlation coefficient for the April 28 2009 dataset across lanes

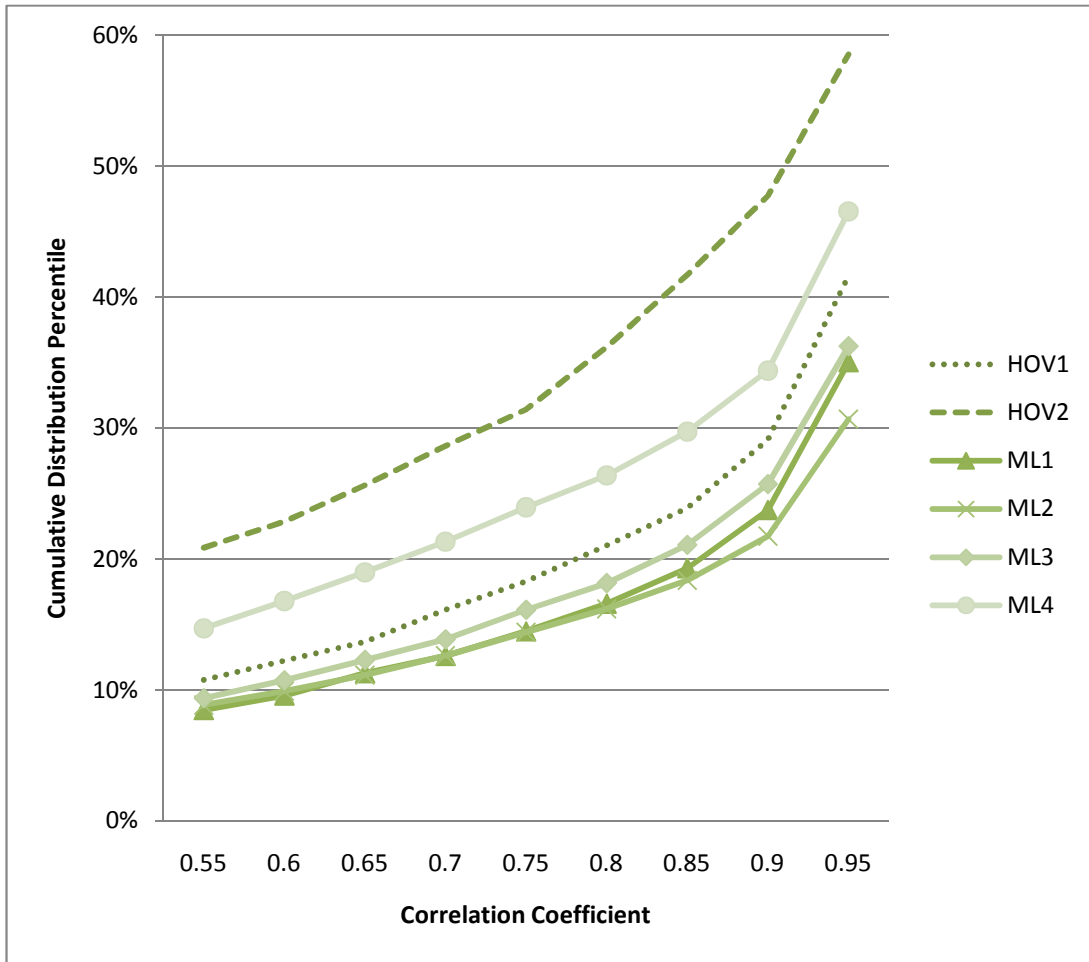


Figure 3-41 Cumulative distribution plot showing percentage of non-repeatable signatures below corresponding correlation coefficient for the May 12 2009 dataset across lanes

### 3.6 Investigation of Heterogeneous Transformation between Sensys™ and Inductive Loop Signatures

This section describes the investigation of the compatibility between signatures obtained from ILD loop sensors and Sensys™ magnetometer sensors using analysis based on advanced algorithms. The signature matching analysis consists of several steps. First, sets of input features are extracted from ILD loop and Sensys™ magnetometer sensors. Then, preliminary analysis consisting of the investigation of feature correlation between sensors is performed to reveal potentially similar characteristics between the two sensor technologies. Last, a neural network model is

designed to transform ILD signatures into features extracted from Sensys™ signatures.

### **3.6.1 Study Site**

The study site for this investigation is the Detector Testbed at the Sand Canyon Detector Station, located on Northbound I-405 Freeway in Irvine, California. This facility is located at post-mile 2.89 and is comprised of two HOV lanes and four ML lanes. HOV lane two serves as an entry and egress between the ML lanes and HOV lane 1. Each lane is equipped with double square 6-foot inductive loop sensors and double Sensys™ magnetometer sensors. Each pair of double inductive loop sensors is placed longitudinally along the lane and spaced at 20 feet between leading edges. Each Sensys™ magnetometer is located in the center of each square inductive loop sensor. This results in a longitudinal spacing of 20 feet between Sensys™ magnetometer sensors in each lane.

### **3.6.2 Signal Preprocessing: Matching ILD and Sensys™ Signatures**

The ILD and Sensys™ signature data were collected independently. Hence, time offsets as well as temporal drifts were present between the ILD and Sensys™ data, which resulted in different ILD and Sensys™-based signature timestamps for each vehicle. Hence, the two signatures corresponding to the same vehicle needed to be matched prior to performing further analysis.

Other issues relating to the differing sensor technology characteristics also need to be addressed to ensure accurate vehicle matching. They include occurrences of tailgating signatures as well as dropped sections in some Sensys™ signatures which needed to be excluded from analysis.

The procedure developed to match the signatures is as follows:

Step 1 For each lane, the starting matches were declared manually by checking the starting times, durations, and headways between

successive vehicles. In this way, the first few matches of the ILD and Sensys™ signatures were made.

- Step 2 Using the manually identified signature pairs as a starting point, headways were calculated between each successive vehicle for both the Sensys™ and ILD signature data separately. The headways were then compared and matches were made if the difference between the Sensys™ and ILD headways was found to be within the threshold value. Tailgating signatures were identified when the difference in headways was greater than the threshold value. For these situations, the headway was recalculated by including the following signature and compared again until the difference was within the threshold value.
- Step 3 A comparison of duration between matching ILD signatures and Sensys™ signatures was performed as validation and to further remove possible mismatched signatures pairs due to detection errors.
- Step 4 The final preparation task removes signatures with dropped sections from the data set. This step helps to further detect Sensys™ signatures with dropped packets which may not have been detected in prior steps. A ‘drop detection algorithm’ was applied to identify the flat part in the Sensys™ signature, if the duration of the drop was bigger than the threshold value, it was identified as a bad signature and was removed from the match list.

Using headways between successive vehicles as the matching criteria, as described in Step 2, has advantages over using a time stamp difference approach which measures the time of a vehicle passing over the detector. First, there exists a minimum headway between vehicles under any traffic condition. Hence, a headway threshold can be set without introducing matching errors. Second, because headway is a marginal time measurement, it is relatively insensitive to differential clock drifts present in the dataset compared with absolute measures such as time stamps. Third, using headway information allows for direct detection of tailgating signatures as opposed to a timestamp difference approach, where each signature would need to be analyzed in order to detect tailgating signatures. Further, due to the large number of signatures available in our dataset, the criteria thresholds in steps 2 and 3 were set to

be very strict values. This ensures that the final set of matched signature pairs had minimal errors.

### 3.6.3 Correlation Analysis

Correlation analysis of the extracted data points from ILD and Sensys™ signatures was performed to explore the compatibility between ILD and Sensys™ data. The procedure for the correlation between each matched signature pair follows three main steps. First, the raw signature values are obtained for each pair. Second, a feature vector is obtained by interpolating each signature pair. From the interpolation, 30 data points representing equally-spaced magnitude values are determined. Finally, the two feature vectors (ILD and Sensys™) are compared via the Pearson Correlation Coefficient.

The Pearson Correlation Coefficient measures the correlation between two variables and is widely used as an indicator of linear dependence. The feature vectors extracted from both the Z-axis and X-axis of Sensys™ signatures were compared with those obtained from ILD signatures. Results of the correlation analysis between the signature feature vectors extracted from ILD and the Sensys™ Z-axis and X-axis are summarized in Table 3-3 and Table 3-4, respectively.

Table 3-3 Number of signature pairs by correlation values between ILD and Sensys™ Z-Axis

<i>Lane\Coef</i>	>0.9	>0.5	<-0.5	<-0.9
1	0	119	787	24
2	0	18	89	4
3	1	73	409	7
4	1	113	766	23
5	5	120	797	22
6	3	75	562	19
<b>All Lanes</b>	10	518	3410	99

Table 3-4 Number of signature pairs by correlation values between ILD and Sensys™ X-Axis

<i>Lane\Coef</i>	>0.9	>0.5	<-0.5	<-0.9
1	0	450	521	2
2	1	63	35	0
3	2	235	239	1
4	1	537	399	1
5	2	522	429	0
6	2	383	264	1
<b>All Lanes</b>	8	2190	1887	5

From the Table 3-3 and Table 3-4, it can be observed that the Z-axis Sensys™ signatures show better correlation with ILD signatures with an inverse relationship (shown as a negative correlation). However, Table 3-5 shows that about 30 percent of the signature pairs still show a correlation of less than -0.5 between the feature vectors obtained from ILD and Sensys™ Z-axis signatures, and less than 1 percent of the signature pairs show a correlation coefficient of -0.9 or less. It is evident that only a slight correlation exists between the Sensys™ and ILD signatures. Table 3-5 summarizes the number and percentage of signature pairs according to the correlation value.

Table 3-5 Number and Percentage of signature pairs by correlation values between ILD and Sensys™ Z-Axis

<i>Lane\Coef</i>	<-0.5		<-0.9		<i>Total Matched Pairs</i>
1	787	30.5%	24	0.9%	2,579
2	89	31.0%	4	1.4%	287
3	409	30.4%	7	0.5%	1,346
4	766	31.0%	23	0.9%	2,470
5	797	30.1%	22	0.8%	2,649
6	562	29.8%	19	1.0%	1,884
<b>All Lanes</b>	3410	30.4%	99	0.9%	11,215

### **3.6.4 Exploratory Heterogeneous Transformation Analysis**

Further exploratory analysis was performed to investigate the potential of signature feature transformation between ILD and Sensys™ signatures. The approach used in this study extracts interpolated data points from normalized ILD signatures as input features and the sign of interpolated data points from Sensys™ signatures as target features. The input features obtained from ILD signatures are then trained iteratively via artificial neural networks (ANNs) to predict their corresponding target features. ANNs were chosen for their inherent ability to recognize hidden patterns in multi-dimensional data that are beyond the ability of human perception.

#### **3.6.4.1 Data validation**

An additional criterion was considered to improve the accuracy of vehicle matches in this analysis. This procedure involved the comparison of durations between ILD signatures and their corresponding matched Sensys™ signatures. Matches were only considered if the absolute difference between the ILD and Sensys™ signature durations is less than half of the duration of the ILD signature. From this validation analysis a further 892 vehicles were discarded from the dataset from the correlation analysis described in Section 3.5.3, leaving 10,323 vehicles for the heterogeneous transformation analysis.

#### **3.6.4.2 Inductive Loop Signature Extracted Features**

To obtain the ILD features, each signature is first normalized by dividing the overall signature by its peak magnitude. This yields a signature with a peak magnitude of 1.0 shown as a blue plot in Figure 3-42. 20 equally-spaced interpolated data points are then extracted from this normalized signature (shown as red crosses in Figure 3-42) to be used as the input feature vector.

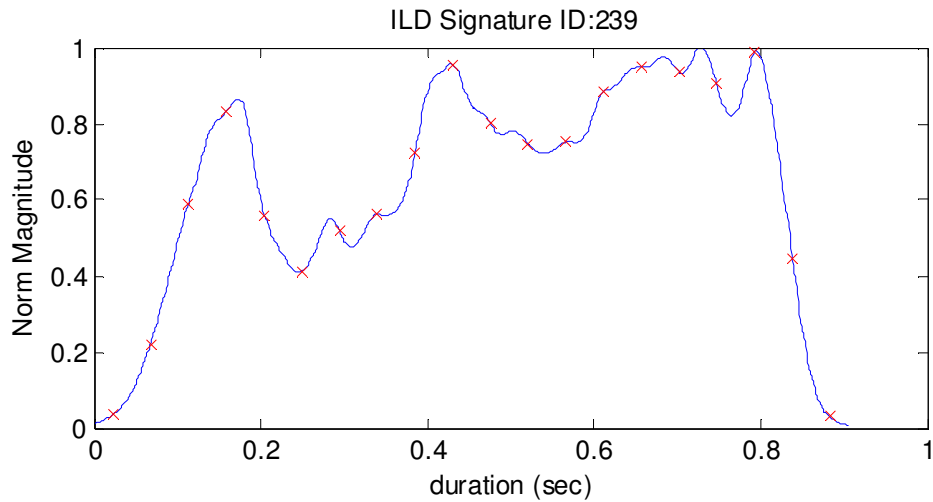


Figure 3-42 Extracting features from an ILD signature for heterogeneous transformation analysis

#### 3.6.4.3 Sensys™ Signature Extracted Features

Sensys™ features are obtained by first determining the positive and negative regions of the signature. 20 equally-spaced data points are then obtained from each signature. The data points generally take either of two values: 1 if the interpolated point is greater than zero and -1 if it is below zero. If the interpolated point lies exactly at zero, then the data point would also be assigned a zero value, although this occurrence is rare. Figure 3-43 shows extracted data points (shown as red crosses) from a Sensys™ signature (shown as a blue plot).

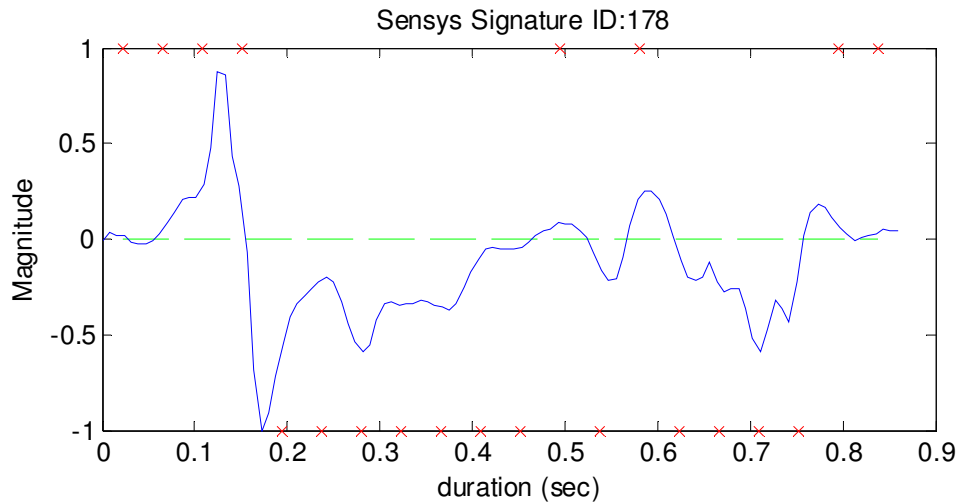


Figure 3-43 Extracting features from a Sensys™ signature for heterogeneous transformation analysis

#### 3.6.4.4 Neural Network Model Architecture and Data Organization

A multi-layer feedforward neural network (MLFNN) was used to train the ILD input features to predict the Sensys target features accurately. The MLFNN was designed 20 neurons at the input layer corresponding to the ILD input features and 20 neurons in the output layer corresponding to the number of Sensys target features. Two hidden layers were implemented in the MLFNN, with each hidden layer size varying between 5 and 20 neurons in steps of 5.

The dataset used in this analysis was partitioned into three sub-sets. 60 percent was used for training each MLFNN configuration, 20 percent was used for validation, which served as a stopping criterion, preventing over-training of the MLFNN by stopping training when performance of the validation data fails to improve over a successive number of iterations. The remaining 20 percent of the dataset was used as test data to evaluate the performance of each trained data.

#### 3.6.4.5 Analysis of Results

The results from the best trained MLFNN on the test dataset of 2,065 vehicles is shown in Figure 3-44. The model correctly predicted the corresponding 20 Sensys™

target features in only 1.2 percent of the test data. It predicted 16 out of 20 Sensys™ target features in over 32.2 percent of the test cases. And with a 50 percent probability, the model is able to predict over 14 out of 20 (70 percent) Sensys™ target features correctly.

The poor results from this transformation analysis corroborate the correlation analysis results from Section 3.6.3, and indicate that the characteristics of ILD and Sensys™ signatures are not compatible. This indicates that heterogeneous transformation between ILD and Sensys™ signatures is not viable, especially in the application of vehicle re-identification. Furthermore, it should be noted that the ILD and Sensys™ signatures obtained for this analysis were obtained from the same location, and had been extensively cleaned to remove bad signature data as well as potential error matches. Hence, results are expected to be significantly poorer in real-world vehicle re-identification applications where there would be a significant distance spanning the sensors and erroneous signature data cannot be as easily identified and removed.

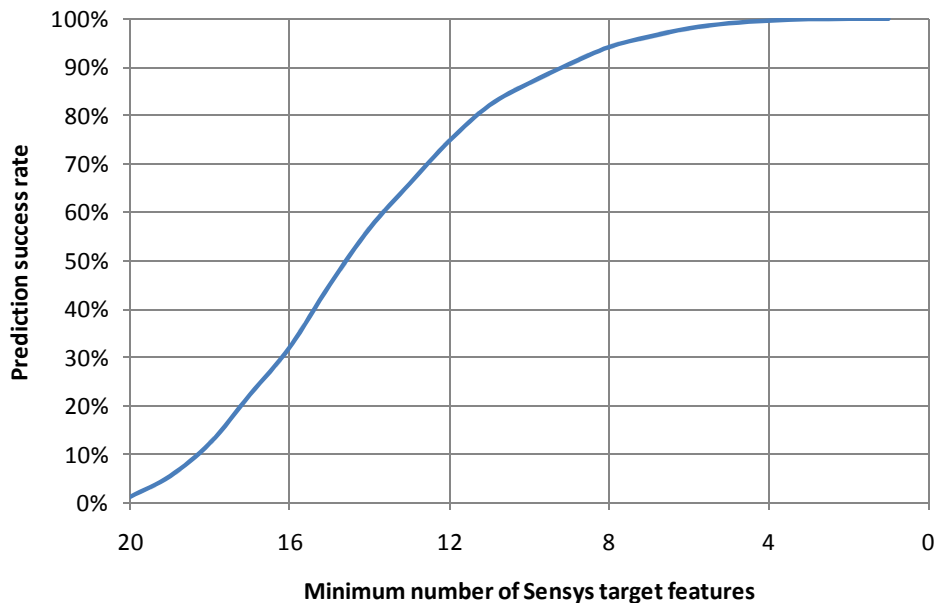


Figure 3-44 Percentage of vehicles with minimum number of Sensys™ target features predicted correctly

### **3.7 Summary of Findings**

#### **3.7.1 Blade™ Inductive Sensors**

3.5-inch surface-mounted Blade™ inductive sensors generate the most distinct wheel spike features within the Blade™ signature. However, the signature magnitude is small for high clearance vehicles and may affect vehicle detection performance if background noise signals are present and significant. Larger 8-inch Blade™ inductive sensor configurations addressed this concern, however, with an increase observation of upturned wheel spikes especially in large commercial vehicles.

Interference between adjacent Blade™ inductive sensors along the same lane was identified as the likely cause of observed noise issues as well as repeatability issues in double Blade™ inductive sensor installations. Further investigations with Blade™ inductive sensor configurations are recommended to determine the optimal configuration which addresses noise and repeatability concerns while still generating signature features that are suitable for advanced traffic analysis.

#### **3.7.2 Analysis of Sensys™ Data in Conventional Mode**

The investigation performed has yielded the following findings from the comparison of Sensys™ traffic measures versus ILD in conventional mode:

- Sensys™ volume measures were found to be on average 6.05 percent lower than ILD along the Northbound I-405 freeway at Sand Canyon.
- Sensys™ occupancies were found to be significantly higher than ILD – measuring 25.87 percent higher on average. This may have implications on estimating speeds, travel times and traffic densities.
- Sensys™ occupancy measures are highly correlated with ILD measures, hence, they can be effectively corrected using a correction factor. However, the correction factor can only be estimated if there are ILDs in close proximity to the installed Sensys™ sensors, and correction factors may not be

transferrable because Sensys™ sensors are sensitive to the earth's magnetic field which may vary by location.

### **3.7.3 Analysis of Quality and Repeatability of Sensys™ Data in Signature Mode**

Dropped data packets have been identified as an issue of concern for Sensys™ Magnetometers when operating in signature mode. It was found that the frequency of dropped data packets increases with longer duration vehicle signatures associated with longer vehicles such as large commercial vehicles or slower vehicles during congested traffic periods. The elevation of the Sensys™ Access Point as well as its distance from Sensys™ Magnetometers was not found to have a significant influence on rate of data packet drops.

### **3.7.4 Investigation of Heterogeneous Transformation between Inductive Loop and Sensys™ Signatures**

The correlation analysis between ILD and Sensys™ signatures shows only a slight correlation. A further investigation of heterogeneous transformation between ILD and Sensys™ signatures yielded poor results, which corroborated the findings from the correlation analysis. This indicates that re-identification of vehicles across a section spanning detector stations equipped with ILD and Sensys™ signature technologies is probably not viable.

## **CHAPTER 4 REAL-TIME TRAFFIC PERFORMANCE MEASUREMENT SYSTEM: FIELD AND COMMUNICATIONS DEPLOYMENT**

### **4.1 Overview of Field, Communications and Data Processing Framework**

This chapter presents and describes the Real Time Performance Measurement System (RTPMS) framework components including the field data processing system, the performance measurement system, the database server architecture, and field and communications deployment.

Field computational resources and the bandwidth of field communication links are often limiting factors in traffic operations. This was a key consideration in the design of RTPMS. The RTPMS consists of six modules, as illustrated in Figure 4-1. The field data preprocessing system first processes the raw vehicle signature data via the Signature Examination Module to detect bad and/or abnormal vehicle signatures. The Real-Time Reidentification 2 (RTREID-2) Piece-wise Slope Rate (PSR) Generation Module then extracts PSR values while the Speed Estimation Module estimates single loop speed from each vehicle signature. The PSR values and estimated speeds from each field unit are then sent to the RTREID-2 server through a CORBA interface. The Real-Time Vehicle Classification (RTVC) and RTREID-2 modules are subsequently performed to obtain vehicle class and vehicle tracking information for each individual vehicle. Finally, the UCI\_PeMS Module queries the RTPMS database and computes real-time performance indices and estimates.

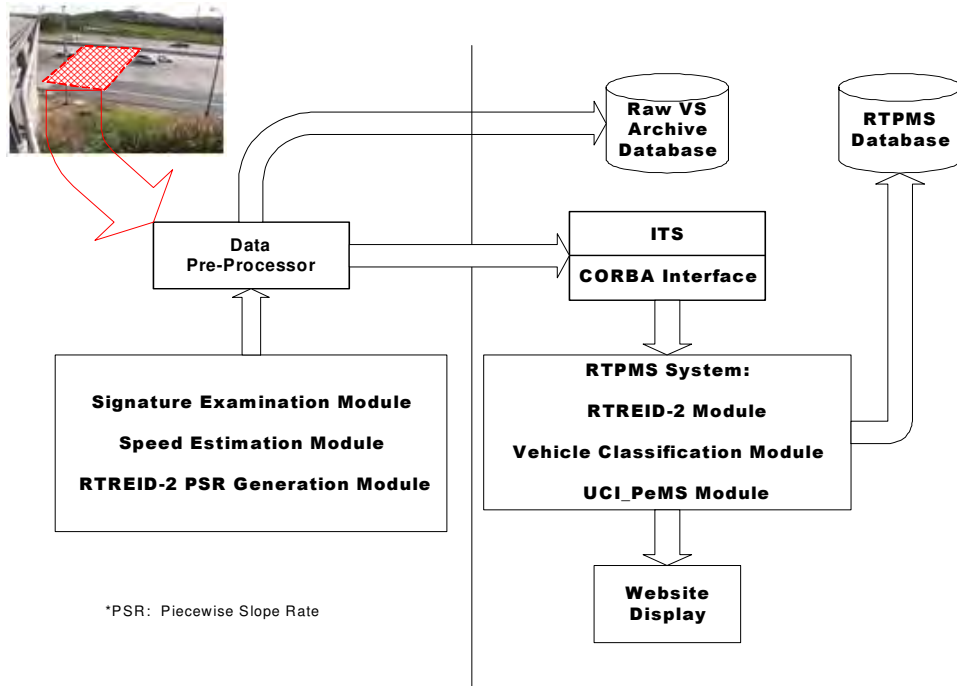


Figure 4-1 RTPMS Module Framework

RTPMS is divided into two sub-systems: a field data pre-processing system and a performance measurement system. The field data preprocessing system includes all field PCs that obtain and process raw vehicle signature data, while the performance measurement system consists of four servers designed to generate and display real-time performance measurements. The current RTPMS architecture is illustrated in Figure 4-2. The box labeled ITS represents resources that are currently located within the Institute of Transportation Studies (ITS) at the University of California, Irvine (UCI).

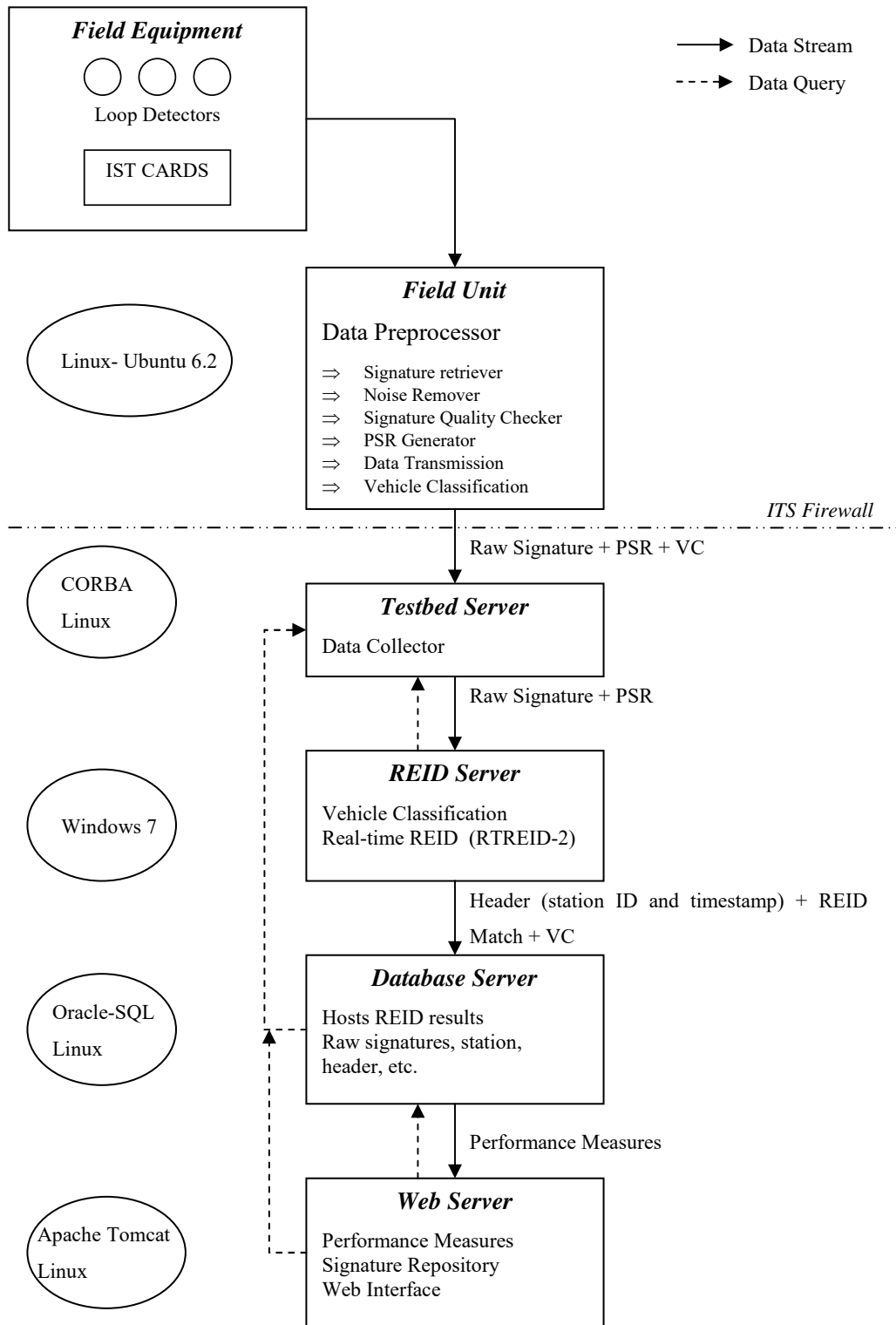


Figure 4-2 RTPMS Architecture

## 4.2 Field Hardware Configuration

This section describes the hardware configuration recommended for setting up traffic cabinets to support RTPMS.

### 4.2.1 Recommended Traffic Cabinet Hardware Components

A typical freeway traffic cabinet of an inductive loop detector station consists of a traffic controller (typically type 170 or 2070), an input file which houses inductive loop detector cards, a power supply unit and terminal blocks. The traffic cabinet hardware configuration to support RTPMS has been designed to require minimal modifications to the existing layout. This ensures that the RTPMS can operate in parallel with existing traffic operations. Figure 4-3 shows the additional hardware equipment required: swapping out existing conventional inductive loop detector card with advanced IST-222 inductive loop detector cards and the installation of a field processing system (field unit).

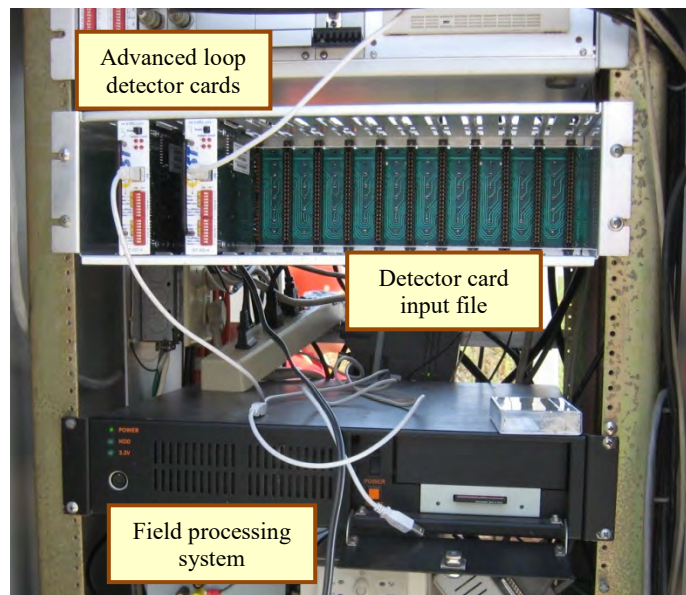


Figure 4-3 Traffic cabinet showing advanced loop detector cards and rack-mounted field computer

The advanced loop detector cards are connected to the field unit via USB cables. Since all signature data is transmitted to the field unit through the USB

interface, the RTPMS is independent of and transparent to the traffic controller unit. Hence, connections on the detector card input file do not need to be spliced or modified in any way, eliminating possibilities of compromising existing traffic operations. In addition, communications between the field unit and the REID server is performed through a wireless modem installed within the field unit, so the RTPMS hardware is not dependent on any existing communications infrastructure set up within the cabinet. In fact, a single power outlet is the only resource required for the RTPMS hardware.

## **4.2.2 Field Data Processing System (Field Unit)**

### **4.2.2.1 Overview**

Each field computer contains a data pre-processor module which generates two types of data: raw vehicle signatures and RTPMS features. The raw vehicle signatures are unprocessed vehicle signatures obtained from advanced detector cards. The RTPMS features consist of PSR values which are used for vehicle re-identification and vehicle classification by the performance measurement system. Figure 4-4 shows the flow of processes within each field unit.

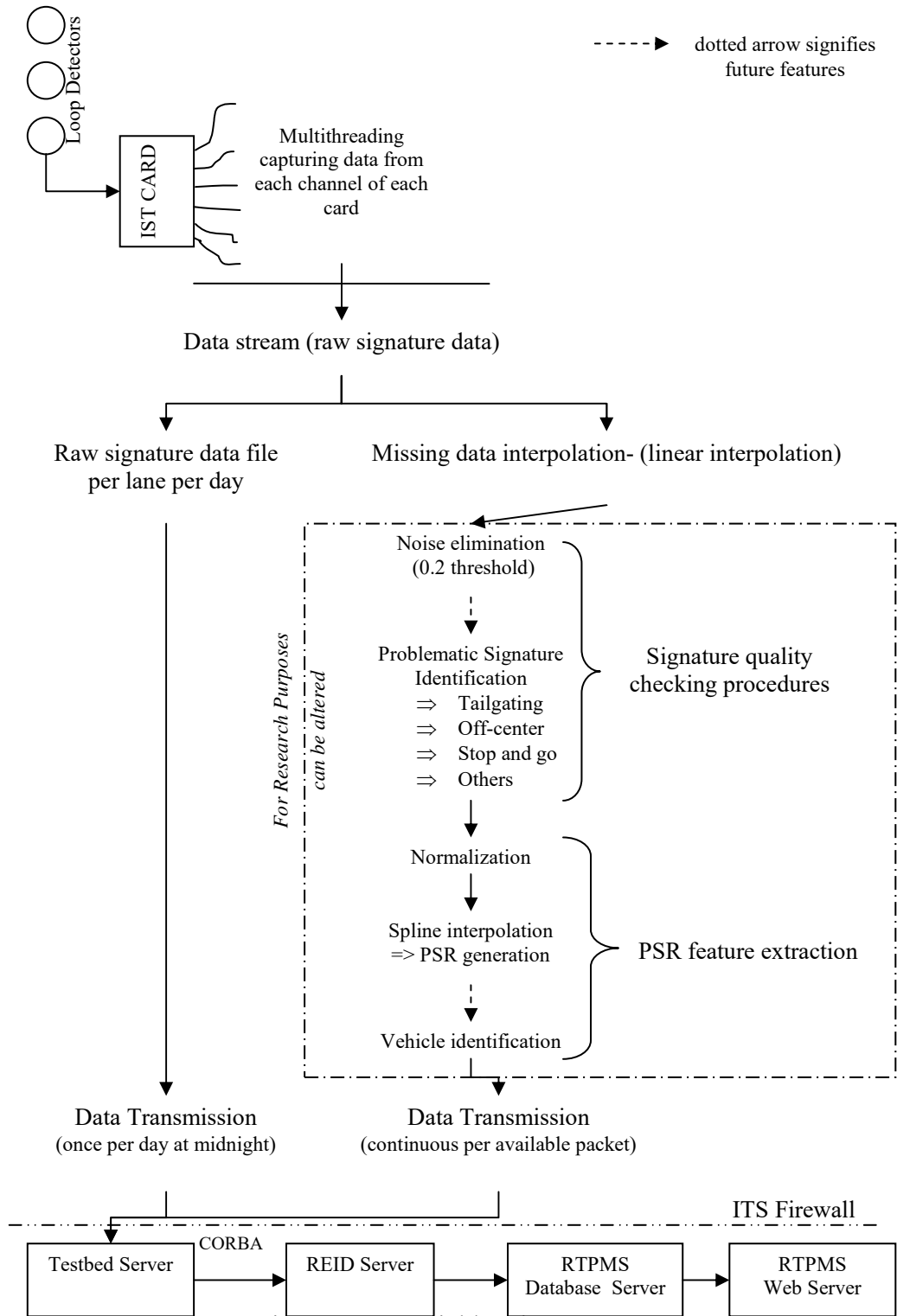


Figure 4-4 Field Unit processes

#### 4.2.2.2 Field Unit Hardware Setup

The field unit hardware consists of a field computer additionally equipped with a high-speed compact flash card connected via a Compact Flash Drive through the IDE interface and a wireless modem connected via an add-on PCMCIA interface as shown in Figure 4-5. The Linux operating system, detector card software as well as signature data is stored within the compact flash card, eliminating the need for physical hard drives which are sensitive to extreme environments. The wireless modem provides communications for transmitting signature data.

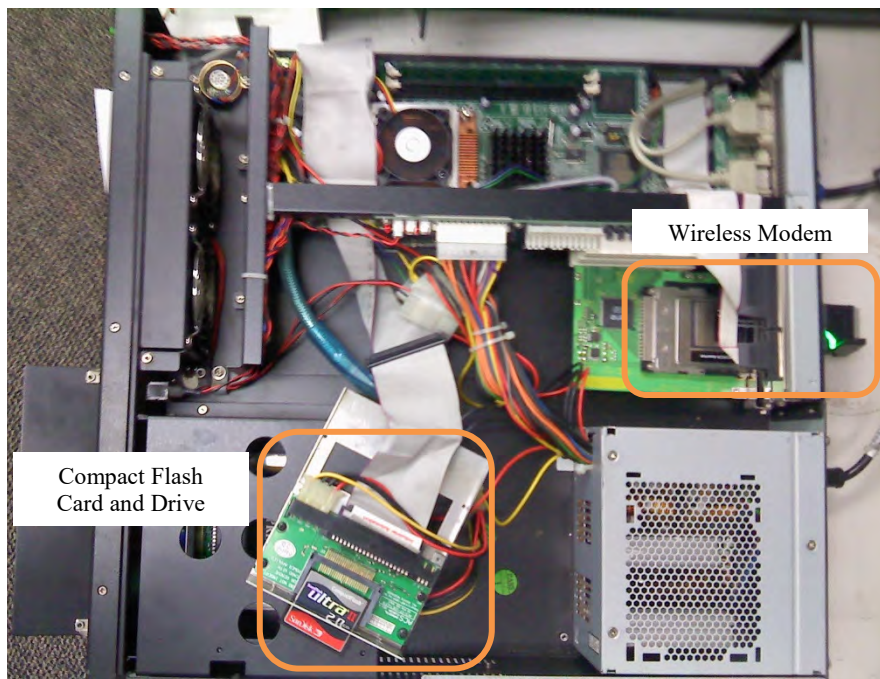


Figure 4-5 Additional hardware components of field unit

#### 4.2.3 Advanced Loop Detector Cards

Standard bivalent loop detector cards are capable of measuring a vehicle's presence while advanced loop detector cards are capable of collecting vehicle signature data, which are measurements of the inductance changes as the vehicle passes over the loop. Inductive Signature Technologies, Inc. produces the IST-222 Standard Signature Output Detector Cards which were used for this project. These cards are directly compatible with existing traffic controllers to obtain conventional traffic

measures such as flow and occupancy. The cards sample at 1,200 samples per second, producing very detailed signatures. The IST-222 card is connected to the field processing unit by a USB port on the front of the detector card.

### **4.3 Performance Measurement System**

There are four servers in the performance measurement system: RTREID-2, Data Collector, RTPMS Web, and Database servers. The Data Collector is programmed in CORBA and communicates with the field units wirelessly. The Data Collector receives raw vehicle signature data and RTPMS features, and subsequently feeds the RTPMS server with RTPMS features. The vehicle re-identification and vehicle classification tasks are managed by the RTREID-2 server. The raw vehicle signature data obtained from the field as well as the outputs of the RTREID-2 server are sent to the Database server for storage. The RTPMS Web server obtains information from the Database server to execute performance evaluation and display advanced traffic performance results.

### **4.4 Database Server Architecture**

The RTPMS database server is located on the permanent host, [trantor.its.uci.edu](http://trantor.its.uci.edu), in the Institute of Transportation Studies (ITS) at the University of California, Irvine (UCI). The database server is equipped with the Oracle 9i database software. Oracle was chosen as it supports the development of a stable and reliable system for multiple simultaneous data entries and queries.

The RTPMS database server is designed to operate with an optimal balance of speed of performance and low space requirements. It consists of two main data structure components: static lookup tables and signature and REID output tables. The static lookup tables are managed by the database administrator, and are used to setup the RTPMS with site-specific information. The signature and REID output tables store results from the re-identification and classification modules for the purpose of evaluating performance measures. The RTPMS database is also designed

with several built-in queries to speed up the search for frequently looked up data. This saves the Database server from significant delay due to parsing repeated long queries. These built-in queries also reduce the search parameters in web-based queries required to obtain data—speeding up the search process.

#### 4.4.1 Lookup Tables

Lookup Tables are used to store information on static data used in RTPMS queries for output to the web interface. Corridor, detector card, vehicle class, section, and station information are all stored as look-up tables.

##### 4.4.1.1 Corridor Information

The corridor information is stored in the Corridor Lookup Table (Table 4-1). This table is used to store information about each corridor in the database.

Table 4-1 Corridor Lookup Table (LOOKUP\_CORRIDORS)

<i>Field Name</i>	<i>Description</i>
<b>CORRIDOR_ID</b>	Reference number for each corridor
<b>CORRIDOR_NAME</b>	Defined name of the available corridors
<b>STCTY_FIPS</b>	Coded value for city
<b>CITY</b>	Name of city in which corridor lies
<b>DIRECTION_ID</b>	Coded value for direction (NB = 1)
<b>LAT_COORD</b>	Latitude Coordinate
<b>LONG_COORD</b>	Longitude Coordinate
<b>START_PM</b>	Starting post-mile
<b>END_PM</b>	Ending post-mile
<b>ROUTE</b>	Route of corridor
<b>DESCRIPTION</b>	Location description of corridor
<b>ROUTE_NAME</b>	Name of route
<b>DIR</b>	Cardinal direction (North, South, East, West)

#### 4.4.1.2 Detector Card Information

The Detector Card Lookup Table (Table 4-2) stores information about each detector card. Each card's location, lane assignment, and configuration are stored in this table.

Table 4-2 Detector Card Lookup Table (LOOKUP\_DET\_CARD\_LN)

<i>Field Name</i>	<i>Description</i>
<b>CARD_LN_ID</b>	Reference number of the detector card-lane assignment
<b>DET_CARD_ID</b>	IST-222 card number printed on detector card
<b>FRONT_LOOP_CHANNEL</b>	Channel of the detector card assigned to the leading sensor in the lane
<b>CARD_CONFIG_ID</b>	Determines if both channels of the detector card are allocated to the same lane or if they are allocated to different lanes
<b>SLOT_NO</b>	Physical location of detector card in the input file
<b>STATION_ID</b>	Station where card is located
<b>LANE</b>	Lane assignment of the detector card
<b>LANE_TYPE_ID</b>	Main line (101), merging lane (102), or HOV (103) lane type

#### 4.4.1.3 Section Information

The Section Lookup Table (Table 4-3) stores the information defining each section. This table is necessary for defining the stations at each end of the section, the length of the section, and the number of lanes in that section. The variables **EFFECTIVE\_LANES\_ML** and **EFFECTIVE\_LANES\_HOV** are necessary to define the number of lanes in a section when the upstream and downstream stations have a different number of lanes, i.e. there is a merge lane or dropped lane within the section.

Table 4-3 Section Lookup Table (LOOKUP\_SECTIONS)

<i>Field Name</i>	<i>Description</i>
<b>SECTION_ID</b>	Reference number for the section
<b>UP_STN_ID</b>	ID of the upstream station
<b>DN_STN_ID</b>	ID of the downstream station
<b>SECTION_NAME</b>	Text description of the section
<b>LENGTH_MI</b>	Length (miles) of the section
<b>EFFECTIVE_LANES_ML</b>	Effective number of main line lanes within a section
<b>EFFECTIVE_LANES_HOV</b>	Effective number of HOV lanes within a section

#### 4.4.1.4 Corridor Information

The corridor lookup table associates the individual sections to the corridor. Multiple sections make up each corridor and a single section can belong to more than one corridor. This table defines these relationships.

Table 4-4 Corridor Lookup Table (LOOKUP\_SECT\_CORR)

<i>Field Name</i>	<i>Description</i>
<b>SECT_CORR_ID</b>	Reference number of the corridor and section combination
<b>CORRIDOR_ID</b>	Corridor identification number
<b>SECTION_ID</b>	Section identification number
<b>SECTION_ORDER</b>	Number referring to the order of the section within the corridor

#### 4.4.1.5 Station Information

The Station Information Lookup Table (Table 4-5) stores each station's ID, name, loop configuration, post-mile, and latitude and longitude coordinates. When referencing a corridor or section the station information of that section is referenced in this table.

Table 4-5 Station Information Lookup Table (LOOKUP\_STATIONS)

<i>Field Name</i>	<i>Description</i>
<b>STATION_ID</b>	Reference number for each station
<b>STATION_NAME</b>	Name of the station
<b>CABINET_ID</b>	Caltrans cabinet identification number
<b>ROAD_NAME_ID</b>	
<b>NUM_LANES</b>	Number of lanes
<b>LOOP_TYPE_ID</b>	Round loop (1) or square loop (2)
<b>LOOP_CONFIG_ID</b>	Double (2) or Single (1) loops
<b>DIRECTION_ID</b>	Northbound (1) or Southbound (2)
<b>POSTMILE</b>	Station post-mile
<b>LAT_COORD</b>	Latitude coordinate
<b>LONG_COORD</b>	Longitude coordinate

#### 4.4.2 Signature Table

The Signature Table (Table 4-6) stores information for each signature including duration, sample count, and timestamp. The table is appended whenever new data is available.

Table 4-6 Signature Table (RTPMS\_VEH\_SIG)

<i>Field Name</i>	<i>Description</i>
<b>ID</b>	Reference identification number
<b>SIG_ID</b>	Signature identification number
<b>CARDLN_ID</b>	Detector card identification number from which the signature came
<b>STN_ID</b>	Station identification number from where the signature was captured
<b>LANE</b>	Lane number of where the signature came
<b>DURATION</b>	Time length of the signature
<b>VEHCLASS_ID</b>	Vehicle classification reference value
<b>SCOUNT</b>	Number of samples (data points) in the signature
<b>TIMESTAMP</b>	Time the signature was captured, i.e. time at which the vehicle passed over the loop

#### 4.4.3 REID Table

The REID Table (Table 4-7) stores the matched vehicle signature pairs that are produced by the REID algorithm. This table is appended whenever new vehicles are re-identified.

Table 4-7 REID Results Table (RTPMS\_REID\_OUTPUT)

<i>Field Name</i>	<i>Description</i>
<b>ID</b>	Reference number for the matched pair of vehicles
<b>UP_SIG_ID</b>	Identification number of the vehicle at the upstream station
<b>UP_LANE_ID</b>	Lane number of the vehicle at the upstream station
<b>DN_SIG_ID</b>	Identification number of the vehicle at the downstream station
<b>DN_LANE_ID</b>	Lane number of the vehicle at the downstream station
<b>SECTION_ID</b>	Section over which the matched vehicle traversed

#### **4.5 Field Deployment**

The RTPMS is currently undergoing a real-time implementation which consists of equipping detector stations in Detector Testbed along the Northbound I-405N freeway with field units configured wireless communications hardware followed by a system shake-down to identify and address operational issues. In addition to the mainline detector stations, on and off ramp detector locations will also be included in the system. The field units at these locations are running the Ubuntu Linux operating system. Data transmission is performed using wireless modems as illustrated in Figure 4-6. The status and IP information are updated in the RTPMS database at UCI ITS, and the CORBA interface of RTPMS has been tested and modified for stability to ensure smooth data transmission from the field units.

At the time of writing this report, the deployment status of RTPMS stations along the Northbound I-405 freeway in the City of Irvine, California is presented in Table 4-8. Mainline stations provide vehicle re-identification, signature results and archived signature data, while ramp meter stations provide signature results and archived signature data. Two ramp locations at Irvine Center Drive have been removed from the deployment plan because they are located upstream of the first mainline detector station located at cabinet V2474 just south of the CA-133 freeway interchange. A third location at cabinet V2603 (post mile 5.01) is temporarily removed from the deployment plan due to its proximity to the adjacent location at cabinet V2604 (post mile 5.05). All other mainline count stations have been deployed to provide continuous RTPMS coverage along the freeway corridor from South of CA-133 Freeway (postmile 1.6) to Red Hill Ave (postmile 8.4), spanning 6.8 miles. Several ramp locations have not been deployed due to insufficient operational field units. New improved field units are currently being evaluated for replacement of the existing field units. The evaluation is supported by the California Traffic Management Labs (CTMLabs) under the direction of the Institute of Transportation Studies at the University of California, Irvine. Continued deployment of the remaining detector stations will also be undertaken by CTMLabs.

Table 4-8 List of RTPMS detector stations with deployment status

Caltrans Cabinet Number	Cabinet Location	RTPMS Station Name	RTPMS Station ID	Post mile	Description	Deployment Status	
1	E4331	Enterprise @ Irvine Center Dr. 1	ICD_R1	4501	0.93	Ramp Meter	Cancelled
2	E4332	Enterprise @ Irvine Center Dr. 2	ICD_R2	4502	1.11	Ramp Meter	Cancelled
3	V2474	I-405 S @ South of 133	S133	450	1.6	Mainline Count Station	Deployed
4	UCI 1	Laguna Canyon	LC1	451	2.23	Detector Testbed	Deployed
5	ET040	I-405 N @ Laguna Canyon Rd.	LC2	452	2.35	Mainline Count Station	Deployed
6	UCI 1	Sand Canyon Off-ramp	SCOR	4531	none	Detector Testbed	
7	ET040	Sand Canyon	SC	453	2.89	Detector Testbed	Deployed
8	E4551	I-405 N @ Sand Canyon	SC_R	4541	2.99	Ramp Meter	Deployed
9	V2040	I-405 N @ N. of Sand Canyon	N_SC	454	3.31	Mainline Count Station	Deployed
10	E4335	I-405 N @ Jeffrey 1	JEFF_R1	4551	3.86	Ramp Meter	
11	E4336	I-405 N @ Jeffrey 2	JEFF_R2	4552	4.03	Ramp Meter	
12	V2603	I-405 S @ Yale	YALE	455	5.01	Mainline Count Station	Cancelled
13	V2604	I-405 S @ Spruce	SPR	456	5.05	Mainline Count Station	Deployed
14	E4341	I-405 N @ Culver Dr. 1	CLV_R1	4571	5.55	Ramp Meter	Deployed
15	E4342	I-405 N @ Culver Dr. 2	CLV_R2	4572	5.74	Ramp Meter	
16	V2602	I-405 S @ Harvard Ave.	HRVD	457	6.1	Mainline Count Station	Deployed
17	E4343	I-405 N @ Jamboree 1	JAMB_R1	4581	6.85	Ramp Meter	
18	E4344	I-405 N @ Jamboree 2	JAMB_R2	4582	7.07	Ramp Meter	
19	E4345	I-405 N @ MacArthur 1	MACA_R	4583	7.73	Ramp Meter	
20	V2433	I-405 S @ Airport	AIRP	458	8.27	Mainline Count Station	Deployed
21	V2605	I-405 S @ Red Hill	RH	459	8.4	Mainline Count Station	Deployed

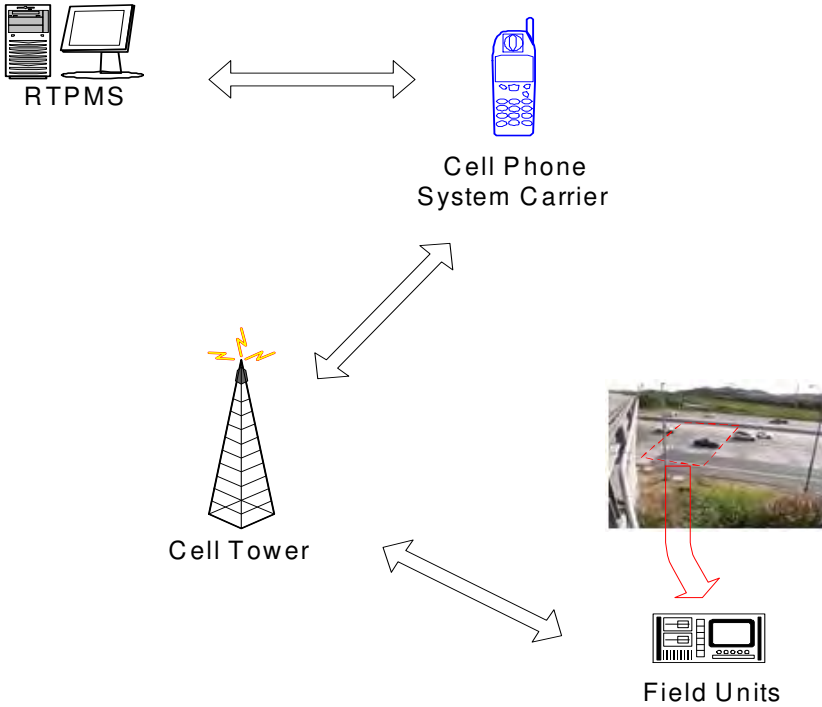


Figure 4-6 Communications Framework for RTPMS

## CHAPTER 5 REAL-TIME TRAFFIC PERFORMANCE MEASUREMENT SYSTEM: WEB SERVER DEPLOYMENT

### 5.1 Overview of Web and Database Framework

This chapter describes the design and on-going development of RTPMS web and database architecture. The RTPMS web and database framework consists of two main components: the RTPMS Database Server and RTPMS Web Server as shown in Figure 5-1. Communications between these components facilitate the exchange of information between users and the RTPMS Servers to provide user-requested data.

The browser resides on the user's computer. It provides the front-end user interface display which allows the user to request specific data requests through a series of text and graphical selections. The graphical displays are designed to provide the user with intuitive and comprehensive traffic performance measures.

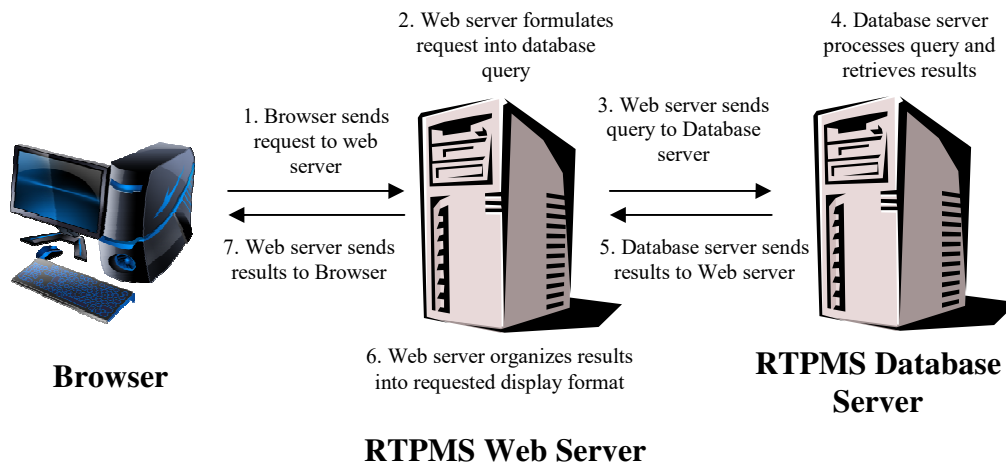


Figure 5-1 RTPMS Web and Database Framework

### 5.2 Web Server Design

The RTPMS web server is currently temporarily hosted on moon.its.uci.edu in UCI ITS. The web server runs on the Windows XP Professional operating system and is

equipped with Apache Tomcat, a servlet container developed by the Apache Software Foundation (ASF) which provides a "pure Java" HTTP web server environment for Java-based web pages—the chosen technology for the development of the web architecture for this project. The fully developed web server will be transferred to and permanently hosted on the California Traffic Management Laboratories (CTMLabs) server in the UCI ITS.

### 5.3 RTPMS Web Interface Modules

There has been a sustained trend for traffic information to be displayed on map-like interfaces to provide users with appreciation of network traffic conditions such as those found in Google Maps, PeMs and SigAlert as shown in Figure 5-2. These interfaces provide the additional benefit of providing a broad overview of traffic performance over a regional traffic network.

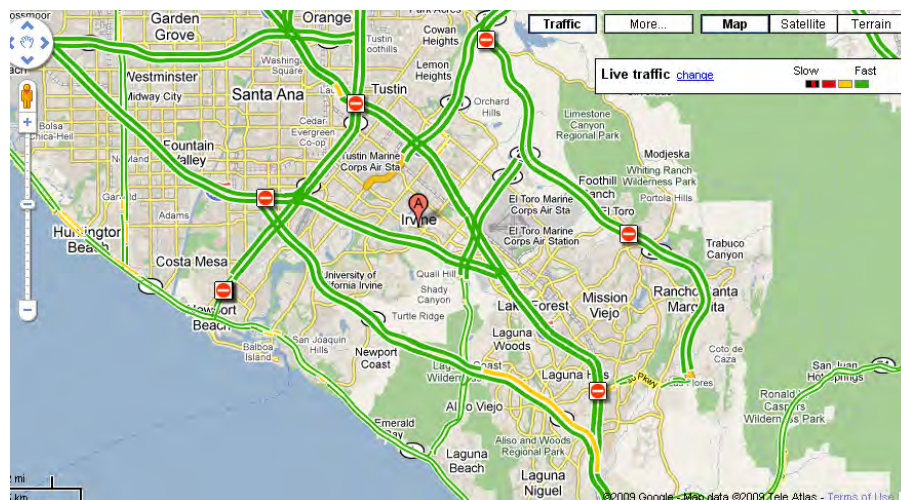


Figure 5-2 Sample Traffic Performance Interface from Google Maps

#### 5.3.1 Real-time Google Maps interactive navigation interface

The RTPMS Google Maps interactive interface provides an enhanced visualization and demonstration of the traffic performance measurements using the Google Maps Application Programming Interface (API). When a user requests the web page, the web page first calls the API to display the Google Maps for the area; it then retrieves

real-time traffic information from the database server and displays it on the map interface.

In Figure 5-3, the web page displays the Google Map for the Detector Testbed site on Northbound I-405 in Irvine, California. Zooming and panning are provided by the underlying Google Maps interface, which also offers map, satellite and hybrid views of the network. The highway sections refresh automatically to show real-time traffic levels.

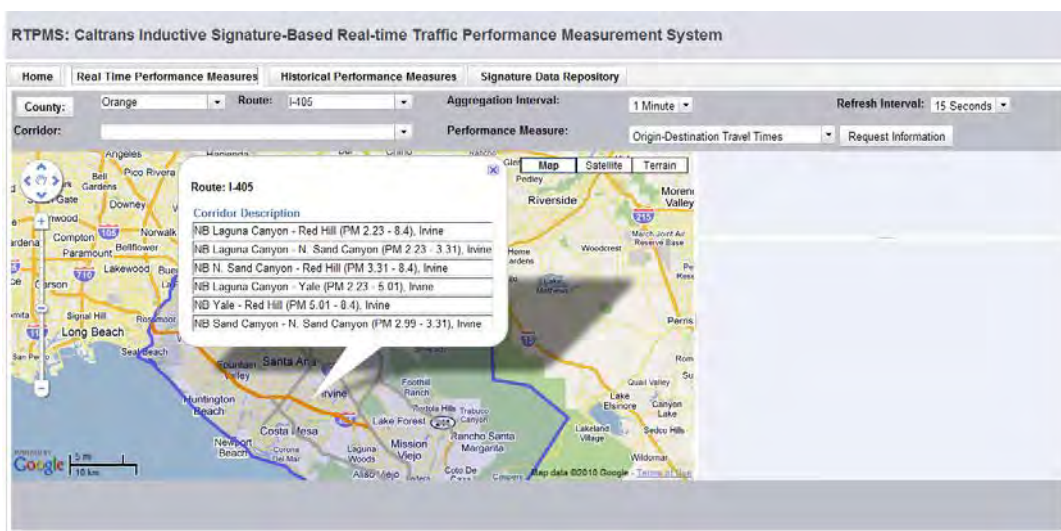


Figure 5-3 Google Maps-based RTPMS Interface

Users can switch between a mainline and HOV display. The aggregation time interval and refresh interval are also adjustable. An overview of the current traffic status, e.g., section travel times and mean speeds, as well as corridor travel time for both mainline and HOV lanes of the entire corridor are shown in the control panel—also automatically updated in real-time.

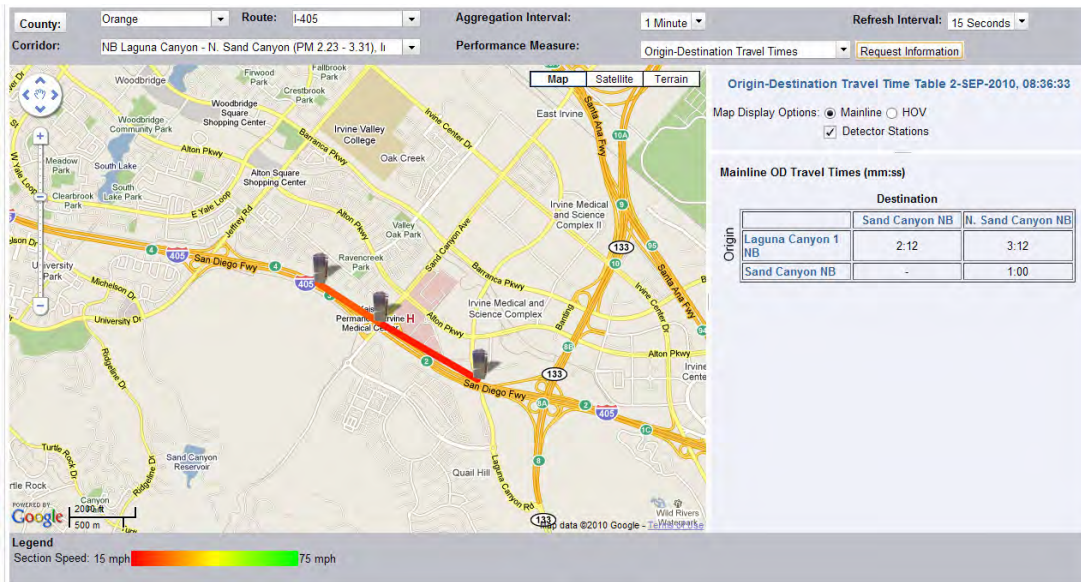


Figure 5-4 Detector Station Information Display from Google Maps-based RTPMS Interface

### 5.3.2 Real-Time Performance Measures

The new Real-Time Performance Measures are displayed for each station that is reporting real-time data from the field. The currently developed queries include:

1. Origin-Destination Travel Times
2. Lane-Lane Section Travel-Time Matrix
3. Lane-Lane Section Speed Matrix
4. Section Speeds and Densities

#### 5.3.2.1 Input Query Interface

The new query interface for real-time data consists of user input selections by either pull down menus or mouse over selection from the Google™ Map interface. Users are able to select the desired county, route, and corridor from the map or pull down menu. Once selected users can then select date, start time, end time, duration, time step (aggregation levels), and performance measurement type from the pull down menus as shown in Figure 5-5. Sample outputs are discussed in the following subsections.

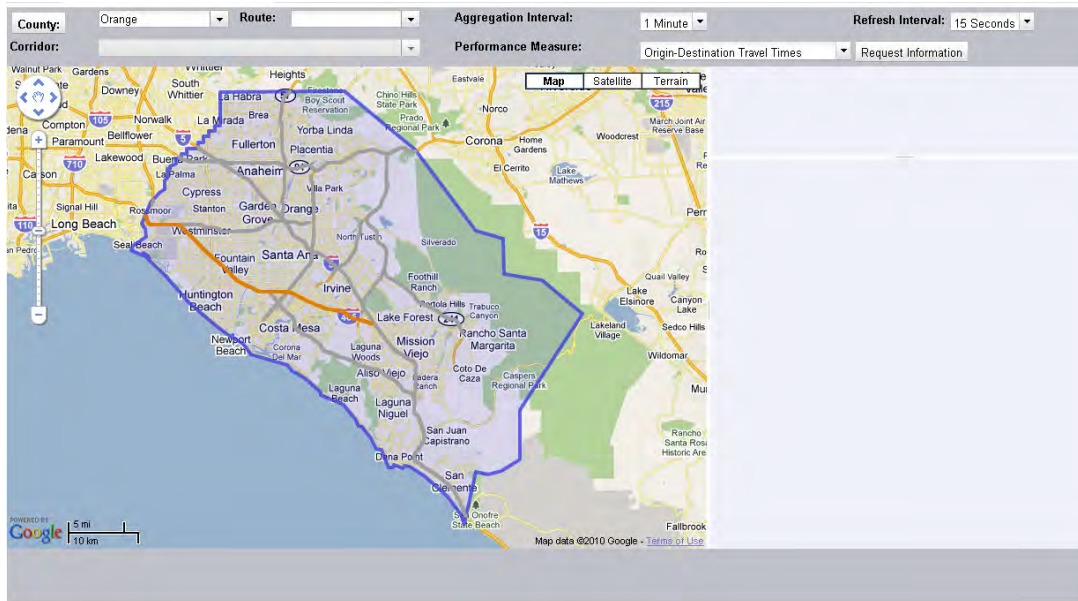


Figure 5-5 Real-time Performance Measures interactive user input query interface

### 5.3.2.2 Table and Graphical Outputs

The outputs for real-time data are available when real-time data is streaming from the field. Each output consists of a table or matrix type display as well as a graphical representation on the Google map interface. The display features can be toggled between HOV and mainline facility types.

#### Origin-Destination Travel Times

Each corridor possesses multiple origins and destinations formed by unique upstream and downstream detector station pairs. The origin-destination travel times associated with each corridor are presented in a matrix table where each cell of the matrix shows the current travel time from the origin (row) to the destination (column). For example, the I-405 Northbound corridor from South of the CA-133 Freeway to Red Hill would display six origins and six destinations spanning seven detector stations associated with the corridor as shown in Table 5-1. This results in 21 origin-destination pairs. An example of the origin-destination travel time matrix encompassing the entire corridor from South of the 133 to Airport is shown in Figure 5-6.

Table 5-1 Detector Stations corresponding to I-405 Northbound corridor from South of the CA-133 Freeway to Red Hill

<i>RTPMS Station ID</i>	<i>Detector Station Name</i>	<i>Post mile</i>
450	S. CA-133	1.6
452	Laguna Canyon 2 NB	2.35
454	N. Sand Canyon NB	3.31
456	Spruce NB	5.05
457	Harvard NB	6.2
458	Airport NB	8.27
459	Red Hill NB	8.4

Mainline OD Travel Times (mm:ss)

		Destination					
		Laguna Canyon 2 NB	N. Sand Canyon NB	Spruce NB	Harvard NB	Airport NB	Red Hill NB
Origin	S. CA-133	00:36	01:21	02:46	03:35	05:15	05:21
	Laguna Canyon 2 NB		00:45	02:10	02:59	04:39	04:45
	N. Sand Canyon NB			01:25	02:14	03:54	04:00
	Spruce NB				00:49	02:29	02:35
	Harvard NB					01:40	01:46
	Airport NB						00:06
	Red Hill NB						

Figure 5-6 Origin-Destination Travel Time Matrix for the S. CA-133 - Red Hill Corridor

Lane-Lane Travel-Time Matrix

The Lane-Lane Travel-Time Matrix displays the travel times by lane in matrix form with the columns representing the downstream lane selection and the rows representing the upstream lane selection of each re-identified vehicle (Figure 5-7).

This matrix takes into account the lane changes of the vehicles and therefore presents a more detailed representation traffic conditions within each section.

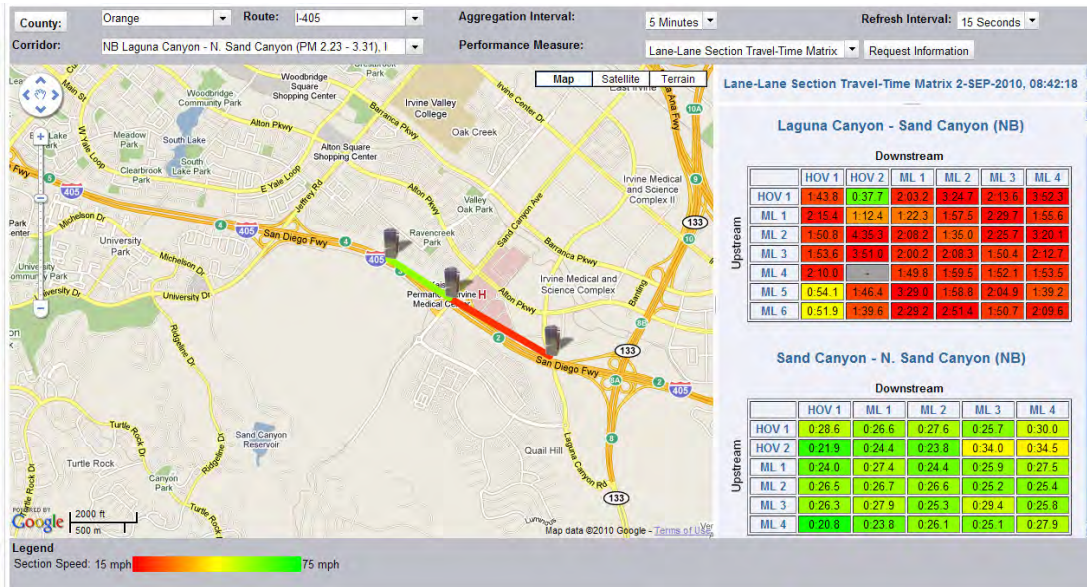


Figure 5-7 Sample Lane-Lane Travel Time Matrix Format

Lane-Lane Section Speed Matrix

The Lane-Lane Section Speed Matrix follows the same principle as the travel time matrix but reports the speeds of vehicles as they traverse the section and make lane changes. The speeds are also displayed on the map interface as a continuous color band from 15 mph (red) to 75 mph (green) (Figure 5-8).

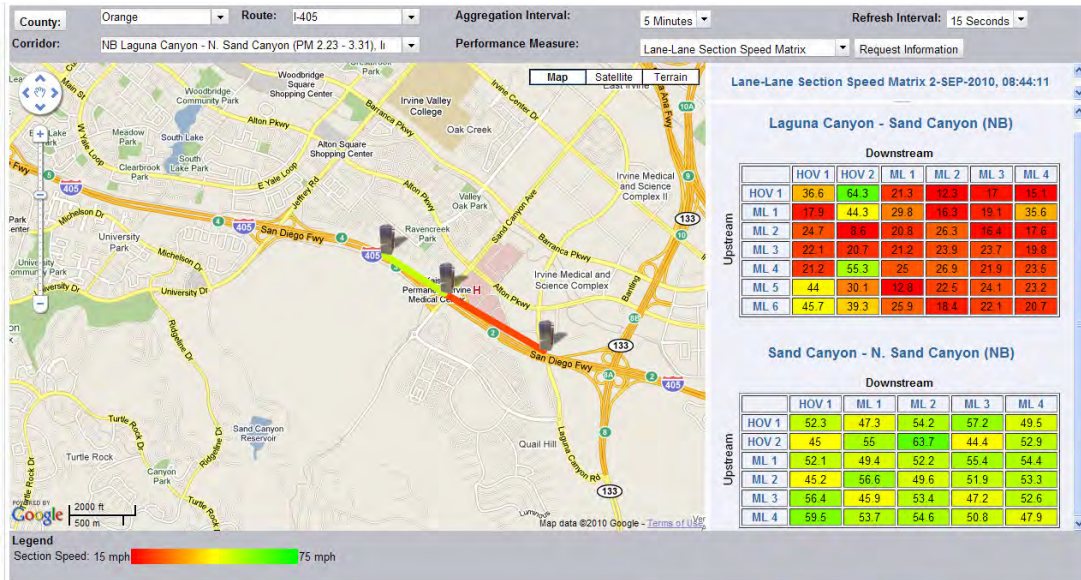


Figure 5-8 Sample Lane-Lane Section Speed Display

Section Speeds and Densities

Section speeds and densities are displayed together as a graphical display on the Google™ map interface. Density is displayed as the thickness of the line, and the speed is displayed as the color of the line along the section between two stations. The speed is a color contour ranging from 15 mph (red) to 75 mph (green) and the density ranges from 0 vehicles per miles per lane (vpmpl) (all grey box) to 125 vpmpl (box completely filled) (Figure 5-9). The value for maximum density, 125 vpmpl, is defined as the jam density of the freeway segment, i.e. the density at which traffic is no longer moving. Additionally, a table is also displayed and contains information on mainline and HOV median speed and density for each section comprising the corridor.

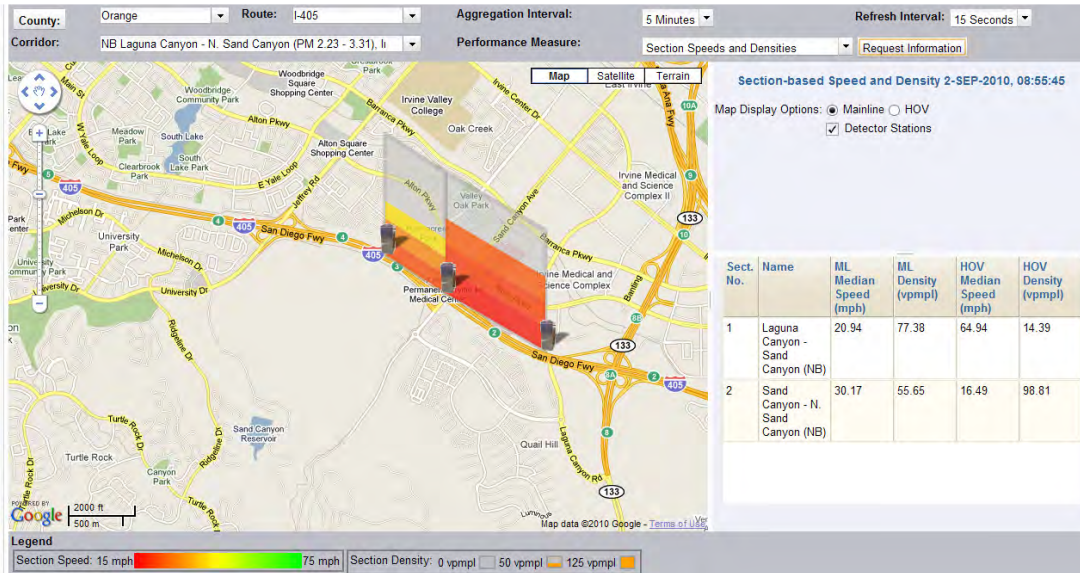


Figure 5-9 Sample Section Speeds and Densities Display

### 5.3.3 Historical Query Interface

The new Historical Query Interface provides traffic operators and researchers access to archived data within the RTPMS. This is a useful tool for performing advanced research studies to gain further insight into traffic performance impacts. This section describes the historical query and display modules developed to date. The modules of the historical query interface currently include:

1. Corridor travel time by facility
2. Corridor speed by facility
3. Corridor average delay by facility
4. Corridor total delay by facility
5. Section-based density contour map for main line lanes

Each query provides a graphical display on the map and a traceable timeline chart. The timeline charts provide an interactive graphical chart display for the travel time, speed, and delay measures using the Annotated Timeline visualization API developed by Google. This interactive interface allows the user to retrieve time and facility-specific traffic performance information by placing the mouse cursor over

the region of interest within the chart. Users can also zoom into and scroll across more specific time periods using the range selector provided at the bottom of the chart interface.

### 5.3.3.1 Input Query Interface

The query interface consists of user input selections to obtain requested performance historical measurements. Currently, users are able to query by county, route, corridor, date, start time, end time, duration, time step (aggregation levels), and performance measurement type as shown in Figure 5-10. Sample outputs are discussed in the following sub-sections.

The screenshot shows the RTPMS query interface with the following fields and values:

RTPMS: Caltrans Inductive Signature-Based Real-time Traffic Performance Measurement System							
Home	Real Time Performance Measures	Historical Performance Measures	Signature Data Repository				
County:	Orange	Route:	I-405	Date:	9/7/2010	Start Time:	6:00 AM
Corridor:	NB Laguna Canyon - N. Sand Canyon (PM 2.23 - 3.31), I		Time Step:	5 Minutes	End Time:	6:00 PM	
Performance Measure:	Corridor Travel Time By Facility		Request Information				

Figure 5-10 Historical Performance Measures Query Inputs

### 5.3.3.2 Table and Graphical Outputs

#### Corridor Travel Time by Facility

The corridor travel time performance displays an interactive table that presents overall time-aggregated corridor travel times, differentiated by mainline and HOV lane facilities as shown in Figure 5-11. The time aggregated corridor travel times are computed from the sum of average section travel times within the corridor for each corresponding time interval.

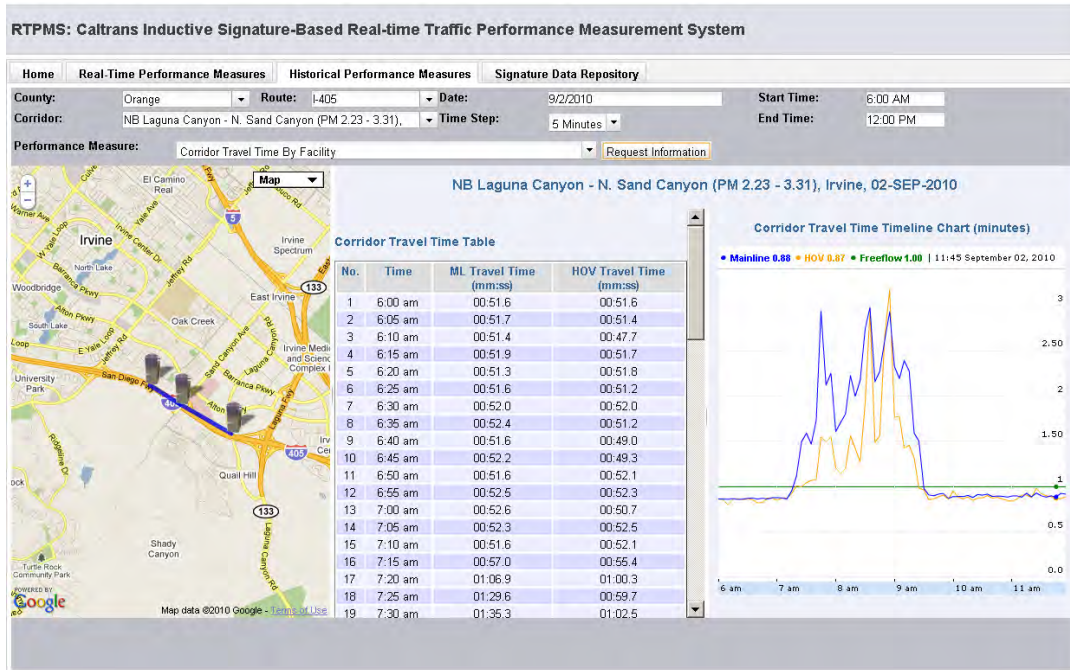


Figure 5-11 Sample Corridor Travel Time by Facility Display

Corridor Speed by Facility

The corridor speed by facility performance measure displays the time aggregated average speed to traverse the corridor for each time period associated with the selected corridor. Each corridor speed measure presented is distinguished by facility type (mainline and HOV lanes) as shown in Figure 5-12.

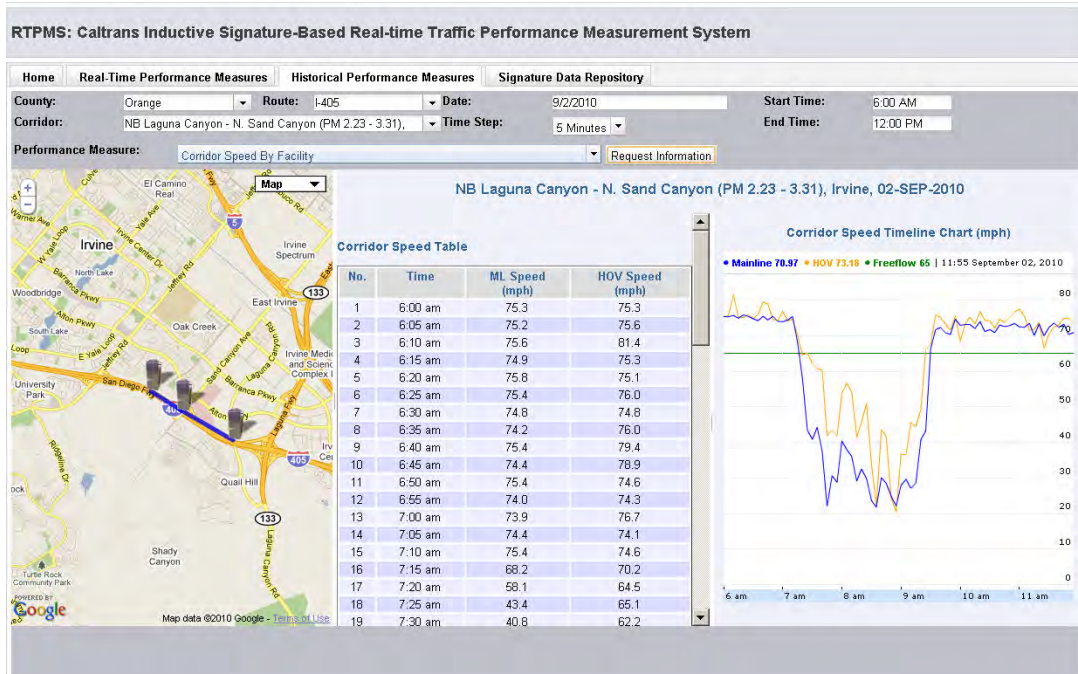


Figure 5-12 Sample Corridor Speed by Facility Display

Corridor Average Delay by Facility

The corridor average delay performance measure presents the average delay experienced by each vehicle in minutes across time of day by facility as shown in Figure 5-13. The blue line represents corridor delay from the mainline lanes while the orange line represents delay from the HOV lane. The delay is taken as the additional minutes of travel required compared to expected travel time under free flow conditions defined in this application as travel at the speed limit (defined here as 65 mph for the I-405 freeway corridor in Irvine, CA). The Corridor Total Delay Timeline Chart in vehicle-hours is also available as an output (Figure 5-14).

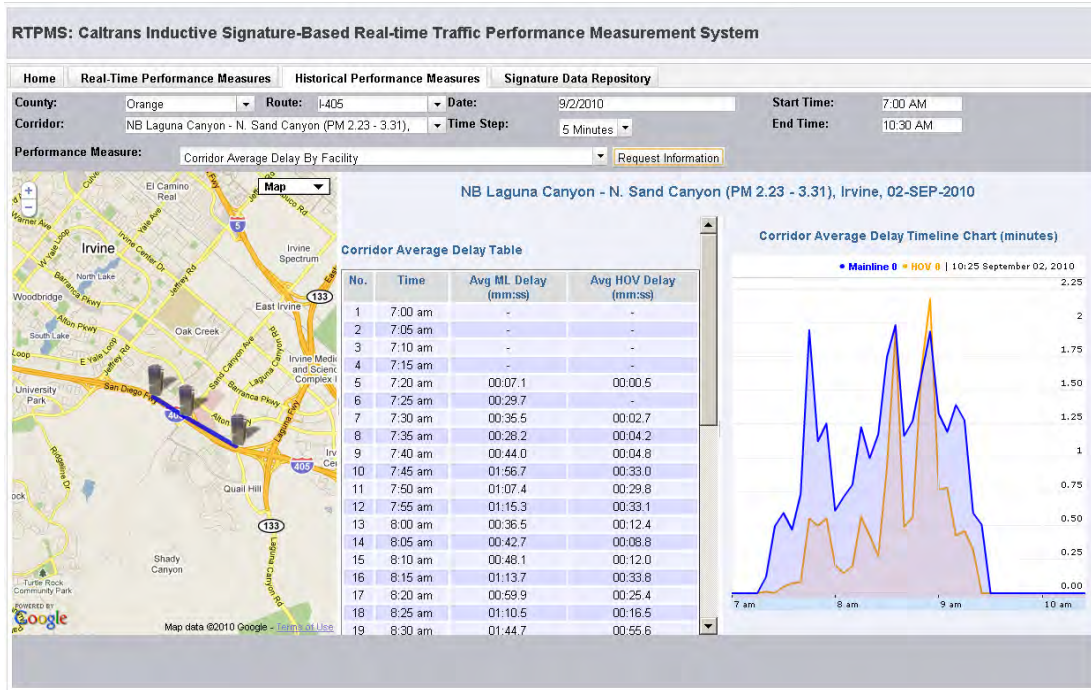


Figure 5-13 Sample Corridor Average Delay Timeline Chart Display (minutes per vehicle)

Corridor Total Delay by Facility

The corridor total delay performance measure presents the total delay experienced by all vehicles within the corridor in vehicle-hours across time of day by facility as shown in Figure 5-14. The blue line represents the total corridor delay from the mainline lanes while the orange line represents total delay from the HOV lane. The total delay is taken as the additional time of travel required compared to the expected travel time under free flow conditions defined in this application as travel at the speed limit (65 mph for the I-405 freeway corridor in Irvine, CA) multiplied by the number of vehicles that experience that delay.

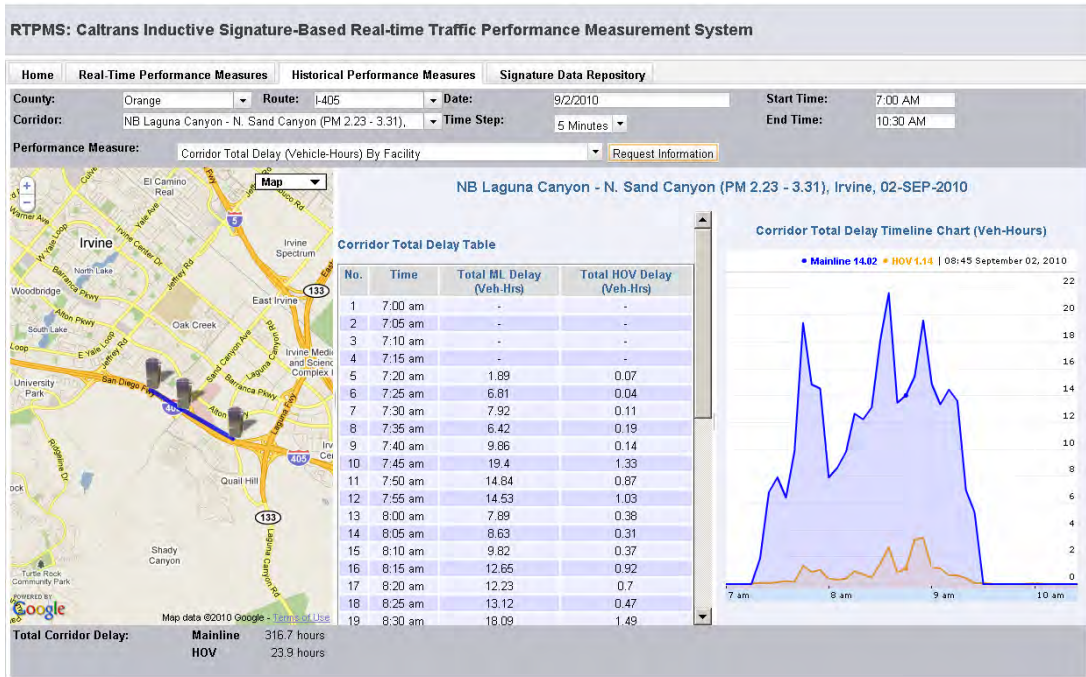


Figure 5-14 Sample Corridor Total Delay Timeline Chart Display (Vehicle-Hours)

Section-Based Density Contour Map

The Section-Based Density Contour Map provides a graphical display of the change in density conditions by time of day and distance along the section. The horizontal axis displays the distance separating each station and the vertical axis displays the time of day. The legend along the bottom of the page depicts the color reference for each density condition, with 125 vehicles per mile per lane (vpmpl) as the upper bound and 0 vpmpl as the lower bound. Figure 5-15 shows a sample contour map for September 2<sup>nd</sup>, 2010 data.

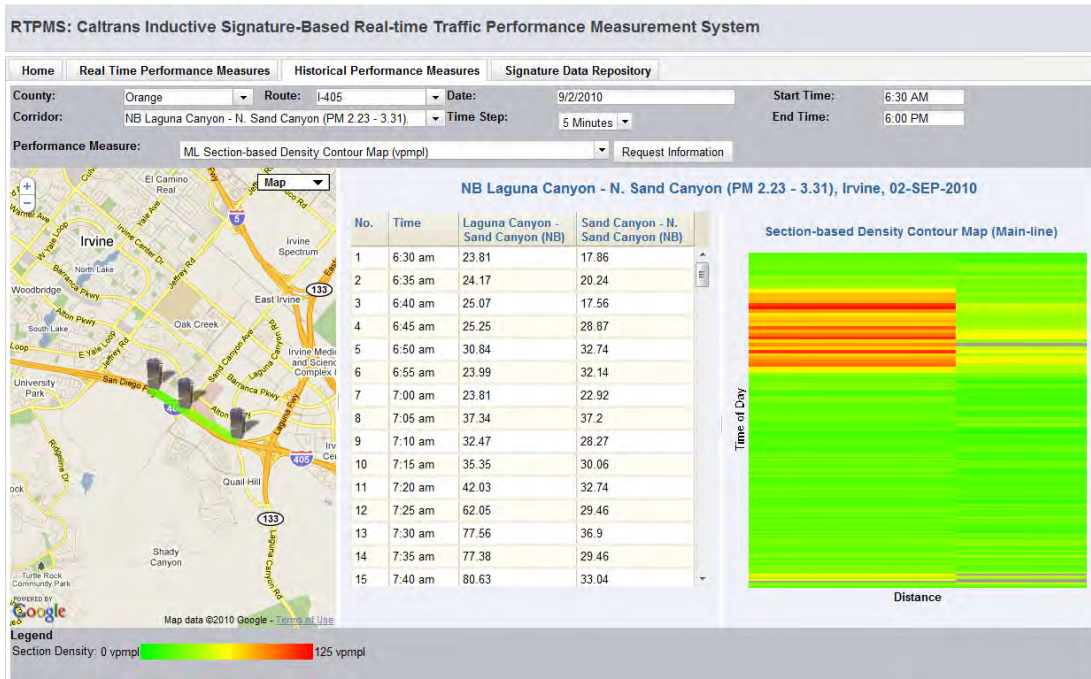


Figure 5-15 Sample Section-based Density Contour Map

### 5.3.4 Signature Data Repository

In addition to real-time and historical data, the current version of RTPMS also includes a signature data repository. The raw signature data can be downloaded by selecting the county, route, corridor, and station for which data is desired. Days for which there is available data appear in bold on the monthly calendar, which displays once the input data has been selected by the user. The user can select the day that they would like to download and then finally download each lane’s data. The downloaded raw signature file requires a decoder, which has been provided as part of RTPMS. Users are able to use the decoder to turn the binary raw signature data into a text file they can then use for research purposes. Figure 5-16 shows an example of the Signature Data Repository for September 2, 2010, at the Laguna Canyon 1 NB detector station.

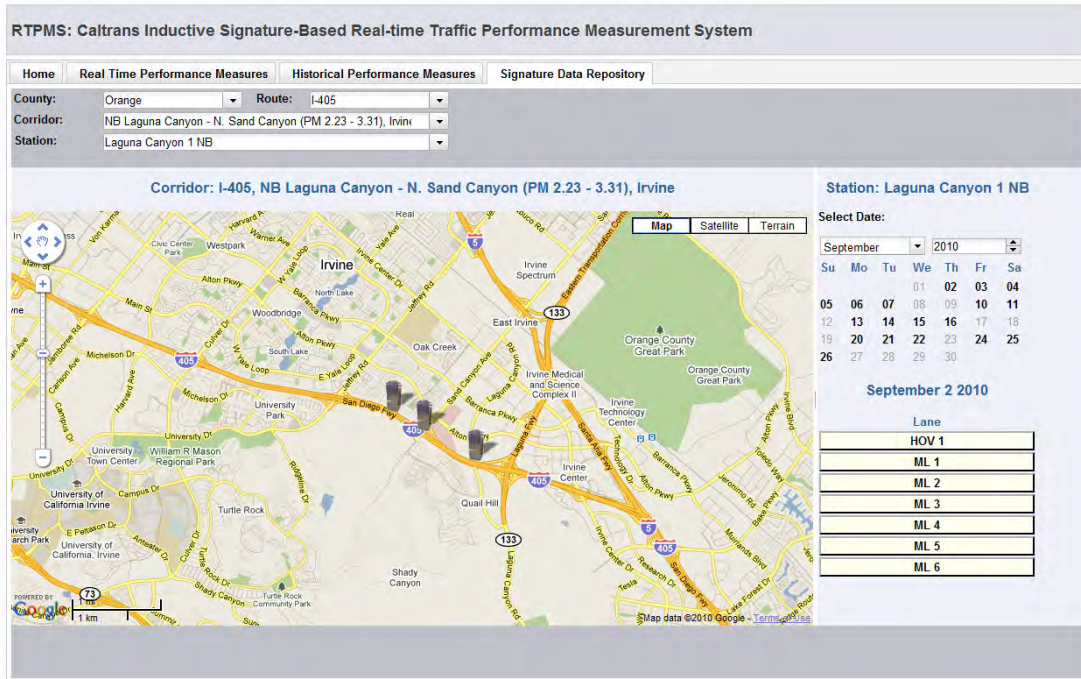


Figure 5-16 Signature Data Repository

## **CHAPTER 6 CONCLUSION**

Effective real-time traffic detection systems which are able to obtain accurate, detailed and timely freeway performance measures are a prerequisite for efficient transportation system operations. Advanced real-time traffic performance measurement provides timely and detailed assessment of traffic conditions and is the cornerstone for achieving optimal operations of the freeway network. It assists in the in-depth understanding of traffic impacts in congestion-prone metropolitan areas, the knowledge of which is essential to determine the best mitigating solutions. This study has yielded several significant findings relating to the potential of alternative advanced traffic surveillance technologies compared with Inductive Loop Detector (ILD) signatures. This study has also expanded and developed advanced tools for the field deployment of the Real-time Traffic Performance Measurement System (RTPMS).

### **6.1 Alternative Advanced Traffic Surveillance Technologies**

The Blade™ inductive system and Sensys™ wireless magnetometers were investigated to identify alternative technologies to ILD signatures which are capable of providing deployable advanced traffic surveillance.

The study of the Blade™ inductive system yielded proposed sensor configurations that may be suitable for obtaining speed profiles from vehicles to enable recovery of vehicle inductive signatures that have been distorted by acceleration and deceleration effects. However, the system was not sufficiently mature for deployment on the I-405 freeway. This was due to insufficient evaluation on the reliability and feasibility of the installation specifications provided by the manufacturer. Safety concerns were also raised relating to possible pavement damage due to the geometry of the cuts required for installation of the sensors. Additionally, but perhaps not as critically, installation of the Blade™ sensors would require temporary lane closures which are costly and required significant coordination across several agencies. Due to these concerns, the Blade™ inductive

system was not deployed on the I-405, and its evaluation was confined to surface-mounted installation within the University of California, Irvine campus.

The investigation of Sensys™ wireless magnetometers revealed the potential of Sensys™ in providing reliable conventional traffic data such as volume and occupancy information as well as to augment the ILD signature system through heterogeneous transformation of signatures between ILD and Sensys™ sensors. The results from the analysis of conventional data indicated that while volume counts from Sensys™ were comparable with ILDs with errors of about six percent, occupancy measures at the test site were significantly higher than ILDs. While factoring techniques can be used to adjust the Sensys™ occupancy measures, they still need the presence of existing ILDs for validation of measurement accuracy. Spikes in occupancy measurements were also a concern, as they appeared abruptly and seemed to be random in nature. The investigation of transformation between ILD and Sensys™ signatures showed almost no correlation in the initial analysis of interpolated features obtained from signatures pairs obtained from the same vehicle. A further transformation analysis using artificial neural networks yielded similarly poor results, corroborating the findings from the correlation analysis. These findings indicate that Sensys™ signatures are probably not compatible with ILD signatures. However, because their features are independent from ILD signatures, data fusion of these two technologies could help to improve the performance of advanced traffic surveillance applications if both technologies are deployed in a same location.

## **6.2 Real-time Traffic Performance Measurement System**

This study has refined the components of the prototype RTPMS first developed under PATH Task Order 5304 for full deployment in the Detector Testbed on the Northbound I-405 freeway corridor in the City of Irvine, California. Modifications were made to the RTPMS to improve the reliability of connections from multiple field units to the CORBA server.

A new advanced integrated web-user interface using advanced technologies such as Asynchronous JavaScript and XML (AJAX) was developed to provide advanced queries for real-time as well as archived traffic performance measures, which are displayed in a highly interactive environment. Real-time performance measures include advanced traffic performance measures not obtainable through conventional ILD systems such as section densities, lane-lane section speeds and travel times and speed distributions within each section. Archived reports also provide advanced measures such as corridor travel times, speeds, delays, section densities and vehicle classifications by time of day. These advanced traffic performance measures provide users with unprecedented insight into current and historical traffic conditions to design and evaluate corridor management strategies. A repository for access to archived signature data was also developed as a separate module within the RTPMS web interface. This signature repository allows the research community to further investigate the potential of ILD signatures in providing improved traffic surveillance applications.

### **6.3 Implementation Strategies and Future Research**

At the completion of this project, a majority of stations have been fully implemented with field computers, detector cards, and wireless modems in the Detector Testbed. As a continuation of the work in this project, deployment of equipment to the remaining stations designated in the project proposal will be carried out. Continual expansion of the online tools available through the RTPMS web-interface is proposed for future work.

A critical issue facing continued deployment of the stations along the northbound I-405 corridor is the aging field units, most which are almost ten years old. While most of them have been retrofitted for improved performance and reliability, the upgrades were only expected to be a cost-effective solution in the short term, as most components in these units are reaching the limit of their service life. The recommendation for future support of this project is to acquire newer,

fanless field units that are more reliable and are better able to quickly process and transfer data from the field to the RTPMS servers. The new units will have no moving parts such as fans and hard drives. This eliminates potential system failures due to wear and temperature cycles, and is expected to provide extended service life over the old units. This would improve the reliability of the system and reduce long term maintenance costs, while the higher performance processors equipped with these new units will also help to reduce delays associated with transferring data from the field to the servers in ITS.

Several future research studies and initiatives can be performed to expand on the framework of the RTPMS and leverage on the efforts already invested in the development of the system. The following are a list of recommended efforts:

1. Develop real-time and archived measurement corridor-based emissions estimation tools,
2. Design re-identification algorithms to incorporate on- and off-ramp locations,
3. Develop advanced ramp metering algorithms which are able to harness the information yielded from RTPMS, and
4. Deploy additional freeway and parallel arterial corridors to investigate performance of traffic networks

Emissions estimation based on RTPMS is currently being developed under a study funded by the University of California Institute of Transportation Studies Multi-campus Research Program and Initiative on Sustainable Transportation. One of this study's objectives is to yield real-time and archived emissions estimation tools using the MOVES emissions model.

Design of more sophisticated re-identification algorithms to incorporate on- and off-ramp locations are required due to the acceleration-stop-deceleration patterns which are characteristic of traffic inflow and outflow of the ramps. The ability to

correctly re-identify on- and off-ramp vehicles with mainline vehicles would yield even more comprehensive applications for RTPMS, such as providing full freeway facility travel times for vehicles.

Advanced ramp metering algorithms based on the RTPMS framework will be able to harness its advanced section-based traffic measures. This will offer further potential for improved management of ramp traffic under critical conditions where traffic flow and density measures estimated from point sources may not provide sufficient insight.

It is recommended that RTPMS be deployed in additional freeway corridors such as the CA-55 and I-5 freeways. These freeways, which together with the I-405 corridor form the Irvine golden triangle, will provide a unique and valuable testbed for testing and deploying new traffic operations and management strategies using advanced traffic information from RTPMS. A further implementation along arterial corridors parallel to these freeways will also yield insight in understanding relationships between adjacent arterial and freeway corridor traffic performance and travel behavior.

## REFERENCES

- [1] Palen, J. The need for surveillance in intelligent transportation systems. *Intellimotion*, Vol. 6, No. 1, University of California PATH, Berkeley, pp. 1–3, 1997.
- [2] Coifman, B. and E. Ergueta. Improved Reidentification and travel time Measurement on Congested Freeways. *ASCE Journal of Transportation Engineering*, Vol. 129, No. 5, September 2003.
- [3] Freeway Performance Measurement System (PeMS). University of California, Berkeley, PATH, and CalTrans. <http://pems.eecs.berkeley.edu/> Accessed May 12, 2009.
- [4] Kühne, R. D., and S. Immes. Freeway Control Systems for Using Section-Related Traffic Variable Detection. *Pacific Rim TransTech Conference*, Seattle, Washington, 1993.
- [5] Ritchie, S.G. and C. Sun. *Section related measures of traffic system performance: Final Report*. Publication UCB-ITS-PRR-98-33. California PATH, University of California, Berkeley, 1998.
- [6] Sun, C., S.G. Ritchie, and K. Tsai. Algorithm Development for Derivation of Section-Related Measures of Traffic System Performance Using Inductive Loop Detectors. In *Transportation Research Record: Journal of the Transportation Research Board*, No. 1643, Transportation Research Board of the National Academies, Washington, D.C., 1998, pp. 171-180.
- [7] Oh, C., A. Tok, and S. G. Ritchie. Real-Time Freeway Level of Service Using Inductive-Signature-Based Vehicle Reidentification System. *IEEE Transactions on Intelligent Transportation Systems*, Vol. 6, No. 2, 2005, pp. 138-146.
- [8] Jeng, S., S.G. Ritchie, and Y.C. Tok. Freeway Corridor Performance Measurement Based on Vehicle Reidentification. In *Proceedings of the Transportation Research Board 86<sup>th</sup> Annual Meeting*, Washington D.C., January 2007.
- [9] Hall, F. L., and B. N. Persaud. Evaluation of Speed Estimates Made with Single-Detector Data from Freeway Traffic Management Systems. In *Transportation Research Record: Journal of the Transportation Research Board*, No. 1232, Transportation Research Board of the National Academies, Washington, D.C., 1989, pp. 9-16.
- [10] Dailey, D. J. A Statistical Algorithm for Estimating Speed from Single Loop Volume and Occupancy Measurements. *Transportation Research: Part B*, Vol. 33, No. 5, 1999, pp. 313–322.
- [11] Coifman, B. Improved Velocity Estimation using Single Loop Detectors. *Transportation Research: Part A*, Vol. 35, 2001, pp 863-880.

- [12] Hellinga, B. Improving Freeway Speed Estimated from Single Loop Detectors. *ASCE Journal of Transportation Engineering*, Vol. 128, No. 1, 2002, pp 58-67.
- [13] Sun, C. Use of Vehicle Signature Analysis and Lexicographic Optimization for Vehicle Reidentification on Freeways. Ph.D. Thesis, University of California, Irvine, 1998.
- [14] Jeng, S. and S.G. Ritchie. New Inductive Signature Data Compression and Transformation Method for Online Vehicle Reidentification. In *Proceedings of the Transportation Research Board 85<sup>th</sup> Annual Meeting*, Washington D.C., January 2006.
- [15] Kwon, T.M. Blind Deconvolution of Vehicle Inductance Signatures for Travel-Time Estimation. Report MN/RC-2006-06. Minnesota DOT, February 2006.
- [16] Coifman, B. Vehicle Reidentification and Travel Time Measurement in Real-Time on Freeways Using the Existing Loop Detector Infrastructure. In *Transportation Research Record: Journal of the Transportation Research Board*, No. 1643, Transportation Research Board of the National Academies, Washington, D.C., 1998, pp. 181-191.
- [17] Coifman, B. and M. Cassidy. Vehicle Reidentification and Travel Time Measurement on Congested Freeways. *Transportation Research: Part A*, Vol. 36, 2002, pp. 889-917.
- [18] Coifman, B. Estimating Density and Lane Inflow on a Freeway Segment. *Transportation Research: Part A*, Vol. 37, No 8, 2003, pp. 689-701.
- [19] Li, R., G. Rose, and M. Sarvi. Evaluation of Speed-Based Travel Time Estimation Models. *ASCE Journal of Transportation Engineering*, Vol. 132, No. 7, 2006, pp 540-547.
- [20] Cortes, C E, Lavanya, R, Oh, J-S, Jayakrishnan, R. General Purpose Methodology for Estimation Link Travel Time with Multiple-Point Detection of Traffic. *Transportation Research Record No. 1802*, Transportation Research Board, 2002, pp 181-189.
- [21] Van Lint, J. W. C. and N. J. van der Zijpp. An Improved Travel Time Estimation Algorithm using Dual Loop Detectors. In *Proceedings of the Transportation Research Board 82nd Annual Meeting*, Washington, D.C., January 2003.
- [22] Sun, L., J. Yang, and H. Mahmassani. Travel time estimation based on piecewise truncated quadratic speed trajectory. *Transportation Research: Part A*, Vol. 42, No. 1, 2008, pp. 173-186.
- [23] Nam, D. H., and D. R. Drew. Traffic Dynamics: Method for Estimating Freeway Travel Times in Real Time from Flow Measurements. *ASCE Journal of Transportation Engineering*, Vol. 122, No. 3, 1996, pp. 185-191.

- [24] Vanajakshi, L. D, B.M. Williams, and L. R. Rilett. Improved Flow-Based Travel Time Estimation Method from Point Detector Data for Freeways. *ASCE Journal of Transportation Engineering*, Vol. 135, No. 1, 2009, pp. 26-36.
- [25] Dailey, D. J. Travel Time Estimation using Cross-Correlational Techniques. *Transportation Research: Part B*, Vol. 27, No. 2, 1993, pp. 97-107.
- [26] Petty, K. F., P. Bickel, M. Ostland, J. Rice, F. Schoenberg, J. Jiang, and Y. Rotov, Accurate Estimation of Travel Times from Single-Loop Detectors. *Transportation Research: Part A*, Vol. 32, No. 1, 1998, pp. 1-17.
- [27] Coifman, B. and S. Krishnamurthy. Vehicle reidentification and travel time measurement across freeway junctions using the existing detector infrastructure. *Transportation Research: Part C*, Vol. 15, No. 3, 2007, pp. 135-153.
- [28] Oh, S., S.G. Ritchie, and C. Oh. Real-time Traffic Measurement from Single Loop Inductive Signatures. In *Transportation Research Record: Journal of the Transportation Research Board*, No. 1804, Transportation Research Board of the National Academies, Washington, D.C., 2002, pp. 98-106.
- [29] Gazis, D. and C. Knapp. On-line Estimation of Traffic Densities from Time-Series of Flow and Speed Data. *Transportation Science*, Vol. 5, No. 3, 1971, pp. 282-301.
- [30] Vanajakshi, L. and L.R. Rilett. Loop Detector Data Diagnostics based on Conservation of Vehicles Principle. In *Transportation Research Record: Journal of the Transportation Research Board*, No. 1870, Transportation Research Board of the National Academies, Washington, D.C., 2004, pp. 162-169.
- [31] Lin, W.H. and D. Ahanotu. *Validating the Basic Cell Transmission Model on a Single Freeway Link*. PATH Technical Note 95-3, Institute of Transportation Studies, University of California, Berkeley, 1994.
- [32] Munoz, L., X. Sun, R. Horowitz, and L. Alvarez. A piecewise-linearized CTM and parameter calibration methodology. In *Transportation Research Record: Journal of the Transportation Research Board*, No. 1965, Transportation Research Board of the National Academies, Washington, D.C., 2006, pp. 183-191.
- [33] Herrera, J. and A. Bayen. Traffic Flow Reconstruction using Mobile Sensors and Loop Detector Data. In *Proceedings of the Transportation Research Board 87<sup>th</sup> Annual Meeting*, Washington D.C., January 2008.
- [34] Mimbela, L.E.Y. and L.A. Klein. *Summary of Vehicle Detection and Surveillance Technologies Used in Intelligent Transportation Systems*. Submitted to FHWA Intelligent Transportation Systems Joint Program Office, November 30, 2000.

- [35] Gordon, R.L. and W. Tighe. *Traffic Control Systems Handbook*. Publication FHWA-HOP-06-006. FHWA, U.S. Department of Transportation, October 2005.
- [36] *Traffic Detector Handbook Third Edition Volume 1*, Federal Highway Administration, Publication No. FHWA-HRT-06-108, October 2006.
- [37] Martin, P.T., Y. Feng, and X. Wang. Detector Technology Evaluation. Utah Department of Transportation, Report No. UTL-1002-64. November 2003.
- [38] Turner, S. M. Advanced Techniques for Travel Time Data Collection. *Transportation Research Record No. 1551*, Transportation Research Board, Washington, D.C., 1996, pp. 51-58.
- [39] Coifman, B. and S. Kim. Speed estimation and length based vehicle classification from freeway single loop detectors. *Transportation Research: Part C*, Vol. 17, 2009, pp 349-364.
- [40] Park, S., S.G. Ritchie, and C. Oh. An Innovative Single Loop Speed Estimation Models with Advanced Loop Data. In *Proceedings of the Transportation Research Board 86<sup>th</sup> Annual Meeting*, Washington D.C., January 2007.
- [41] Tok, Y.C., S.V. Hernandez, and S.G. Ritchie. Accurate individual vehicle speeds from single inductive loop signatures. In *Proceedings of the Transportation Research Board 88<sup>th</sup> Annual Meeting*, Washington D.C., January 2009.
- [42] Holt, R. B., B. L. Smith, B. B. Park. *An Investigation of Travel Time Estimation Based on Point Sensors*. Report No. STL-2003-03. Smart Travel Lab, Charlottesville, VA, August 2003.
- [43] Cassidy, M. and B. Coifman. Relation among average speed, flow, and density and analogous relations between density and occupancy. In *Transportation Research Record: Journal of the Transportation Research Board*, No. 1591, Transportation Research Board of the National Academies, Washington, D.C., 1997, pp. 1-6.
- [44] Golob, T., W.W. Recker, and V. Alvarez. Freeway safety as a function of traffic flow. *Accident Analysis and Prevention*, Vol. 36, Is. 6, 2003, pp. 933-946.
- [45] *Highway Capacity Manual*, Transportation Research Board, Washington D.C., 2000 (Standard U.S. version).
- [46] Bickel, P.J., Chen, C., Kwon, J., Rice, J., Varaiya, P. and van Zwet, E. Traffic Flow on a Freeway Network. In Denison, D.D. et al. (Eds.) *Nonlinear Estimation and Classification*, New York, Springer, 2003.
- [47] Zhang, L., L.R. Rilett, E.G. Jones, B. Naik, J. Appiah. Analysis of Aggregated and Disaggregated Traffic Data Obtained from Nonintrusive Traffic Detection Sensors. In *Proceedings of the Transportation Research Board 86<sup>th</sup> Annual Meeting*, Washington D.C., January 2007.

- [48] Hall, F.L. The Relationship between Occupancy and Density. *Transportation Forum*, Vol. 3-3, Dec. 1986, pp. 46-52.
- [49] Roess, R.P., E.S. Prassas, and W.R. McShane. *Traffic Engineering Third Edition*. Prentice Hall, New Jersey, 2004.
- [50] May, A.D. *Traffic Flow Fundamentals*. Prentice Hall, New Jersey, 1990.
- [51] Greenshields, B. A study of traffic capacity. *Highway Research Board Proceedings*, Vol. 14, 1935, pp. 448–477.
- [52] Hu, X. and D. Yang. Estimation of Traffic Density on Urban Freeways. *Journal of Transportation Systems Engineering and Information Technology*, Vol. 8, Is. 3, 2008, pp. 79-82.
- [53] Nahi, N. and A. Trivedi. Recursive estimation of traffic variables: Section density and average speed. *Transportation Science Vol 7, Is 3*, 1973, pp. 269–286.
- [54] Gazis, D. and M. Szeto. Design of density measuring systems for roadways. *Transportation research Record No. 495*, Transportation Research Board, 1974, pp. 44-52.
- [55] Cremer, M. and K. Putensen. Monitoring of Traffic Density Profiles using Measurements from Loop Detectors and Vehicle Trip Data. *Large Urban Systems*, Proceedings of the Advanced Traffic Management Conference, 1993.
- [56] Daganzo, C. F. The CTM: A dynamic representation of highway traffic consistent with hydrodynamic theory. *Transportation Research: Part B*, Vol. 28, No. 4, 1994, pp. 269-287.
- [57] Munoz, L., X. Sun, R. Horowitz, and L. Alvarez. Traffic Density Estimation and the CTM. *Proceedings of the American Control Conference*, Denver, Co., June 4-6, 2003.
- [58] Sun, C., S. G. Ritchie, K. Tsai, and R. Jayakrishnan. Use of Vehicle Signature Analysis and Lexicographic Optimization for Vehicle Reidentification on Freeways. *Transportation Research: Part C*, Vol. 7, No. 4, 1999, pp. 167-185.
- [59] *Travel Time Data Collection Handbook*. Federal Highway Administration (FHWA), Rep. No. FHWA-PL-98-035, Washington, D.C., 1998.
- [60] Sun, C. and Ritchie, S. Individual Vehicle Speed Estimation Using Single Loop Inductive Waveforms. *Journal of Transportation Engineering*, Vol. 125, No. 6, 1999, pp. 531-538.
- [61] Sun, C. G. Arr, and R.D. Ramachandran. An investigation of the use of Vehicle Reidentification for deriving travel time and travel time distribution. In *Proceedings of the Transportation Research Board 82<sup>th</sup> Annual Meeting*, Washington D.C., January 2003.